DISSERTATION

SEX-SPECIFIC CARDIOMETABOLIC RESPONSES TO CHRONIC STRESS AND THE IMPACT OF PREFRONTAL-MEDULLARY REGULATION

Submitted by

Carley Dearing

Department of Biomedical Sciences

In partial fulfillment of the requirements

For the Degree of Doctor of Philosophy

Colorado State University

Fort Collins, Colorado

Spring 2024

Doctoral Committee:

Advisor: Brent Myers

Bret Smith
Anna Fails
Kim Hoke

ABSTRACT

SEX-SPECFIC CARDIOMETABOLIC RESPONSES TO CHRONIC STRESS AND THE IMPACT OF PREFRONTAL-MEDULLARY REGULATION

Globally, cardiovascular and metabolic disease are leading causes of death and years lived with disability. Chronic stress is an etiologic factor in both diseases and biologic sex plays an important role in the progression and prognosis of each. However, the neurobiological basis of how chronic stress exposure intersects with sex, cardiovascular, and metabolic function to impact systemic physiology is poorly understood. Prior studies from our group indicate that, in rats, the prefrontal infralimbic cortex (IL)-rostral ventrolateral medulla (RVLM) circuit inhibits sympathetic and endocrine responses to stress. Therefore, we aimed to address the overarching hypothesis that the IL-RVLM circuit is necessary for homeostatic function and mitigation of deleterious changes to metabolic, cardiac, and microvascular function following chronic stress. To this end, an intersectional genetic approach was used to induce Cre-dependent expression of tetanus toxin light chain and inhibit neurotransmitter release from RVLM-projecting IL neurons in male and female rats. Rats were then exposed to 2 weeks of chronic variable stress (CVS). Metabolic function was assessed with a fasted glucose tolerance test. Cardiovascular function was examined with echocardiography and non-invasive hemodynamics. Additionally, microvascular function was quantified via *ex-vivo* resistance arteriole pressure myography. Our results indicate that glucose tolerance, left ventricular structure, and vascular function are all impacted in a sex-dependent manner. Following chronic stress, circuit-intact females show glucodysregulation characterized by decreased glucose clearance, elevated corticosterone, and insulin insensitivity. Regardless of stress, circuit inhibition in females also impaired glucoregulation but was characterized by elevated glucagon

with no compensatory insulin response. Circuit inhibition also increased relative heart size, increased endothelial-dependent vasodilation at both normotensive and hypertensive pressures, and increased myogenic tone and diastolic wall strain. These changes indicate that chronic stress in females leads to broad endocrine-autonomic dysregulation of glucose homeostasis and microvascular function that is exacerbated by IL-RVLM inhibition. While chronic stress in males resulted in an adaptive metabolic response and no changes in normotensive vasodilation, circuit inhibition in chronically-stressed males lead to glucodysregulation and increased endothelial-dependent vasodilation at hypertensive pressures. Additionally, these animals had reduced ventricular wall thickness in diastole. Broadly, these results support the hypothesis that the IL-RVLM circuit is necessary for appropriate glucose homeostasis and vascular function and that circuit inhibition and chronic stress lead to sex-specific responses that may differentially impact the progression of cardiovascular and metabolic disease.

ACKNOWLEDGEMTS

I would like to thank my advisor, Brent Myers, for his help in navigating the difficulty of the dual DVM-PhD program. My success can be attributed to his unwavering support and mentorship. The current and former members of the Myers lab were also instrumental to the success of these projects and creating a welcoming and collaborative community. These projects are only complete because of the help of Ema Lukinic, Ella Sandford, Courtney Bouchet, Derek Schaeuble, and the many other members of our lab.

I would also like the thank the following for their support in the projects - my committee members: Anna Fails, Bret Smith, Kim Hoke, and Bob Handa; our collaborators both at CSU and the University of Cincinnati: Adam Chicco, Chris Gentile, Greg Amberg, Rachel Morano, and Lawson Wuslin; and the DVM-PhD directors: Dan Regan, Anne Avery, Sue VandeWoude, and Ed Hoover. Importantly, I would like to thank Dan Regan for the advice and coffee throughout this time. Additionally, the support network of other DVM-PhD students is a vital part of thriving throughout this process.

These projects were supported by NIH funding sources: F30 OD032120 to C. Dearing, T32 GM136628 to the DVM-PhD program, and R01 HL150559 to B. Myers.

Finally, I would like to thank my family and friends for their support throughout my career. Their support has made my success possible and has given me the foundation to handle the challenges this program affords. Most importantly, I would like to thank my husband, Tommy Dearing, for all that he does, including technical support.

TABLE OF CONTENTS

CHAPTER 1: SEX DIFFERENCES IN AUTONOMIC RESPONSES TO STRESS: IMPLICATIONS FOR CARDIOMETABOLIC PHYSIOLOGY[1]

1. Introduction

Chronic stress exposure is increasingly prevalent in modern society. Whether interpersonal, economic/occupational, sociocultural, environmental, or a combination of these, stress is a fundamental part of daily life for many people. Subsequently, chronic stress is a significant contributor to cardiometabolic and psychiatric disorders including the global leading causes of death, cardiovascular disease (1, 2), and years lived with disability, depression (3). While the detrimental effects of stress are well documented, the majority of physiological studies have been conducted in males. Emerging evidence indicates that females respond to stress differently (4); therefore, this review focuses on the current understanding of how sex impacts stress-related physiologic outcomes.

Stress can be operationally defined as any real or perceived stimulus that challenges homeostasis or well-being (5) and results in both perception and subsequent physiologic responses (6). Exposure to acute stress initiates a homeostatic response that promotes adaptation (5, 7). However, chronic stress, defined as long-term exposure to real or perceived threats leading to repeated activation of physiologic systems, can tax adaptive capacity (8, 9). While chronic exposure to stressors and subsequent allostatic load have increased in society (10), certain populations are impacted to a greater extent than others. In particular, socioeconomic disadvantage associates with increased perceived stress (11, 12), higher

[1]Dearing, C., Handa, R. J., & Myers, B. (2022). Sex differences in autonomic responses to stress: implications for cardiometabolic physiology. American Journal of Physiology-Endocrinology and Metabolism, 323(3), E281-E289.

allostatic load (13), flattened diurnal cortisol profiles (14), inflammation (15), changes in DNA methylation (16), and, consequently, increased risk of psychiatric (17), cardiovascular (18, 19), and metabolic disease (20).

Metabolic syndrome is characterized by a set of clinical signs including insulin resistance, hyperlipidemia, abdominal obesity, and hypertension that creates predispositions for type-two diabetes mellitus and cardiovascular disease (21). While the development of metabolic disease is multifactorial, stress is widely recognized as a causative agent (22). Specifically, chronic stress positively correlates with the development of metabolic syndrome in both children (20, 23) and adults (24). Similarly, chronic stress worsens the progression of cardiovascular disease (25).

Cardiometabolic disorders are frequently co-morbid with mood disorders (3). Additionally, the reciprocal relationship between cardiometabolic and depressive disorders further contributes to years lived with disability (3, 26). While depressive disorders are also complex and multifactorial, chronic stress commonly exacerbates mood symptoms (27). In addition, depression has inflammatory and immunomodulatory components related to increased cortisol (28, 29). Importantly, mood and cardiometabolic comorbidity disproportionately affect females (30). However, basic physiologic investigations into the consequences of chronic stress have only recently taken female subjects into account.

2. Autonomic and endocrine stress responses

The autonomic nervous system (ANS) modulates the physiology of organ systems to maintain homeostasis through the integration of sympathetic norepinephrine and vagal parasympathetic acetylcholine signaling (31). In response to stressors, the ANS prepares the body to respond to real or perceived threats. The prototypical acute stress response is

characterized by rapid activation of the sympathetic nervous system to prime the body for action, resulting in a wide range of physiologic changes including: epinephrine and norepinephrine release, increased heart rate and respiration, glucose mobilization, peripheral vasodilation, and visceral vasoconstriction (32).

The hypothalamic-pituitary-adrenal (HPA) axis aids in homeostatic regulation of stress responses over a longer timeframe through the release of glucocorticoids (cortisol in humans, corticosterone in rats and mice) from the adrenal cortex (9). Broadly, glucocorticoids act to increase gluconeogenesis through the promotion of a catabolic state that is essential for stress responding (5). The HPA axis response is initiated by corticotropin releasing hormone (CRH) neurons in the paraventricular hypothalamus. CRH then acts on the anterior pituitary to cause the release of adrenocorticotropic hormone (ACTH), which stimulates synthesis and release of glucocorticoids from the adrenal cortex into systemic circulation. Glucocorticoids then bind mineralocorticoid (MR) and glucocorticoid receptors (GR) to inhibit further release of CRH via negative feedback. Further, HPA axis activity is regulated through multiple mechanisms including descending neural inputs (33), the recruitment and synchronicity of CRH neurons during acute stress (34), and rhythmicity on both ultradian and circadian timescales (35). Importantly, acute autonomic and endocrine stress responses dynamically interact to integrate physiologic states and promote adaptation.

In contrast to adaptive acute stress responses, chronic stress produces different physiologic outcomes, both autonomically and hormonally. Chronic stress leads to prolonged sympathetic stimulation, vagal withdrawal, and subsequent autonomic imbalance. Dysregulation of sympathetic/parasympathetic balance results in cardiovascular changes including baroreflex blunting (36), reduced heart rate variability (37), decreased blood pressure variability (38), and diminished neurovascular coupling (39). Importantly, chronic stress-induced autonomic imbalance is impacted by hormonal signaling. For example, inhibition of CRH receptors 1 and 2

in the limbic bed nucleus of the stria terminalis increases arterial pressure and impairs baroreflex (40). Chronic stress also leads to prolonged HPA axis activation which can manifest in adrenal hyperplasia and hypertrophy, suggesting greater cumulative exposure to glucocorticoids and epinephrine (41). While chronic stress disrupts glucocorticoid rhythmicity, multiple studies have reported differing effects on diurnal cortisol profiles. A flattening of diurnal cortisol curves is common (42); however, a study of chronic stress in adolescents found that those with the highest genetic risk for HPA axis-linked disease, such as mood disorders, had a pattern of lower morning cortisol coupled with a flatter diurnal curve. Those with lower genetic risk had elevated morning cortisol and a steep diurnal curve. Ultimately, these variable outcomes indicate a genetic component to the consequences of chronic stress (43).

3. Gonadal hormones: estrogens and progesterone

Historically, rodent stress research has focused largely on male subjects or has not considered the effect of sex on physiological outcomes. Therefore, sex-dependent autonomic regulation during chronic stress is an emerging area for understanding sex differences in disease incidence, as well as potential clinical targets. While the rate of metabolic syndrome is similar in males and females (44), females are at greater risk for developing cardiovascular and depressive disorders despite high variability in the prevalence of these disorders across the lifespan (45, 46). In addition to cardiovascular disease being the primary cause of death in women (47), women are at twice the risk for developing major depressive disorder (48). Underscoring these disease predilections are a number of uniquely female experiences including pregnancy, parturition, and conditions, like polycystic ovarian syndrome, that affect female reproductive physiology (30, 49).

Although female sex hormones, centrally estrogens and progesterone, are not unique to females, they are cyclically variable due to menstrual or estrous cycling and change with age. Evidence suggests that female-specific responses to stress are cycle phase-dependent with greater HPA axis reactivity in early proestrus, a period characterized by high estrogens and low progesterone (50). The effects of estrogens are primarily mediated by three estrogen receptors (ERs): ERα, ERβ, and g-protein coupled ER (GPER). While there are several estrogens that bind ERs, estradiol predominates in cycling females and estrone predominates following reproductive senescence (51). The production of estradiol primarily occurs through the aromatization of testosterone. Progesterone effects are mediated by intracellular and membrane-bound progesterone receptors (PRs) and $GABA_A$ receptors. Importantly, ERs and PRs are found throughout the body (**Fig. 1**) and have wide-reaching effects on most physiologic systems (52–56). Generally, estrogens are thought to convey protective cardiometabolic effects in females (57–64), as well as males (65, 66). While many of these effects are activational and life-stage dependent, there is also evidence of sex-dependent organizational effects of steroid hormones (67). Sex steroid receptors are also found in select cells throughout the brain and gonadal hormone action in the central nervous system is an ongoing field of study.

Importantly, neurons that activate autonomic and endocrine stress responding are regulated by a network of cortical and limbic structures, allowing for emotional-regulatory regions to modulate stress responses (68). Ovarian hormones have widespread effects on the activity of these corticolimbic regions, potentially accounting for sex differences in stress physiology (69, 70). In fact, estradiol administration in ovariectomized female rats mediates chronic stress-induced morphological plasticity (71) and brain-derived neurotrophic factor expression in the prefrontal cortex (72), a region that has sexually divergent modulatory effects on HPA axis, cardiovascular, and glucoregulatory stress responses (73). Interestingly, a study of gonadectomized and intact rats found that chronically stressed ovariectomized females had

increased plasma estradiol compared to unstressed controls (74), suggesting that extra-ovarian estradiol synthesis may be recruited by chronic stress. Further, aromatase-dependent ERα signaling in the prefrontal cortex of ovariectomized female rodents prevents neurobehavioral changes following repeated stress (75).

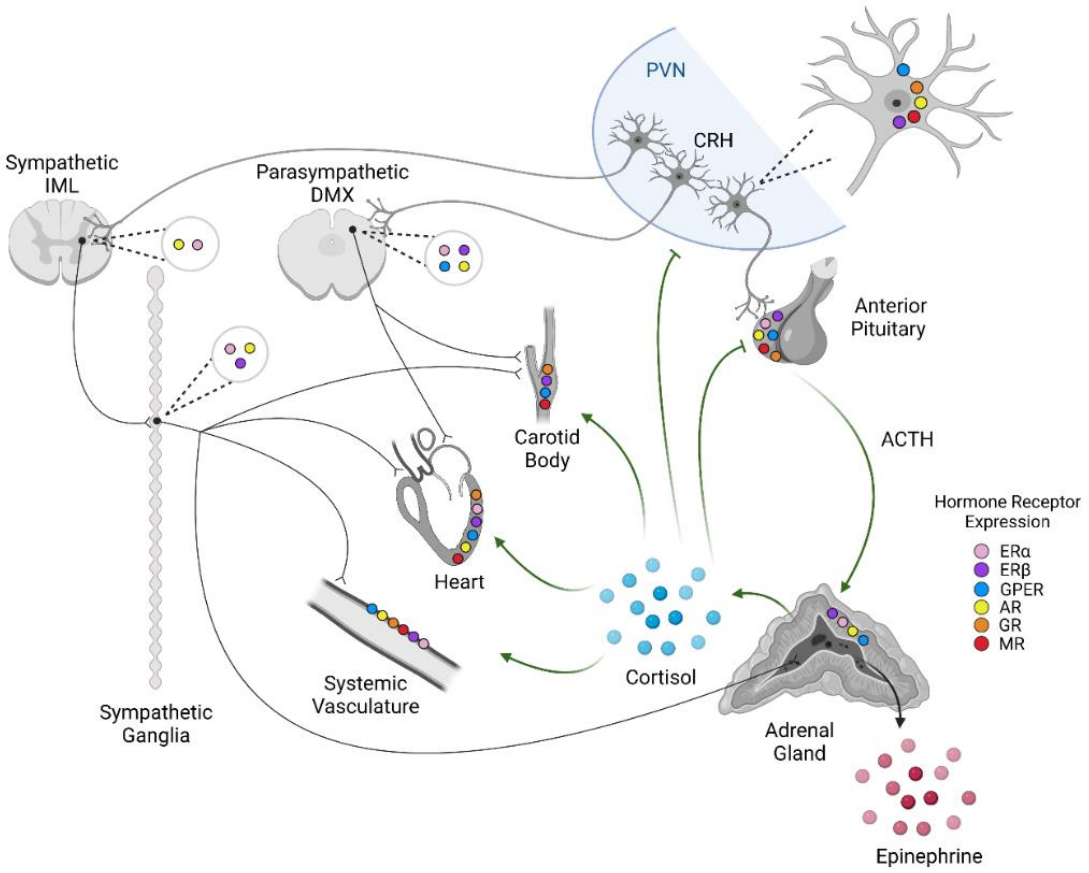

Figure 1: Stress and gonadal hormone receptor expression across neuroendocrine and cardiovascular organs. CRH neurons in the paraventricular nucleus (PVN) of the hypothalamus initiate both autonomic and HPA axis responses to stress. CRH acts on anterior pituitary corticotropes to cause the release of ACTH and the subsequent synthesis and release of glucocorticoids (cortisol in humans, corticosterone in rats and mice) from the adrenal cortex. Glucocorticoids have systemic action on cardiovascular responses and provide negative feedback on the PVN and anterior pituitary. CRH neurons also synapse in the sympathetic intermediolateral nucleus (IML) and the parasympathetic dorsal motor nucleus of the vagus (DMX). Efferents of the DMX innervate both the carotid body and heart to influence cardiac and baroreflex activity but are generally not found in the systemic vasculature. Efferents of the IML

act through sympathetic ganglia to stimulate cardiovascular activity and the release of epinephrine from the adrenal medulla, which acts systemically. Additionally, stress and gonadal hormone receptors regulate activity in a tissue-dependent manner. It is important to note that receptor distribution has not been completely characterized and further study is warranted. Thus, the absence of reports on expression does not indicate that receptors are not present. CRH neurons express estrogen receptors β (ERβ), G protein-coupled estrogen receptor (GPER) (76), and androgen receptors (AR) (77), as well as glucocorticoid receptors (GR) (78) and mineralocorticoid receptors (MR) (79). Similarly, the anterior pituitary expresses ERα, ERβ (80), GPER (81), AR (82), GR, and MR (83). The adrenal cortex expresses ERα, ERβ, GPER, and AR (84). The IML is known to express ERα (85) and AR (86). The DMX shows ERα, ERβ (87), GPER (88), and AR (86) expression. Sympathetic ganglia express ERα, ERβ (89), and AR (90). Cardiac tissue (91–93) and systemic vasculature (94–98) express ERα, ERβ, GPER, and AR, as well as GR and MR. The carotid body shows ERβ (99), GPER (100), GR (101), and MR expression (102). While many of the mechanistic interactions are yet to be elucidated, the integration of these systems modulates stress responses in sex-, age-, and tissue-dependent manners that impact the physiologic outcomes of chronic stress. Created with BioRender.com.

The hippocampus, a key limbic structure that moderates stress responding (103), is also a site of estrogen action. Hippocampal ERα agonism is protective against chronic stress-induced depressive behaviors in female rats (104). Thus, potential protective effects of central nervous system ERα signaling against the negative outcomes associated with chronic stress require further exploration. There is also sexual dimorphism in the hypothalamic rostral anteroventral periventricular nucleus which expresses CRH receptor 1 in female but not male mice (105). These cells also co-express both ERα and GR, indicating the presence of a sex-specific stress hormone-responsive nucleus in female mice that may contribute to sexually-divergent homeostatic responses (105). Additionally, injection of estradiol into the nucleus of the solitary tract or rostral ventrolateral medulla, brainstem preautonomic nuclei, of ovariectomized rats enhances baroreflex sensitivity and reduces arterial pressure (106). Further, in both the paraventricular nucleus and rostral ventrolateral medulla, ERβ, but not ERα, contributes to protection against aldosterone/salt-induced hypertension in female rats (107). Thus, ovarian hormones act in multiple brain regions in a receptor-specific manner to modulate cardiovascular physiology.

The sexually dimorphic distribution of gonadal steroid receptors and their activation by circulating estrogens impacts the development of hypertension, likely through sympathoinhibitory effects (108). This is supported by the increase in hypertension seen in postmenopausal women compared to premenopausal women that is, in part, due to a loss of the protective effects of estrogens, centrally estradiol (109). These protective effects are also seen following chronic stress. Chronically stressed cycling female rats maintain vasoactive metabolite profiles, higher NO and lower H_2O_2, and vascular reactivity compared to both chronically stressed ovariectomized female and male rats. Thus, ovarian hormones mitigate the proinflammatory and prooxidant effects of chronic stress that mediate vascular dysfunction (110).

Taken together, sex-specific physiologic responses to chronic stress are impacted by the organizational and activational actions of sex steroids. These responses are integrated across neuroendocrine, autonomic, and cardiovascular systems. This places additional importance on determining how these interactions are mediated and how they affect long-term health outcomes in both females and males.

4. Gonadal hormones: testosterone

Although testosterone is not unique to males, it plays an important role in male-specific responses to chronic stress. The central effects of androgens are mediated by androgen receptors (AR) by binding either testosterone or dihydrotestosterone. Generally, androgens are protective against the development of metabolic syndrome, while male testosterone deficiency associates with signs of metabolic dysfunction such as insulin resistance (111). Further, hypotestosteronemia in rats, via orchidectomy, leads to a progressive rise in systolic and diastolic blood pressure that is reduced by the administration of exogenous androgens (112).

The anti-hypertensive effects of endogenous testosterone in male rats are mediated by estrogen-independent genomic and non-genomic mechanisms that reduce kidney renin-angiotensin expression and subsequently reduce fluid retention and increase systemic vasodilation (113). Additionally, androgen deficiency is thought to increase the risk of hypertension through increased visceral adiposity, which promotes chronic inflammation that contributes to endothelial dysfunction and hypertension. This cardiometabolic susceptibility is seen in both men and postmenopausal women, who have a reduction in adrenal and ovarian androgens (114). Similarly, testosterone prevents the development of depressive-like symptoms. For instance, testosterone treatment following chronic variable stress reduces passive coping behaviors as well as basal corticosterone and adrenal mass (115). However, research on the mechanistic consequences of AR signaling during chronic stress is limited with more work needed to determine the basis for cardiometabolic regulation.

While causal effects of androgens on autonomic stress regulation are not well understood, chronic stress decreases expression of the cytochrome P450 protein CYP11A1, subsequently reducing testosterone (116). The reduction in testosterone may play a role in male neuroendocrine regulation, including glucocorticoid secretion, as testosterone inhibits HPA axis stress responses in male rats. Specifically, implantation of testosterone in the hypothalamic medial preoptic area reduces ACTH responses to acute stress, an effect that may be mediated through AR or ER due to the presence of aromatase. Additionally, elevated testosterone increases GR binding in the medial preoptic area, possibly contributing to negative feedback inhibition of the HPA axis (117). Taken together, reduced testosterone following chronic stress likely factors into HPA axis dysregulation. However, it is unclear how cardiovascular outcomes may be impacted.

5. Sex differences in autonomic integration

In addition to the acute actions of gonadal hormones, sex differences in stress responding may also arise from organizational and/or chromosomal effects that lead to variations in autonomic signaling. This is particularly evident in cardiovascular physiology. While blood pressure and muscle sympathetic nerve activity are directly related in males, these two physiologic measures are unrelated in actively cycling young women (118). This is attributed to increased β-adrenergic relative to α-adrenergic activity. However, postmenopausal women show the positive relationship between blood pressure and muscle sympathetic nerve activity observed in males. Further, premenopausal women undergoing an acute stress event such as maximal exercise have cardioprotective effects that originate from lower resting sympathetic tone and a more rapid vagal response compared to age-matched males (119). Additionally, women have increased parasympathetic activity in response to acute painful stimuli compared to men (120).

Generally, vagal activity increases heart rate variability and lowers both heart rate and blood pressure. However, this regulation varies across sex, cycle, and life stage. In females, cycle phases characterized by low estrogens are associated with increased basal heart rate and arterial pressure, as well as decreased baroreflex sensitivity (121). Conversely, high estrogenic phases are associated with increased cardiovascular autonomic modulation (121). Postmenopausal women also show decreased vagal responses and heart rate variability (122, 123) that are reversed by estrogen replacement therapy (124). Interestingly, vagal activity influences β-adrenergic signaling in the rat hippocampus (125), indicating that interplay of both central and peripheral neural activation may contribute to the cognitive and vascular protective effects of estrogens. It remains to be determined how these protective effects impact responses to chronic stress; although, recent studies found cycling female rats were resilient to cardiac hypertrophic remodeling (73), and baroreflex impairment following chronic stress

(126).Additionally, female rodents show decreased vascular impairment (110), and resilience to systemic vascular inflammation following chronic stress (127).

Autonomic imbalance also impacts immune regulation. Importantly, inflammatory cytokines have been proposed to link cardiovascular and mood outcomes (128). Further, the regulation of interleukin-1 beta during chronic stress, an inflammatory cytokine elevated in depressive disorders (129) and chronic stress (130), is influenced by β-adrenergic signaling in male, but not female rats (131).Moreover, chronic stress enhances immune reactivity in a sex-dependent manner whereby male rats have excessive innate immune signaling and females show excessive hippocampal immune reactivity (132). Additionally, intact female rats exposed to social defeat stress also show increased interleukin-1 beta in the central amygdala and circulation plasma cytokines (133). These sex-dependent changes, among others, are indicative of broad differences in HPA axis activity and sympatho-vagal balance, likely accounting for sex differences in behavior and physiology.

While a large body of literature indicates that chronic stress sensitizes male HPA axis stress responses to promote glucocorticoid hypersecretion (9), recent studies in female rodents have yielded equivocal results (126). A study focusing on the effects of chronic stress in adolescent rats found that female rats had enhanced HPA axis stress reactivity in adulthood that was attenuated by a GR modulator (134). However, a similar adolescent chronic stress study found decreased HPA axis activation in adult female rats (135). More recently, a longitudinal rodent study found that, compared to male littermates, chronically-stressed female rats have increased HPA axis responses to both psychological and glycemic stressors, as well as impaired glucose tolerance (4). Further, the enhanced glucocorticoid responses to glycemic stress persisted into late adulthood. Taken together, the data to date suggest that chronic stress results in numerous sex-specific physiological changes linked to endocrine and autonomic dysregulation that impact long-term health and disease susceptibility. Conflicting results across

studies indicate that our current understanding of female endocrine regulation during and after chronic stress is incomplete. Additional studies to parse organizational, reproductive cycle, and life-stage effects are likely to uncover significant new information about basic stress biology.

6. Implications

The study of sex-specific autonomic responses to stress is a developing area with many unanswered questions. Determining the underlying mechanisms that promote sex-specific differences in disease occurrence is essential for improving clinical outcomes and may lead to targeted sex-specific preventative care. Additionally, these physiological processes have broad implications for aging pre-, peri-, and post-menopausal women, particularly those with higher allostatic loads due to adverse life events. The higher female incidence of comorbid cardiometabolic and mood disorders, coupled with sexually dimorphic responses to stress, are hypothesized to contribute to increased risk of Alzheimer's disease, which also disproportionately affects women (136). Thus, understanding how the endocrine and autonomic consequences of chronic stress affect health across the lifespan is highly important for improving cardiovascular, metabolic, emotional, and cognitive outcomes.

CHAPTER 2: GLUCOREGULATION AND COPING BEHABIOR AFTER CHRONIC STRESS IN RATS: SEX DIFFERENCES ACROSS THE LIFESPAN[2]

1. Introduction

The neuroendocrine stress response, initiated by threats to homeostasis (7), is essential for mobilizing energy necessary for adaptation and survival (5). However, dysregulated or prolonged stress responses are linked to cardiometabolic dysfunction and neuropsychiatric disorders (8). Globally, metabolic dysfunction contributes to leading causes of death such as cardiovascular disease (1) and diabetes mellitus (2). Additionally, metabolic and depressive disorders have a bi-directional relationship, further contributing to years lived with disability (3, 26).

While the development of metabolic dysfunction is multifactorial, stress is widely recognized as a causative agent (22). Central stress responses influence the neuroendocrine hypothalamic-pituitary-adrenal (HPA) axis, as well as the sympathetic-adrenal-medullary (SAM) axis. Thus, stressful events initiate a cascade of neural and endocrine responses that mobilize energy to alter both physiologic and psychologic states (137). Aberrant activation of these systems by prolonged early life stress is linked to the development of metabolic dysfunction in adulthood (138, 139), as well as psychiatric conditions, including depressive disorders (140, 141). In rodent models, chronic early-life stress increases HPA axis reactivity (139, 142) and impairs neuronal survival and cognition in adulthood (143). Additionally, chronic variable stress (CVS) in young adult rats increases fasting insulin and corticosterone in males (144).

[2]Dearing, C., Morano, R., Ptaskiewicz, E., Mahbod, P., Scheimann, J. R., Franco-Villanueva, A., Wulsin, L., & Myers, B. (2021). Glucoregulation and coping behavior after chronic stress in rats: Sex differences across the lifespan. Hormones and behavior, 136, 105060.

Although pre-clinical studies have found immediate and long-term effects of early life stress on cognitive function (143, 145–149) and endocrine stress reactivity (139, 150–152), these studies have largely focused on males. While there are significant sex differences in the development of psychiatric disorders (153, 154), we are just beginning to learn how biological sex impacts behavioral and metabolic health. Further, studies examining potential sex differences in coping and HPA axis responses after stress in adolescence have generated equivocal results (134, 135), possibly related to group variation and/or timing of assessments.

In the current study, we employed a longitudinal design to test the hypothesis that females may have differential behavioral and metabolic susceptibility to adolescent chronic stress. Furthermore, we sought to examine how early life measures may predict an individual's behavioral and endocrine outcomes later in life. To this end, we assessed the effects of chronic stress during adolescence on coping behavior and glucoregulation in a large cohort of male and female rats both immediately following stress exposure and at 15 months of age. This approach permitted the analysis of stress, sex, and age interactions on coping behaviors, as well as glucocorticoid and glucose responses to psychological and physiological challenges.

2. Methods

2.1 Subjects

Rats were kept on a 12 on 12 off light-dark cycle. Males were kept on a 6:00-18:00 cycle and females were kept on a 9:00-21:00 cycle to maintain the same circadian time during experimentation. Specifically, male assessments were done prior to female assessments on the same day, with both occurring at the same relative time of the light cycle for each sex. Food and water were available *ad libitum*. All experiments were approved by the Institutional Animal Care and Use Committee of the University of Cincinnati (protocol 04-08-03-01) and complied with the

National Institutes of Health Guidelines for the Care and Use of Laboratory animals. All rats had daily welfare assessments by veterinary and/or animal medical service staff.

2.2 Design

As illustrated in **Fig. 2**, a single cohort of rats was generated through in-house breeding of 12 litters of 10 Sprague-Dawley rats each to produce 120 pups (60 rats/sex). Pups were cross fostered as necessary to maintain uniform litter size and equal sex distribution (5 pups/sex/litter). All pups were weaned at postnatal (PN) day 24. At 5 weeks of age, pups were separated into treatment-specific same sex pairs so that 3 rats/sex/litter were assigned to the CVS group and 2 rats/sex/litter were assigned to No CVS. Pairings were randomized and not limited to littermates. In total, 36 rats/sex were exposed to CVS and 24 rats/sex remained as unstressed controls. All rats were handled regularly with body weight monitored throughout the course of the experiment. Males and females were housed separately in adjacent rooms with light cycles shifted so that all stressors and assessments occurred at the same time each day for both sexes. Due to the scale of the experiment, equal portions of all 4 groups went through sample collection and testing on consecutive days. CVS began at PN 43 with baseline blood samples taken 14 days later. After 20 days of CVS, rats went through the forced swim test (FST) followed 3 days later by a fasted glucose tolerance test (GTT). These early assessments were considered the ‘young’ phase for analyses. Rats then aged for 13 months prior to another baseline blood sample, FST, and GTT. Tissues were then collected for analysis 3 days later at just over 15 months of age. Assessments from this period were considered ‘aged’ for analysis.

2.3 CVS

Exposure to CVS began at PN 43, which is considered late adolescence (142). CVS continued for 20 days to include the transition to adulthood. Rats were exposed to stressors

twice daily (AM and PM) presented in a randomized manner (142, 155, 156). Stressors included restraint (plexiglass tube, 30 min), shaker (100 RPM, 1 hr), damp bedding (1 hr), cold room (4 ˚C, 1 hr), and hypoxia (8% oxygen, 30 min). Rats were also exposed to overnight stressors twice a week. These included housing with an unfamiliar cage mate and single housing for social instability and social isolation, respectively.

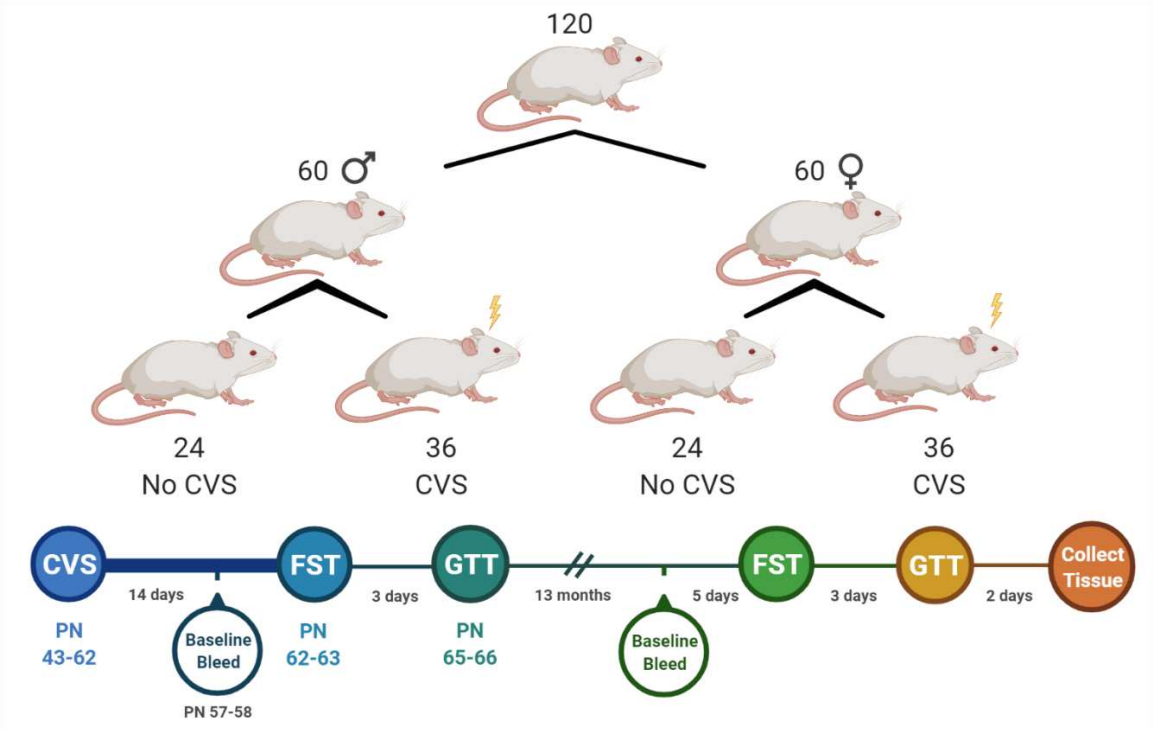

Figure 2: Experimental design and timeline. A single cohort of rats was separated into 4 experimental groups consisting of male and female unstressed controls (No CVS, n = 24/sex) and chronically stressed males and females (CVS, n = 36/sex). These groups underwent endocrine and behavioral assessments immediately following CVS. After aging for 13 months, they were re-tested prior to tissue collection. Created with BioRender.

2.4 Blood collection and analysis

Blood samples (approximately 100 µL) were collected by tail clip in tubes containing 10 µL of 100 mmol/L ethylenediamine tetraacetate (155). Baseline blood was collected on the morning of day 15 in the CVS paradigm prior to daily stressors. Following CVS, rats were

exposed to novel acute stressors that acted as psychologic (FST) and glycemic (GTT) challenges. All 3 assessments (baseline, FST, and GTT) were repeated 13 months later. Blood glucose was determined from tail blood using Bayer Contour Next glucometers and test strips (Ascensia, Parsippany, NJ). Collected blood samples were centrifuged at 3000× g for 15 minutes at 4°C and plasma was stored at -20°C until analysis. Triglyceride and cholesterol levels were determined by the Mouse Metabolic Phenotyping Center at the University of Cincinnati. Plasma corticosterone was measured using an ENZO Corticosterone ELISA (ENZO Life Sciences, Farmingdale, NY) with an intra-assay coefficient of variation of 8.4% and an inter-assay coefficient of variation of 8.2% (157).

2.5 FST

The FST was used as psychological stressor to assess active versus passive coping (158) and endocrine reactivity. As previously described (159), rats were placed in an open-top cylinder (61 cm high x 19 cm diameter) filled with 40 cm of water (23-27 ˚C, 10 minutes). Behavior was recorded with an overhead mounted camera and scored by a blinded observer. The video was analyzed every 5 s for observations of immobility (passive coping) or activity (swimming, climbing, and diving). Additionally, blood was collected at 15, 30, 60, and 120 minutes after the beginning of FST. For females, vaginal swabs were taken after each FST and analyzed for estrous phase by blinded observers.

2.6 GTT

Three days after the FST, rats were fasted for 4 hours prior to a GTT to assess glucose homeostasis and glucocorticoid responses to glycemic challenge (160, 161). A baseline blood sample was collected prior to glucose injection (1.5 g/kg, 20% glucose, i.p.). Blood was then

collected at 15, 30, 45, and 120 minutes post injection. For females, vaginal swabs were taken after each GTT and analyzed for estrous phase by blinded observers.

2.7 Tissue collection

Two days after the final GTT, rats were rapidly anesthetized (5% inhaled isoflurane) and euthanized via rapid decapitation. Mesenteric white adipose tissue (mWAT), inguinal white adipose tissue (iWAT), and adrenal glands were collected and weighed. mWAT was collected to sample visceral adiposity and iWAT to sample subcutaneous adiposity (162, 163). All raw organ weights were corrected for bodyweight.

2.8 Data analysis

Data are expressed as mean ± standard error of the mean. All rats were included in all analyses. All data were analyzed using Prism 8 (GraphPad, San Diego, CA), with statistical significance set at $p < 0.05$ for all tests. Body weight during CVS, as well as plasma corticosterone and blood glucose during FST and GTT were analyzed by 3-way mixed effects analysis with sex, stress condition, and time (repeated) as factors. For significant main or interaction effects, Tukey multiple comparison post-hoc tests were used to compare groups at specific times. Baseline plasma measures, FST behavior, hormonal area under the curve (AUC), aged body weight, and organ weights were analyzed with 2-way ANOVA with sex and stress condition as factors. In the case of main or interaction effects, Tukey multiple comparison post-hoc tests were employed. For inclusion in corticosterone AUC analysis, all time points for each rat were required. Thus, if a blood sample at one time point was of insufficient volume for analysis, that subject was excluded from the AUC calculation. Within-group data were compared across life stages by 1-way ANOVA with age as a factor followed by Tukey multiple comparison post-hoc tests. Additionally, partial eta squared (η_p^2) was calculated as a measure of effect size

following all ANOVA or mixed effects analyses. Pearson correlation two-tailed analyses were run to examine associations between young and aged data within each group. To compare associations across groups, Fisher transformed r values were compared by two-tailed analyses.

3. Results

3.1 Body weight and baseline plasma measures during CVS

Body weight analysis over the course of CVS (**Fig. 3A**) found main effects of sex [$F(1, 116) = 480.5$, $p < 0.0001$, $\eta_p^2 = 0.796$], CVS [$F(1, 116) = 6.866$, $p = 0.01$, $\eta_p^2 = 0.052$], and day [$F(1.590, 184.5) = 3216$, $p < 0.0001$, $\eta_p^2 = 0.611$], as well as sex x day [$F(5, 580) = 341.7$, $p < 0.0001$, $\eta_p^2 = 0.143$] and CVS x day [$F(5, 580) = 4.439$, $p < 0.0006$, $\eta_p^2 = 0.002$] interactions. Post-hoc testing indicated that males had greater body weight than females within stress conditions on all days. Although CVS x day interactions were present across sexes, no significant effects of CVS were observed within sex on specific days. Baseline corticosterone (**Fig. 3B**) had main effects of sex [$F(1, 113) = 10.19$, $p = 0.0018$, $\eta_p^2 = 0.085$] and CVS [$F(1, 113) = 5.410$, $p = 0.0218$, $\eta_p^2 = 0.047$]. Post-hoc analysis found that, within CVS, females had greater ($p < 0.01$) corticosterone than males. Although, the CVS effect in females was not significant ($p < 0.07$). Triglycerides (**Fig. 3C**) showed effects of sex [$F(1, 114) = 92.19$, $p < 0.0001$, $\eta_p^2 = 0.453$] and sex x CVS interaction [$F(1, 114) = 6.161$, $p = 0.0145$, $\eta_p^2 = 0.052$]. Specifically, males had higher triglycerides than females ($p < 0.0001$) in both stress conditions and CVS decreased ($p < 0.05$) triglycerides in females. For plasma cholesterol (**Fig. 3D**), there was a main effect of sex [$F(1, 114) = 17.61$, $p < 0.0001$, $\eta_p^2 = 0.136$] where females had elevated cholesterol ($p < 0.05$) compared to males in both stress conditions. Taken together, these data indicate stress-independent sex differences in triglyceride and cholesterol regulation while CVS increases corticosterone and lowers triglycerides in females.

3.2 Young FST

Behavior during the FST was quantified to determine coping responses to acute psychological stress. Immobility (**Fig. 4A**), a passive behavioral response, showed effects of sex [$F(1, 116) = 32.06$, $p < 0.0001$, $\eta_p^2 = 0.216$] and CVS [$F(1, 116) = 3.944$, $p = 0.0494$, $\eta_p^2 = 0.032$] where females were more immobile ($p < 0.01$) than males in both stress conditions. Although there was a main effect of CVS, within sex there were no significant differences in immobility (males $p = 0.061$). No significant sex or stress effects were found for climbing or diving behaviors; however, swimming (**Fig. 4B**) showed both sex [$F(1, 116) = 16.62$, $p < 0.0001$, $\eta_p^2 = 0.151$] and CVS [$F(1, 116) = 8.895$, $p = 0.0035$, $\eta_p^2 = 0.087$] effects. Post-hoc analysis found that, in the No CVS groups, females had less ($p < 0.01$) swimming behavior. CVS decreased swimming in males ($p < 0.05$) with no significant difference ($p = 0.078$) from females.

Corticosterone (**Fig. 4C**) was measured to determine sex and stress effects on HPA axis reactivity to an acute behavioral challenge. Although all other data are represented by n = 24/sex No CVS and n = 36/sex CVS, a shipping error resulted in lost blood samples for the young FST corticosterone measurement (1/4 randomly across all groups and time points). Consequently, the reduced sample sizes are: n = 10-24 male No CVS, n = 12-24 female No CVS, n = 17-36 male CVS, and n = 18-36 female CVS. Mixed effects analysis found main effects of sex [$F(1, 116) = 32.16$, $p < 0.0001$, $\eta_p^2 = 0.182$], CVS [$F(1, 116) = 55.03$, $p < 0.0001$, $\eta_p^2 = 0.281$], and time [$F(2.413, 174.3) = 462.2$, $p < 0.0001$, $\eta_p^2 = 0.782$] with sex x time [$F(4, 289) = 11.79$, $p < 0.0001$, $\eta_p^2 = 0.127$] and CVS x time [$F(4, 289) = 13.77$, $p < 0.0001$, $\eta_p^2 = 0.098$] interactions. Post-hoc analysis indicated CVS females had higher corticosterone than

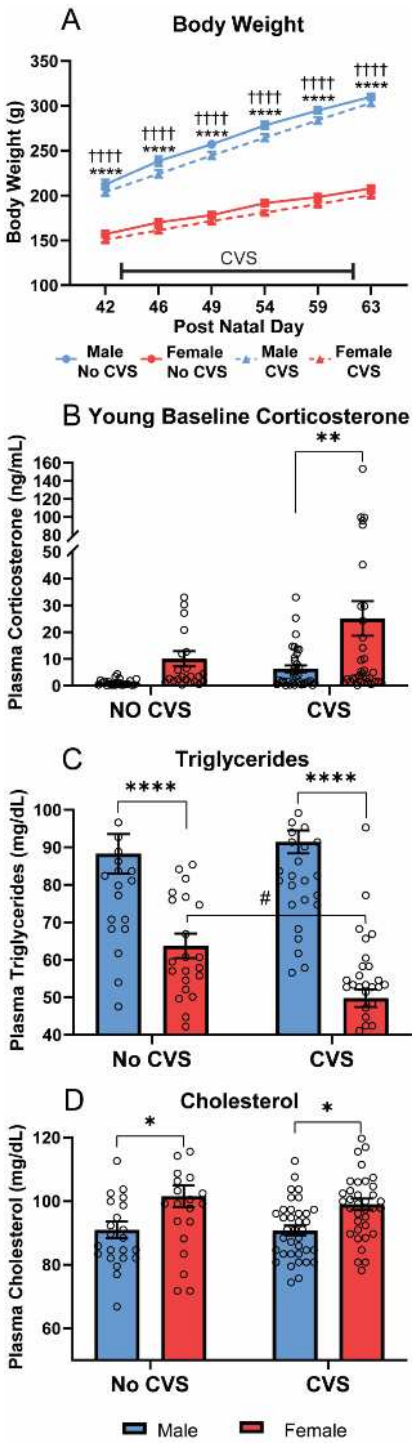

Figure 3: Young metabolic measures. Body weight was measured throughout the course of CVS for both CVS (n = 36/sex) and No CVS (n = 24/sex) controls (**A**). On the morning of CVS day 14, a baseline blood sample was taken to determine plasma corticosterone (**B**), plasma triglycerides (**C**), and plasma cholesterol levels (**D**). Data are expressed as mean ± SEM. * represents sex differences within stress condition, # represents CVS effects within sex, † represents sex differences within CVS over time. *,# $p < 0.05$, ** $p < 0.01$, and ****,†††† $p < 0.0001$.

CVS males 15 min post-FST, while CVS increased corticosterone ($p < 0.05$) in males at 30 and 60 min. Additionally, females had higher corticosterone ($p < 0.01$) at the 90 min recovery time point. AUC analysis of cumulative corticosterone exposure during the FST (**Fig. 4D**) found effects of sex [$F(1, 48) = 11.95$, $p = 0.0012$, $\eta_p^2 = 0.219$] and CVS [$F(1,48) = 27.49$, $p < 0.0001$, $\eta_p^2 = 0.392$]. Specifically, CVS increased total corticosterone ($p < 0.05$) in both sexes but to a greater extent ($p < 0.01$) in females than males.

Glucose mobilization is a component of the stress response reflecting metabolic integration of sympathetic-mediated glucagon release, gluconeogenesis, and glycogenolysis, in addition to longer-term glucocorticoid effects on gluconeogenesis and glycolysis (32, 164). FST exposure (**Fig. 4E**) led to effects of sex [$F(1, 116) = 44.30$, $p < 0.0001$, $\eta_p^2 = 0.175$] and time [$F(2.47, 284.4) = 151.8$, $p < 0.0001$, $\eta_p^2 = 0.379$], with sex x time [$F(3, 346) = 59.55$, $p < 0.0001$, $\eta_p^2 = 0.190$] and CVS x time [$F(3, 346) = 10.74$, $p < 0.0001$, $\eta_p^2 = 0.044$] interactions. From 15-60 min, females had lower ($p < 0.05$) blood glucose than males regardless of stress condition. This was reflected by significant sex effects [$F(1,114) = 48.94$, $p < 0.0001$, $\eta_p^2 = 0.304$] in the AUC analysis (**Fig. 4F**). Collectively, the young FST data indicate that, compared to males, females more passively cope with behavioral challenge and have greater CVS-induced glucocorticoid hypersecretion.

3.3 Young GTT

The GTT was utilized to examine sex and CVS effects on glucose tolerance, as well as glucocorticoid responses to a systemic hyperglycemia stressor. Blood glucose responses to i.p. glucose (**Fig. 5A**) had effects of time [$F(2.41, 279.1) = 387.8$, $p < 0.0001$, $\eta_p^2 = 0.667$], sex x CVS [$F(1, 116) = 5.15$, $p = 0.025$, $\eta_p^2 = 0.017$],sex x time [$F(4, 464) = 12.10$, $p < 0.0001$, $\eta_p^2 = 0.058$], and sex x CVS x time [$F(4, 464) = 2.796$, $p = 0.0257$, $\eta_p^2 = 0.014$] interactions. Post-hoc analysis found that peak glucose (15 min) was greater ($p <0.001$) in CVS females than CVS

males. Further, CVS males had enhanced glucose clearance ($p < 0.01$) 45 min post-injection. Cumulative glucose exposure (**Fig. 5B**) also showed sex x CVS interaction [$F(1, 116) = 4.703$, $p = 0.0322$, $\eta_p^2 = 0.038$] where CVS decreased total glucose in males ($p < 0.05$) and, within CVS, females had greater ($p < 0.05$) total glucose.

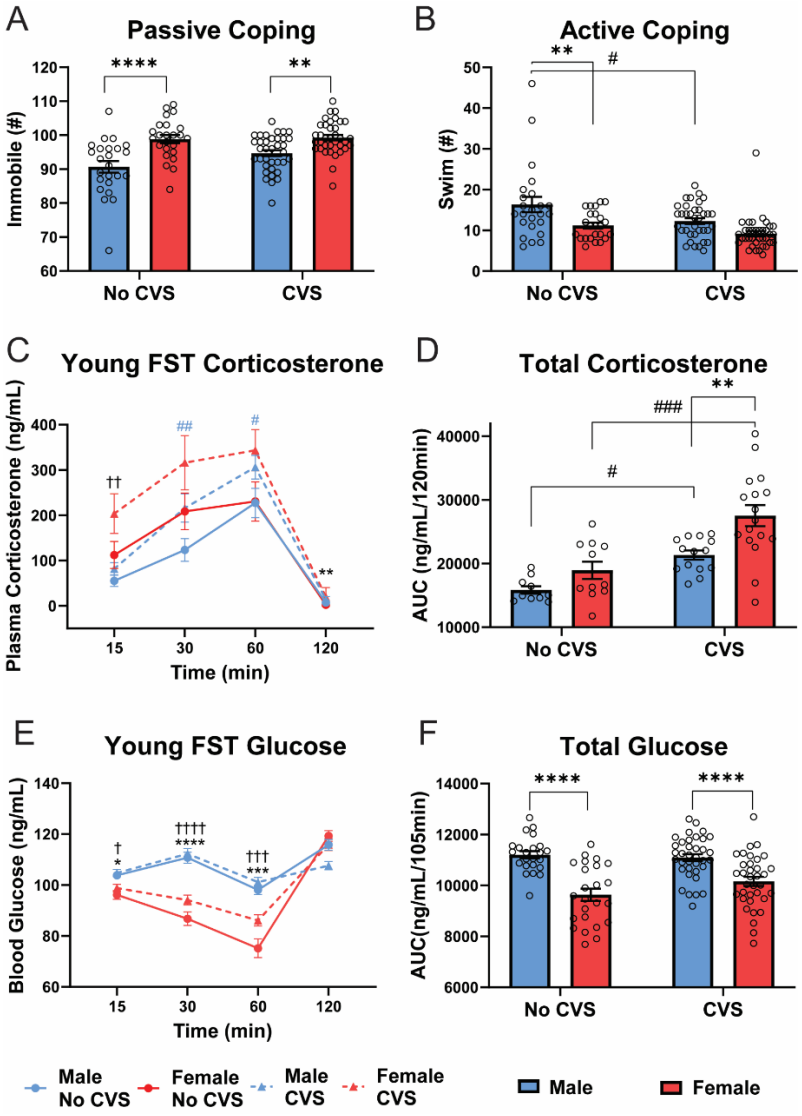

Figure 4: Young FST. During FST, behavioral coping was assessed as passive (**A**) or active (**B**) in No CVS (n = 24/sex) and CVS (n = 36/sex) rats. Blood was taken at 15, 30, 60, and 120 min after the initiation of the 10-min FST. Plasma corticosterone was measured (**C**) and the integrated total corticosterone response was calculated from the AUC (**D**). Blood glucose was also measured at each time point (**E**) and total blood glucose calculated (**F**). Data are expressed as mean ± SEM. * represents sex differences within stress condition, # represents CVS effects

within sex (indicated by color for time-dependent measures), † represents sex differences within CVS over time. *,#,† $p < 0.05$, **,##,†† $p < 0.01$, ***,###,††† $p< 0.001$, and ****,†††† $p < 0.0001$.

In response to glycemic challenge, corticosterone (**Fig. 5C**) had sex [$F(1, 115) = 4.012$, $p = 0.0475$, $\eta_p^2 = 0.029$], CVS [$F(1, 115) = 6.002$, $p = 0.0158$, $\eta_p^2 = 0.017$], and time [$F(2.292, 199.4) = 165.7$, $p < 0.0001$, $\eta_p^2 = 0.625$] effects with a CVS x time interaction [$F(4, 348) = 3.108$, $p = 0.0156$, $\eta_p^2 = 0.014$]. Post-hoc analysis revealed that, within CVS, females had higher ($p < 0.05$) fasting baseline corticosterone than males; additionally, CVS females had higher corticosterone ($p < 0.0001$) at 15 min than CVS males. Analysis of total corticosterone (**Fig. 5D**) indicated a sex effect [$F(1, 35) = 5.687$, $p = 0.0226$, $\eta_p^2 = 0.208$]; however, females were not significantly different from males within either stress condition. Altogether, data from the GTT indicate that CVS improves male glucose clearance without affecting glucocorticoid responses. In contrast, CVS exposed females have impaired glucose tolerance and elevated glucocorticoid reactivity compared to their male counterparts.

3.4 Aged body weight, corticosterone, and somatic measures

With aging and increased body weight (**Fig. S1A**), the sex difference in body weight persisted (**Fig. 6A**). ANOVA indicated effects of sex [$F(1,115) = 1115$, $p < 0.0001$, $\eta_p^2 = 0.907$] with males weighing more ($p < 0.0001$) than females in both stress conditions.

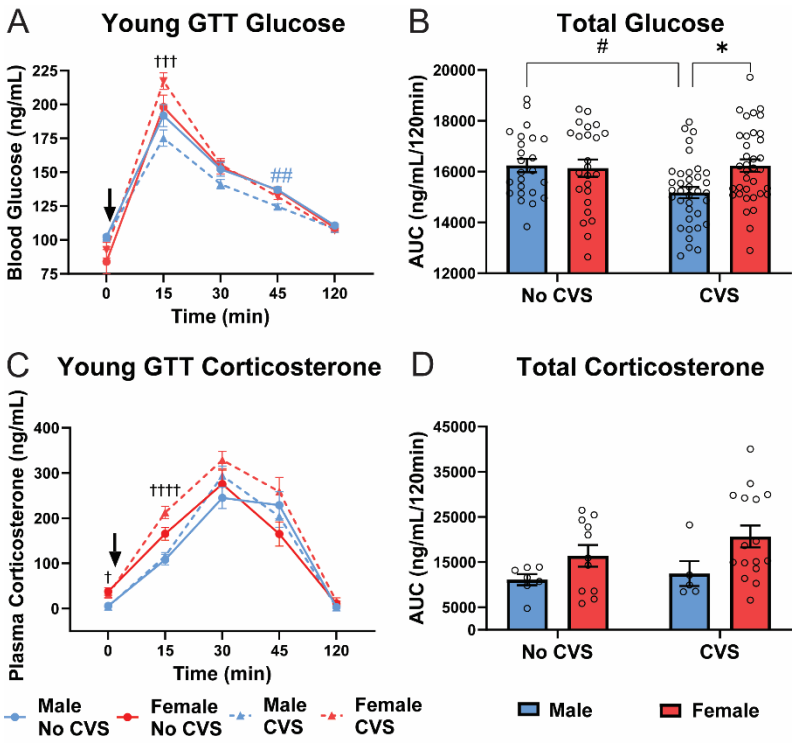

Figure 5: Young GTT. Baseline blood samples (0 min) were taken before glucose injection (1.5 g/kg, i.p.). Blood was taken at 15, 30, 45, and 120 min post injection in No CVS (n = 24/sex) and CVS (n = 36/sex) rats. At each time point, blood glucose was measured (**A**) and total blood glucose was calculated from the AUC (**B**). Plasma corticosterone was also measured (**C**) and cumulative corticosterone determined from the AUC (**D**). Data are expressed as mean ± SEM. ↓ represents glucose bolus, * represents sex differences within stress condition, $^{\#}$ represents CVS effects within sex (indicated by color for time-dependent measures), † represents sex differences within CVS over time. *,$^{\#}$,† $p < 0.05$, $^{\#\#}$ $p < 0.01$, ††† $p < 0.001$, and †††† $p < 0.0001$.

While baseline corticosterone (**Fig. 6B**) robustly increased in all groups (**Fig. S1B**), ANOVA found sex effects [$F(1, 115) = 26.04$, $p < 0.0001$, $\eta_p^2 = 0.186$] where females had higher ($p < 0.01$) resting corticosterone than males regardless of stress exposure. Somatic measures were determined at the conclusion of the study to investigate potential effects of sex and/or stress on adrenal weight, as well as body composition in terms of visceral mWAT and subcutaneous iWAT. Body weight-corrected adrenal indices (**Fig. 6C**) had a sex effect [$F(1, 113) = 251.6$, $p < 0.0001$, $\eta_p^2 = 0.736$] with females having greater ($p < 0.001$) relative adrenal mass. There were no effects on body weight-corrected mWAT (**Fig. 6D**); in contrast, iWAT (**Fig. 6E**) had sex effects [$F(1, 112) = 93.06$, $p < 0.0001$, $\eta_p^2 = 0.461$] where females had less ($p < 0.001$)

subcutaneous adiposity. In all, there were no effects of CVS on baseline corticosterone or somatic measures. However, sex effects were present where females had lower body weight and less subcutaneous fat while their adrenal glands were larger and secreted more corticosterone.

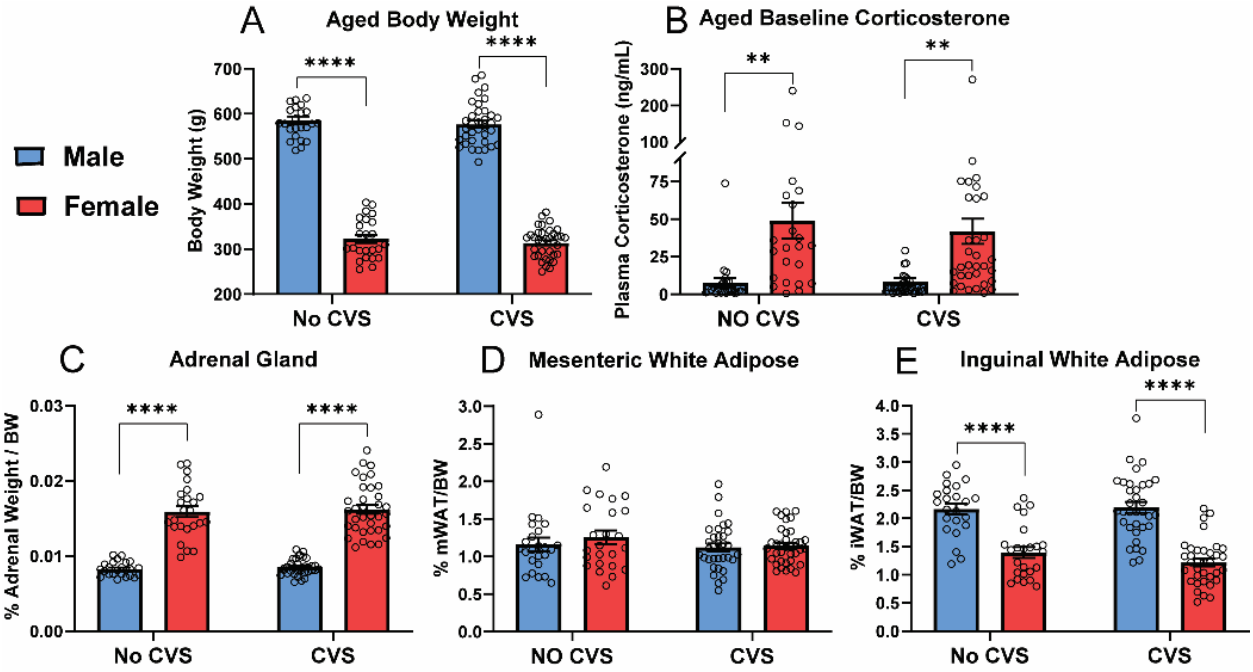

Figure 6: Aged FST. During FST, behavioral coping was assessed as passive (**A**) or active (**B**) in No CVS (n = 24/sex) and CVS (n = 36/sex) rats. Blood was taken at 15, 30, 60, and 120 min after the initiation of the 10-min FST. Plasma corticosterone was measured (**C**) and the total corticosterone response was calculated from the AUC (**D**). Blood glucose was also measured (**E**) and total blood glucose calculated (**F**). Data are expressed as mean ± SEM. * represents sex differences within stress condition and † represents sex differences within CVS over time. *,† $p < 0.05$, **,†† $p < 0.01$, *** $p < 0.001$, and ****,†††† $p < 0.0001$.

3.5 Aged FST

In contrast to young behavior, females were more active than males in the FST at 15 months. Immobility (**Fig. 7A**) showed sex effects [$F(1, 115) = 36.98$, $p < 0.0001$, $\eta_p^2 = 0.282$] with males more immobile ($p < 0.001$) than females in both stress conditions (**Fig. S2A**). Swimming (**Fig. 7B**) also had a sex effect [$F(1, 115) = 15.81$, $p < 0.001$, $\eta_p^2 = 0.146$]. While

there was no significant difference in No CVS groups ($p = 0.085$), CVS females swam more ($p < 0.01$) than CVS males.

Corticosterone responses to FST (**Fig. 7C**) had time [$F(2.52, 246.4) = 114.7$, $p < 0.0001$, $\eta_p^2 = 0.306$] and sex x time [$F(4, 391) = 38.08$, $p < 0.0001$, $\eta_p^2 = 0.215$] effects. Females in both stress groups generated more rapid corticosterone responses with elevated levels at 15 ($p < 0.05$) and 30 ($p < 0.01$) min. However, delayed male recovery from the stressor led to females having lower ($p < 0.05$) corticosterone at 120 min. Given that females had greater corticosterone responses immediately after the stressor and that males showed delayed responses, AUC analysis (**Fig. 7D**) indicated similar total corticosterone exposure in all groups.

Glucose responses to FST in aged rats (**Fig. 7E**) had sex [$F(1, 116) = 77.58$, $p < 0.0001$, $\eta_p^2 = 0.322$] and time effects [$F(2.022, 233.1) = 44.90$, $p < 0.0001$, $\eta_p^2 = 0.099$] with a sex x time [$F(3, 346) = 61.63$, $p < 0.0001$, $\eta_p^2 = 0.132$] interaction. As seen in young rats, males had higher glucose ($p < 0.001$) at 15-60 min in both stress groups. This was reflected in the AUC (**Fig. 7F**) where main effects of sex [$F(1, 114) = 72.41$, $p < 0.0001$, $\eta_p^2 = 0.392$] were present in both stress conditions. In summary, females had less immobility in the FST with CVS females more actively coping. This was coupled with an age-related shift in the temporal dynamics of male and female glucocorticoid responses where females had more rapid stress responses.

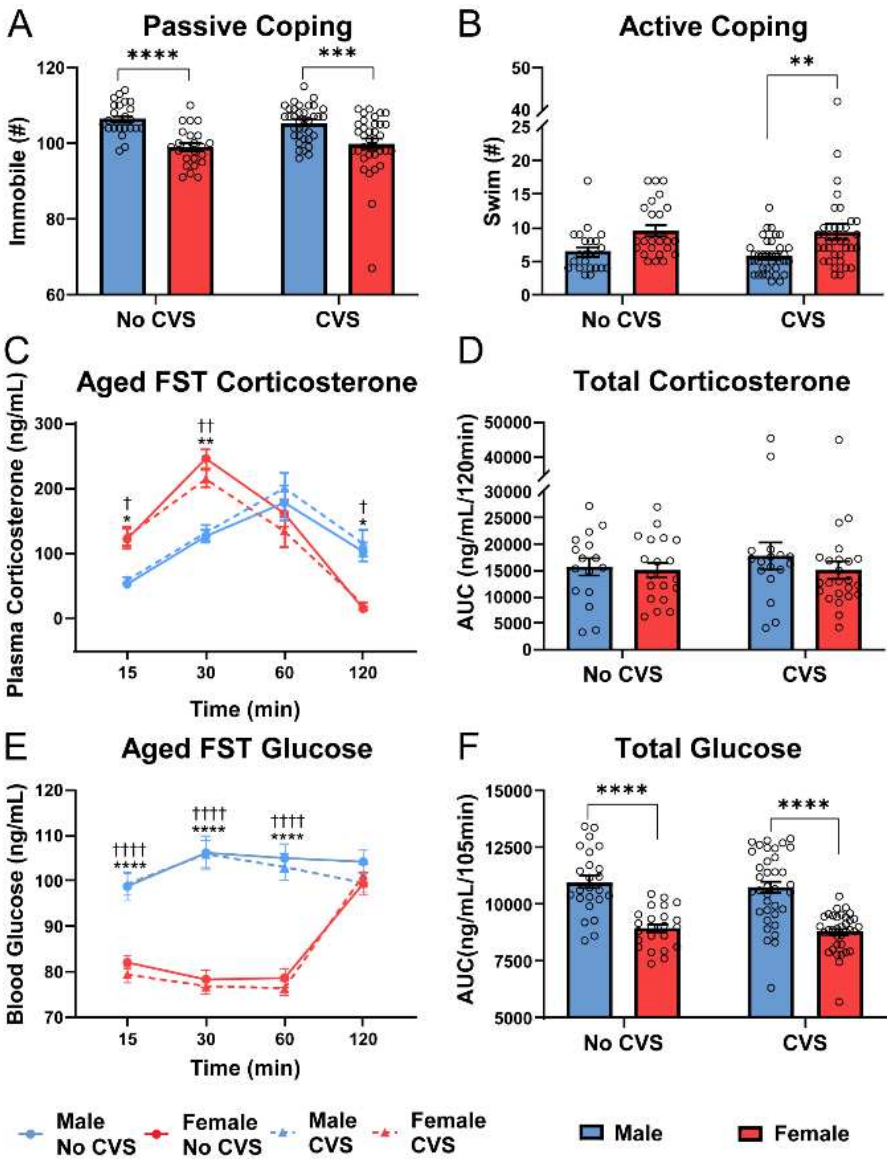

Figure 7: Aged FST. During FST, behavioral coping was assessed as passive (**A**) or active (**B**) in No CVS (n = 24/sex) and CVS (n = 36/sex) rats. Blood was taken at 15, 30, 60, and 120 min after the initiation of the 10-min FST. Plasma corticosterone was measured (**C**) and the total corticosterone response was calculated from the AUC (**D**). Blood glucose was also measured (**E**) and total blood glucose calculated (**F**). Data are expressed as mean ± SEM. * represents sex differences within stress condition and † represents sex differences within CVS over time. *,† $p < 0.05$, **,†† $p < 0.01$, *** $p < 0.001$, and ****,†††† $p < 0.0001$.

3.6 Aged GTT

After aging, the GTT was repeated and analysis of glucose clearance (**Fig. 7A**) found time effects [$F(1.66, 192.4) = 407.9$, $p < 0.0001$, $\eta_p^2 = 0.639$] with no significant group

differences. There were also no significant differences in total glucose (**Fig. 8B**); although, aging decreased male glucose clearance (**Fig. S3B**). Examination of glucocorticoid responses to glycemic challenge (**Fig. 8C**) indicated stress [$F(1, 115) = 5.184$, $p = 0.0246$, $\eta_p^2 = 0.002$] and time [$F(2.83, 251.2) = 253.6$, $p < 0.0001$, $\eta_p^2 = 0.665$] effects with stress x time [$F(4, 355) = 6.055$, $p = 0.0001$, $\eta_p^2 = 0.008$] interactions. Specifically, females exposed to CVS had elevated corticosterone at 15 min compared to CVS males. Although, there were no significant differences in AUC (**Fig. 8D**). Thus, there were no group differences in aged glucose tolerance, but chronically stressed females maintained greater glucocorticoid reactivity relative to their stressed male counterparts.

3.7 Estrous cycle

Estrous cycle was determined for females following each acute stress test (**Table 1**). Given the single cohort design of the study, cycling was random and not staged. However, lifelong cohabitation increased synchronization. For instance, 46 of 60 females were in estrus for young FST. With aging, there was more spread across cycles, especially in the CVS group. As most assessments included rats in all phases, cycle phase was included in correlational analyses to investigate potential effects on behavior and endocrine outcomes.

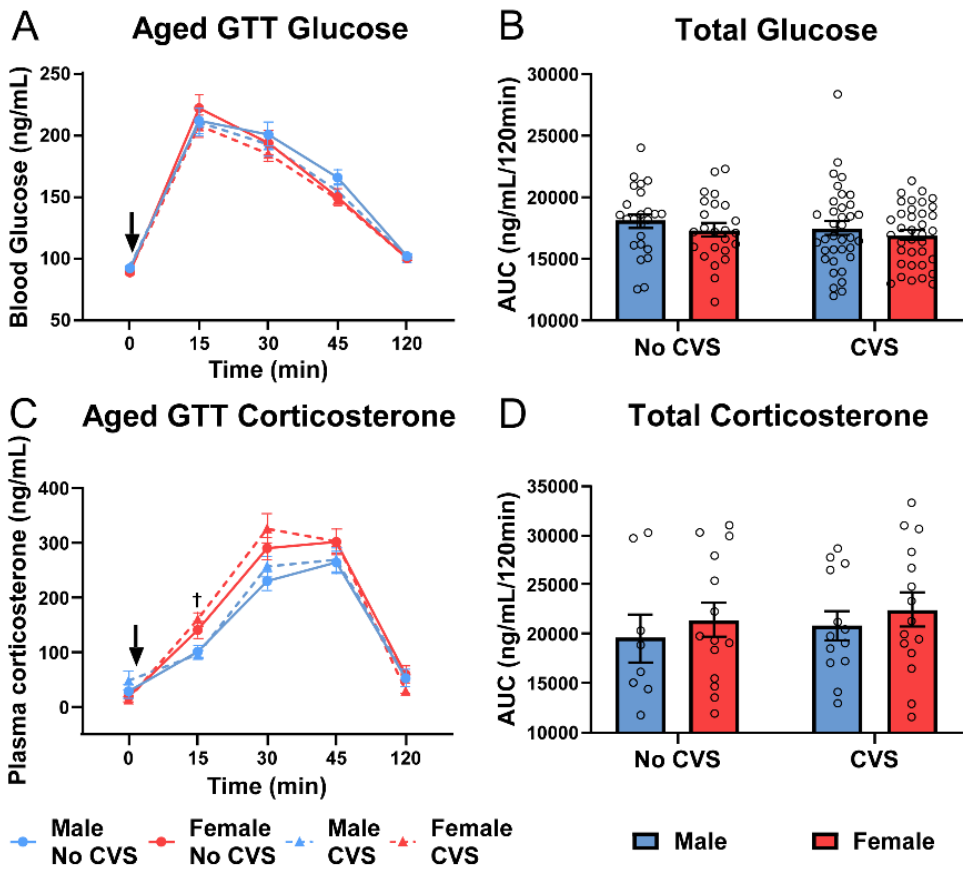

Figure 8: Aged GTT. Baseline blood samples (0 min) were taken before glucose injection (1.5 g/kg, i.p.). Blood was taken at 15, 30, 45, and 120 min post injection in No CVS (n = 24/sex) and CVS (n = 36/sex) rats. At each time point, blood glucose was measured (**A**) and total blood glucose was calculated from the AUC (**B**). Plasma corticosterone was also measured (**C**) and cumulative corticosterone determined from the AUC (**D**). Data are expressed as mean ± SEM. ↓ represents glucose bolus, † represents sex difference within CVS ($p < 0.05$).

Surprisingly, estrous cycle phase did not correlate with coping behavior or endocrine responses; although, cycle phase during each assessment correlated with phase during other assessments. Ultimately, the clustering of females largely into the same cycle phase led to lower sample numbers in the other 3 phases. This limited spread of subjects across phases may have reduced the power to discern cycle-dependent effects.

Table 1: Percentage of rats in each estrous cycle phase during acute tests.

	Phase	Young FST	Young GTT	Aged FST	Aged GTT
No CVS	Proestrus	16.66	33.33	20.83	8.33
	Estrus	75	45.83	62.5	75
	Metestrus	4.16	20.83	8.33	8.33
	Diestrus	4.16	0	8.33	8.33
CVS	Proestrus	16.66	13.88	27.77	22.22
	Estrus	77.77	69.44	44.44	38.88
	Metestrus	5.55	8.33	22.22	16.66
	Diestrus	0	8.33	5.55	22.22

3.8 Regression analysis: CVS males

In males exposed to chronic stress (**Fig. 9B**), numerous associations emerged that were not present in unstressed males. Among data collected in young rats, immobility in the FST positively correlated with corticosterone responses to FST ($r = 0.612$, $p = 0.019$). In contrast, immobility negatively correlated with glucose in the GTT ($r = -0.372$, $p = 0.025$). Baseline corticosterone in young CVS males correlated with multiple outcomes including a positive association with diving behavior ($r = 0.392$, $p = 0.018$) and negative associations with climbing ($r = -0.337$, $p = 0.044$) and cholesterol ($r = -0.354$, $p = 0.034$).

Data collected from aged CVS males indicated that immobility in the FST positively correlated with glucose responses to FST ($r = 0.428$, $p = 0.009$) and corticosterone responses to glycemic challenge ($r = 0.611$, $p = 0.026$). Additionally, aged baseline corticosterone related to adrenal weight ($r = 0.354$, $p = 0.046$) and FST corticosterone responses ($r = 0.567$, $p = 0.018$), while negatively correlating with iWAT ($r = -0.359$, $p = 0.037$). Overall, both young and aged CVS males had positive associations between passive coping and glucocorticoid responses to stressors.

As far as data collected in young rats immediately following CVS that predicted outcomes in aged rats, glucose in the young GTT correlated positively with aged GTT ($r = 0.495$, $p = 0.002$) and climbing behavior ($r = 0.407$, $p = 0.013$) but negatively with FST glucose ($r = -0.438$, $p = 0.007$). Young triglycerides predicted iWAT ($r = 0.371$, $p = 0.018$) and negatively associated with glucose in the aged GTT ($r = -0.386$, $p = 0.019$). Additionally, young baseline corticosterone during CVS predicted GTT glucose ($r = 0.448$, $p = 0.006$) and diving behavior in aged rats ($r = 0.349$, $p = 0.037$). While unstressed males did not have associations at any age between glucocorticoid responses to psychological and physiological stressors, CVS males had a negative correlation between young FST corticosterone responses and aged corticosterone responses to hyperglycemia ($r = -0.873$, $p = 0.023$). Overall, baseline corticosterone in males during CVS not only predicted behavior during the young FST but also aged behavior and glucose tolerance.

3.9 Regression analysis: No CVS females

In young female controls (**Fig. 9C**), triglycerides positively correlated with FST climbing ($r = 0.48$, $p = 0.021$). Additionally, baseline corticosterone positively associated with glucose mobilization during the FST ($r = 0.466$, $p = 0.022$), which associated with corticosterone responses to GTT ($r = 0.79$, $p = 0.004$). Together, these findings indicate that, in contrast to males, female endocrine responses to swim and glycemic stressors are positively related.

In aged No CVS females there were numerous relationships between glucocorticoids and coping behaviors. Specifically, aged baseline corticosterone positively correlated with diving ($r = 0.436$, $p = 0.038$) and FST corticosterone responses ($r = 0.593$, $p = 0.007$). Further, aged FST glucocorticoid responses correlated with climbing behaviors ($r = 0.538$, $p = 0.018$). The aged FST glucocorticoid response also related positively to adrenal weight ($r = 0.495$, $p = 0.031$) and negatively to body weight ($r = -0.635$, $p = 0.003$) and iWAT ($r = -0.473$, $p = 0.041$).

Ultimately, these correlations suggest that adrenal glucocorticoid release is related to active coping in aged females.

Young female data that predicted aged outcomes include corticosterone responses to both glycemic and psychogenic stressors negatively correlating with active coping behaviors after aging. Specifically, young corticosterone responses to hyperglycemia were negatively correlated with aged climbing behavior ($r = -0.630$, $p = 0.037$), while corticosterone responses to forced swim were negatively correlated with diving behavior ($r = -0.636$, $p = 0.047$). In addition, young triglycerides were negatively correlated with immobility after aging ($r = -0.431$, $p = 0.040$). Collectively, these correlations suggest that the female relationship between HPA axis activity and coping behavior changes with age. That is, increased glucocorticoid responses immediately after CVS negatively associate with active coping later in life; in contrast, aged females show a positive relationship between active coping and corticosterone responses.

3.10 Regression analysis: CVS females

In young chronically-stressed females (**Fig. 9D**), there were no associations between behavioral and endocrine measures. In fact, the only correlations among data collected following CVS were positive relationships between baseline corticosterone and corticosterone responses to FST ($r = 0.652$, $p = 0.005$) and immobility in the FST relating to body weight ($r = 0.37$, $p = 0.026$). When compared to No CVS females, these data suggest that prolonged stress exposure may disrupt the female-specific relationships between endocrine responses to psychological and physiological stressors.

With aging, more relationships arose including passive coping negatively relating to body weight ($r = -0.36$, $p = 0.031$) and adiposity (mWAT: $r = -0.355$, $p = 0.034$, iWAT: $r = -0.403$, $p = 0.017$). Additionally, glucose in the FST and GTT correlated ($r = 0.502$, $p = 0.002$), although there was no relationship between glucocorticoid responses in these tests. Moreover, diving

during the FST positively correlated with baseline corticosterone ($r = 0.453$, $p = 0.006$) and negatively correlated with GTT glucose ($r = -0.362$, $p = 0.03$).

Young measures that predicted aged responses included glucose during the young GTT correlating with aged active coping (swim: $r = 0.375$, $p = 0.024$) and glucose during aged FST ($r = 0.342$, $p = 0.044$) and GTT ($r = 0.535$, $p = 0.0007$). Swimming during the aged FST was also positively associated with young triglycerides ($r = 0.361$, $p = 0.03$). In contrast to both No CVS females and chronically-stressed males, CVS females had correlates of aged visceral adiposity. In fact, young immobility correlated positively ($r = 0.41$, $p = 0.013$) and young GTT corticosterone negatively ($r = -0.628$, $p = 0.009$) with mWAT. Collectively, these findings indicate that chronic stress has sex-specific effects on the relationships between passive coping, glucose tolerance, and visceral adiposity over the lifespan.

3.11 Regression analysis: group comparisons

While within group regression analyses are useful for examining associations between behavioral, hormonal, and somatic measures across time, it is important to note that direct comparisons across groups are needed to determine if these associations relate to sex or stress. Furthermore, the presence of a significant correlation in one group does not indicate that the correlation is significantly different from another group. Therefore, correlations were transformed and statistically compared across groups (**Fig. S4**).

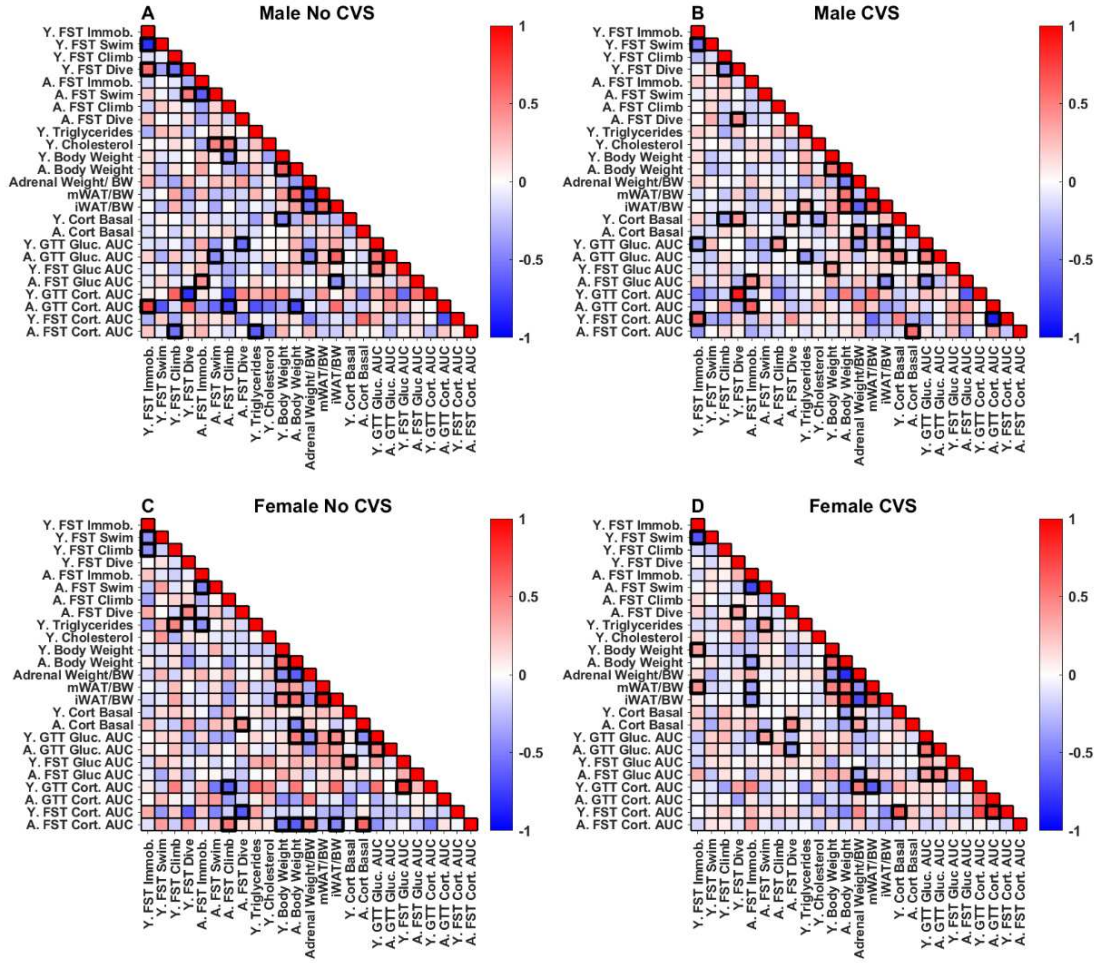

Figure 9: Regression analysis. Pearson correlations were run within each group [No CVS (n = 24/sex) and CVS (n = 36/sex)] for all measures taken throughout the study. Significant associations ($p < 0.05$) are bolded.

4. Discussion

Broadly, this study sought to examine the behavioral and metabolic consequences of adolescent chronic stress in male and female rats across the lifespan. Compared to males immediately after CVS exposure, females exhibited elevations in baseline corticosterone, passive coping behavior, corticosterone responses to behavioral stress, and hyperglycemia-evoked corticosterone, in addition to impaired glucose tolerance.

While there were prominent sex by age interactions, enduring sex differences in the effects of chronic stress were present in coping behavior and corticosterone responses to glycemic challenge. Interestingly, age impacted sex differences in coping behavior, as young females had more passive coping while males were more passive after aging. In fact, regression analysis indicated that young and aged coping behaviors had little relation in any group, suggesting this behavior may represent more of a state than trait variable. In contrast, glucose tolerance was a stable trait across the lifespan in all groups. Collectively, the results indicate that adolescent chronic stress exposure has sex-specific impacts on behavior and metabolic health, partially contributing to differential outcomes later in life.

Adolescent chronic stress exposure leads to a number of physiological changes (134, 135, 139, 142, 150, 165–167), which held true in this study. Particularly, chronically stressed females had increased glucocorticoid responses across the life span which may indicate a broad sensitization of the HPA axis. Additionally, chronically stressed young females had impaired glucose clearance. Taken together, this phenotype may represent impaired metabolic capacity and/or overall dysregulation of endocrine homeostasis. Further, regression analysis indicated that, in chronically stressed females, metabolic indicators including triglycerides and blood glucose were positively correlated with active coping behaviors after aging.

Although numerous studies have reported increased passive coping in females at varying time points after adolescent chronic stress, effects on glucocorticoid responses have been mixed (134, 135, 168). Specifically, adolescent chronic stress in female rats has produced both hypoactivity (135) and sensitization (134) of the HPA axis. The present results found female HPA axis sensitization to both behavioral and glycemic stressors immediately after chronic stress that persisted, in part, into late adulthood. Age differences in stress exposure and data collection, as well as the length of recovery between adolescent stress and adult assessments may contribute to these divergent results. However, the current study simultaneously investigated male and female littermates at multiple time points and found

female glucose intolerance combined with widespread HPA axis sensitization, indicating greater overall endocrine and autonomic reactivity in stressed females across the lifespan.

Interestingly, chronic stress exposure improved glucose tolerance in young males. This associated negatively with young FST immobility and positively with body weight-corrected subcutaneous adiposity at the end of the study, correlations that did not exist in No CVS males. It remains to be determined whether relative differences in adiposity following CVS play a role in the increased rate of glucose clearance. Androgen effects are also possible as testosterone improves glucose tolerance in men (169), and increases active coping in male rats (170).

In both young male and female rats, CVS impacted behavioral and endocrine measures, including elevated glucocorticoid responses to behavioral stress. However, sex differences in the effects of aging more prominently impacted long-term outcomes than CVS. Regardless of stress status, males and females differed in baseline glucocorticoid tone, subcutaneous adiposity, coping behavior, and stress-induced glucose mobilization. In fact, the increased immobility observed in young females was contrasted by an age-related increase in male immobility. This increased male immobility did not relate to bodyweight or adiposity but may reflect androgen decline in males and/or stress resilience in aged females (171). Further, the central processing of stress would be expected to contribute to sex- and stress-specific effects. In fact, 6 weeks after adolescent CVS, FST-induced Fos expression shows sex differences in chronic stress responses. Here, male rats have decreased neural activation in the medial and basolateral amygdala, while females do not (134).

Although glucose tolerance is a well-accepted measure of metabolic function (172), numerous other hormones are critical, most notably insulin. Given the design of sampling blood 5 times each in 2 experiments during the same week, we were limited in the volume we were able to collect. That combined with the demands of processing 2,400 total blood samples across the study, meant sample measurements were prioritized to prominent indicators of both stress reactivity and metabolic regulation. More targeted analysis of insulin in future studies would be

expected to better illuminate sex differences in glucose handling, as well as potential effects on insulin sensitivity. Another design consideration relates to allowing rats to age to 15 months, which should near reproductive senescence (173). This was chosen as a relative translational equivalent of late middle-age. Expanding the age range beyond 18 months would ensure reproductive senescence and may yield differences due to the reduced levels of gonadal hormones at advanced age. Despite the limitations, this study provides novel insights into the longitudinal effects of adolescent chronic stress and a basis for understanding sex-specific pathologies.

Epidemiologic data indicate that males and females develop metabolic syndrome at similar rates (44). However, metabolic syndrome is a predisposing factor to cardiovascular disease (21), which is an increasingly prevalent cause of death in women after midlife (47, 174). Our data suggest that prolonged stress exposure may potentiate physiological and behavioral changes associated with the development of metabolic syndrome and subsequent disease sequelae. These animal data also suggest the possibility that human females may react differently from males to chronic stress in adolescence, and the divergent pathways to metabolic syndrome may require sex-specific interventions. Further investigation may indicate that sex-specific predictive correlations support biomarker development to predict or intervene in future pathology. Given the role of chronic stress in psychiatric and metabolic disorders (22, 24, 25, 27), mitigating the consequences of chronic stress exposure in adolescence has the potential to improve health and quality of life.

CHAPTER 3: SEX-SPECIFIC CARDIAC REMODELING IN AGED RATS AFTER EARLY-LIFE CHRONIC STREESS: ASSOCIATIONS WITH ENDOCRINE AND BEHAVIORAL OUTCOMES[3]

1. Introduction

Cardiovascular disease (CVD) is a leading cause of death both globally (1) and, specifically, a leading cause of death in women (175). However, the rates of cardiovascular disease through the lifespan differ wildly between males and females (176). While rates of CVD steadily increase with age in men, women generally experience lower rates until menopause, at which point rates of CVD increase to, or even exceed, that of men (45). These differences are largely attributed to the protective effects of female reproductive hormones (96, 177), centrally estradiol, on the cardiovascular system that are lost with reproductive senescence (51, 178). Aging associated changes in physiology, like hypertension and increased cholesterol, impact the pathogenesis of CVD in a number of ways and are often used as markers of heart health (26). Centrally, concentric hypertrophic remodeling reduces ventricular volume and increases the workload of the heart (179). Thus, concentric left ventricular hypertrophy (LVH) increases the risk of major cardiovascular events and heart failure (180). However, little is understood about how early life behavior, stress exposure, and autonomic responses impact LVH and the cardiovascular system throughout aging. Differences in these responses may increase susceptibility to cardiovascular remodeling in a sex specific manner.

While stress responses are essential to appropriate homeostatic balance in the face of adversity (5), prolonged stress responses are associated with cardiometabolic dysfunction and

[3] C. Dearing, E. Sandford, N. Olmstead, R. Morano, L. Wulsin, B. Myers. (2024). Sex-specific Cardiac Remodeling in Aged Rats after Early-life Chronic Stress: Associations with Endocrine and Behavioral Outcomes. (*Submitted to Biology of Sex Differences).*

the development of neuropsychiatric disorders (8). Particularly, early-life stress has been shown to have immediate and long-term impacts on cognition and endocrine reactivity in pre-clinical studies (139, 148, 152). Rodent models of chronic early-life stress mirror these impacts with increased stress reactivity in males (144). Additionally, our research has shown that following Chronic Variable Stress (CVS), female rats become hyper-reactive to acute stress with increased corticosterone and impaired glucoregulation. They also exhibit a sex-specific change in coping style with young females exhibiting greater passive coping and young males exhibiting greater active coping during a Forced Swim Test (FST) (4). However, how early-life chronic stress affects cardiovascular remodeling, and consequently CVD risk, after aging in both males and females is unknown.

Following our previously published longitudinal study (4) examining the coping behavior and metabolic impacts of early-life chronic stress exposure in both male and female rats, we used histological analysis to examine cardiac remodeling and test the hypothesis that sex-specific behavioral and endocrine responses impact cardiac susceptibility. To this end, we used assessments of behavioral coping and glucoregulation both immediately following chronic stress exposure and at 15 months of age in a large cohort of male and female rats to assess the effects of both chronic stress and aging on LVH. These analyses shed light on how behavior impacts future cardiac health in a sex-specific manner.

2. Methods

2.1 Subjects

Initial experiments were previously published (4) and were approved by the Institutional Animal Care and Use Committee of the University of Cincinnati (protocol 04-08-03-01) and complied with the National Institutes of Health Guidelines for the Care and Use of Laboratory

Animals. All rats had daily welfare assessments by veterinary and/or medical service staff. Animals were kept on 12 on 12 off light cycles with food and water available *ad libitum*.

2.2 Design

Following on prior experiments, cardiac tissue from all animals was collected and histologically analyzed to look at heart size and relative left ventricular hypertrophy (**Fig. 10A**). Briefly, 120 adolescent rats were randomly assigned to Chronic Variable Stress (CVS) (n = 36/sex) and stress naïve (No CVS) (n = 24/sex) groups. These animals then underwent a 14 day CVS paradigm (142, 155) followed by acute psychogenic (Forced Swim Test [FST]) and metabolic (Glucose Tolerance Test [GTT]) stressors. Animals were then aged to 15 months and acute stressed again. Blood glucocorticoid, somatic, and behavioral measures were quantified (4).

2.3 Cardiac Tissue Collection

Following the final acute stress test rats, rats were anesthetized (5% inhaled isoflurane) and euthanized via rapid decapitation. Hearts were immediately arrested in diastole via an intracardiac injection of 15% potassium chloride. Hearts were removed from the thoracic cavity and great vessels were trimmed to the trunk. Post-mortem clots were extracted, and the hearts were weighed. Tissue was then placed in 4% paraformaldehyde for 24 hours and transferred to 3% sucrose for storage. Raw organ weights were corrected for bodyweight at the time of euthanasia.

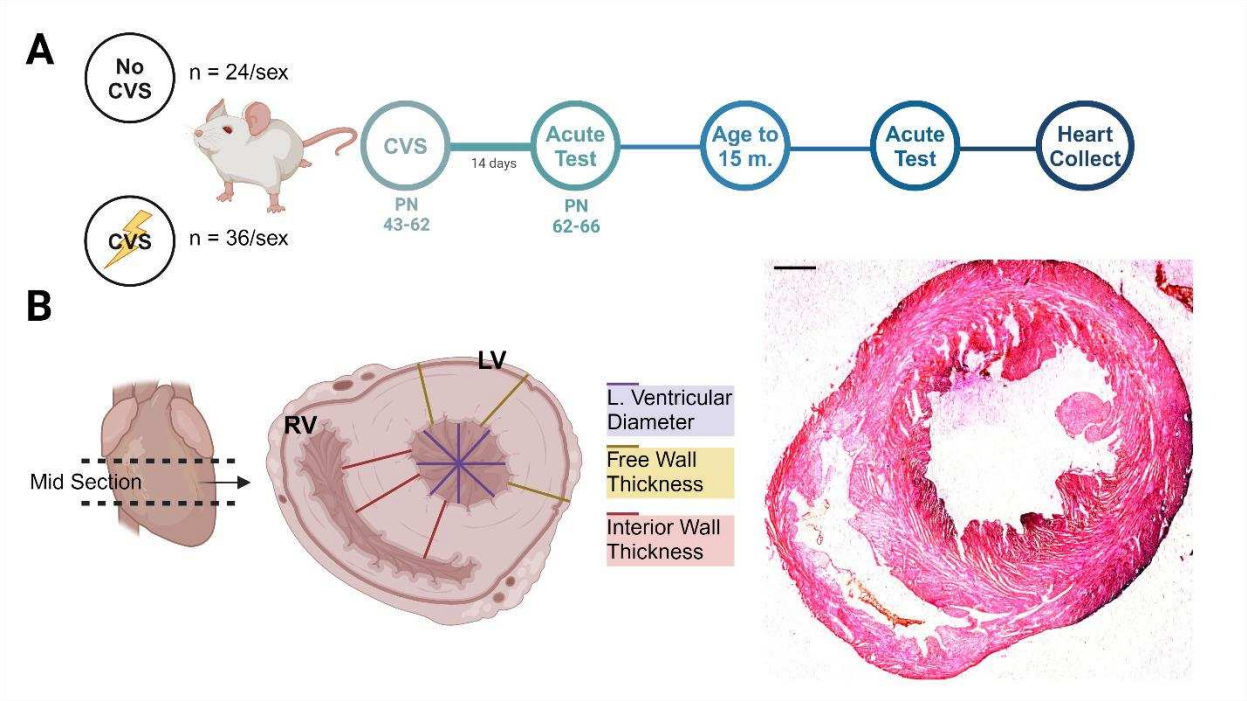

Figure 10. Experimental design. A single cohort of male and female rats underwent chronic stress (No CVS n = 24/sex; CVS n = 36/sex) followed by acute challenge and aging (A). Mid-sections of each heart were stained with H&E and wall and ventricular thickness were measured (B) Scale bar 1mm. Created with BioRender.

2.4 Histologic Processing

Prior to histological evaluation the cardiac tissue was sectioned, dehydrated, and embedded in paraffin in order to allow efficient slicing, imaging, and analysis. The heart tissue was sliced horizontally into 3 increments, the midsection of the heart was placed in a labeled cassette to be dehydrated. Mid-sectioned tissue was placed into a 60% ethanol bath for 10 minutes. It was transferred into a 70% ethanol bath for two 20 minute increments in two different baths. The tissue was soaked in two 95% ethanol baths for 20 minutes increments. The cassette was transferred to a 100% ethanol bath for a total of 60 minutes, transferring the tissue to a new ethanol bath every 20 minutes. Tissue was transferred to a 100% xylene bath for a total of 90 minutes, in 30 and 60 minutes increments. After dehydrating the hearts, the cassettes were

dried and placed into a paraffin soak overnight. The cassettes were removed from the paraffin reservoir and embedded for slicing. The tissue was sliced using a Microm HM 330 microtome at 35 μm. Slices were stained with Hematoxylin and Eosin before drying, cover-slipping, and imaging.

2.5 Imaging and Analysis

Bright Field imaging was performed using a Ziess Axio Imager Z2 microscope. An image was taken for 9 tissue sections per animal to be analyzed. FIJI Image processing was used to analyze these images. For each image three different parameters were measured: left ventricle diameter, left ventricular free wall thickness, and interior wall thickness (**Fig. 10B**). 3-6 measurements were made per image when measuring the free wall and interior wall. The interior wall measurements were made from the endocardium of the left ventricle wall straight to the endocardium of the right ventricle. The free wall measurements were made from starting at the endocardium of the left ventricle out to the serosa. The ventricular diameter was measured at 0, 45, -45, and 90 degrees spanning the entirety of the ventricle. These measurements were then averaged across tissue slice and animal (n = 36-54 biologic replicates/animal).

2.6 Data Analysis

Data are expressed as mean ± standard error of the mean. All rats were included in all analyses. Data were analyzed using Prism 10 (GraphPad, San Diego, CA), with statistical significance set at $p<0.05$ for all tests. Heart size and hypertrophy ratio were analyzed by 2-way ANOVA with sex and stress as factors. Internal comparison of hypertrophy within group was analyzed by 3-way ANOVA with sex, stress, and hypertrophy ratio as factors. All other comparisons of behavioral, somatic, and physiologic responses to Forced Swim and Glucose Tolerance Testing were analyzed by 3-way ANOVA with sex, stress, and left ventricular hypertrophy as factors. Tukey multiple comparisons post-hoc tests were used for all main and

interaction effects. Area under the curve (AUC) analysis was calculated as previously reported (4). Effect size is reported as eta squared (η^2). Pearson correlation two-tailed analyses were used to examine relationships between hypertrophy and acute responses within groups. See supplemental table (**S.1**) for all ANOVA analysis results.

3. Results

Statistical results are focused on effects that are impacted by left ventricular hypertrophy for clarity. In concordance with our prior publication on the effects of stress and sex in these experiments, post-hoc analysis showed many of the same group differences. Therefore, while main effects are stated below, sex and stress specific group differences are outlined in the supplemental material.

3.1 Heart size and hypertrophy

Heart size was considered with 3 measurements: left ventricular diameter, interior wall, and free wall size (**Fig. 11**). 2-way ANOVA comparison of the ventricular diameter found a main effect of stress [$F(1, 111) = 11.62$, $p = 0.0009$, $\eta^2 = 9.326$] with post-hoc analysis indicating the No CVS females had greater left ventricles than both No CVS males ($p = 0.0437$) and CVS males ($p = 0.005$). Interior and free wall measurements both exhibited main effects of sex [$F(1, 110) = 13.71$, $p = 0.0003$, $\eta^2 = 11.0$] and [$F(1, 111) = 19.08$, $p < 0.0001$, $\eta^2 = 14.58$] respectively. Post-hoc analysis of the interior wall measurements indicated CVS males had smaller interior walls than both the No CVS females ($p = 0.045$) and CVS females ($p = 0.0144$). This was also reflected in the free wall analysis with CVS males again showing a smaller free wall than No CVS ($p = 0.0043$) and CVS ($p = 0.0082$) females. Additionally, No CVS males showed significantly smaller free walls than both No CVS ($p = 0.0177$) and CVS females ($p = 0.0367$). There were no significant differences within sex for any heart size measurement.

Left ventricular concentric hypertrophy (LVH) was determined by a Hypertrophy Ratio (HR) of the left ventricular diameter to the free wall thickness. Analysis indicated a main effect of sex [$F(1, 111) = 14.39$, $p = 0.0002$, $\eta^2 = 11.0$] where CVS females showed significantly increased inward remodeling compared to both CVS (0.0009) and No CVS ($p = 0.003$) males. No differences were seen within sex. An internal comparison of the low, mid, and high hypertrophy groups for each sex and stress condition indicated main effects of hypertrophy [$F(2, 103) = 118.1$, $p < 0.0001$, $\eta^2 = 50.77$], sex [$F(1, 103) = 49.89$, $p < 0.0001$, $\eta^2 = 10.72$], and stress [$F(1, 103) = 4.717$, $p = 0.0322$, $\eta^2 = 1.014$]. Additionally, interactions of hypertrophy by sex [$F(2,103) = 5.932$, $p = 0.0036$, $\eta^2 = 2.550$] and sex by stress [$F(1, 103) = 5.520$, $p = 0.0207$, $\eta^2 = 1.186$] were present with the high hypertrophy group being significantly higher in all cases (**Table 2**). The only groups that were not significantly different were the male CVS and both male and female No CVS low and mid hypertrophy (**Fig. 11E**).

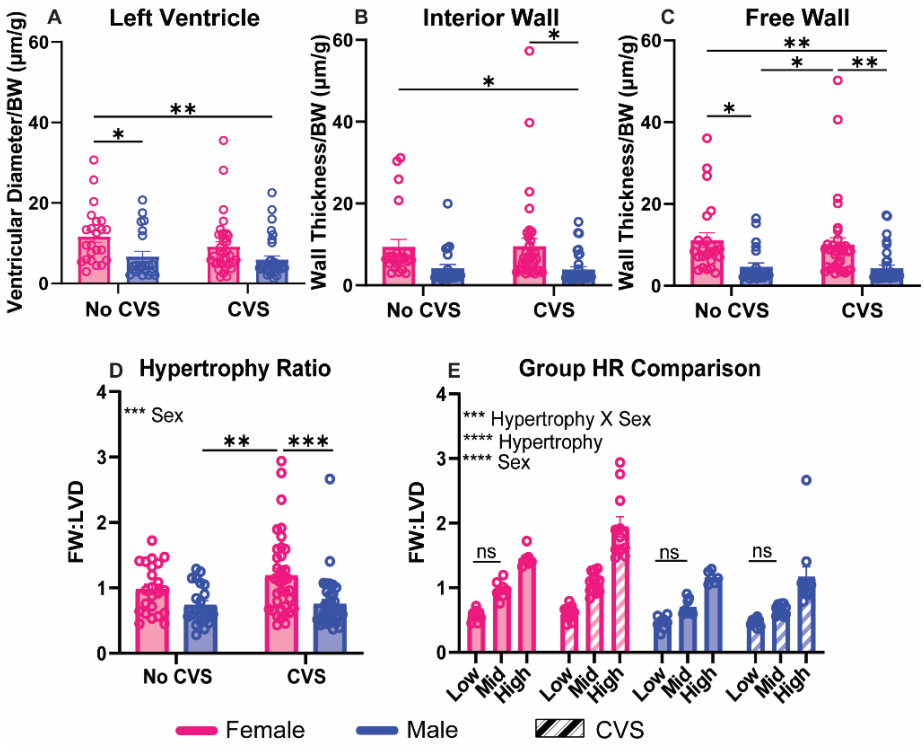

Figure 11. Heart and hypertrophy measurements. The Left ventricle (A), Interior wall (B), and Free wall (C) were measured and corrected for bodyweight at the time of tissue collection. Hypertrophy (HR) is represented by a ratio of the free wall to the left ventricular diameter (D).

Each group was then separated into subpopulations, and these were compared to determine differences between subpopulations (E). Data are expressed as mean ± SEM. * p<0.05, ** p<0.01, *** p<0.001, **** p<0.0001.

Table 2: Statistical comparison of hypertrophy subpopulations by group.

P value between hypertrophy groups

	Female			Male		
	High > Mid	High > Low	Mid > Low	High > Mid	High > Low	Mid > Low
No CVS	p = 0.0147	p = < 0.0001	p = 0.0728	p = 0.0411	p = < 0.0001	p = 0.7317
CVS	p = < 0.0001	p = < 0.0001	p = 0.0008	p = < 0.0002	p = < 0.0001	p = 0.7704

3.2 Behavior

Behavioral coping style (**Fig. 12**) differently impacted future cardiac hypertrophy depending on the age of the animals. When separated into low, mid, and high LVH groups, young passive coping, represented by immobility during FST, impacted LVH with main effects of sex [$F(1,103) = 31.18$, $p < 0.0001$, $\eta^2 = 20.26$], stress [$F(1, 103) = 4.641$, $p = 0.0335$, $\eta^2 = 3.015$] and LVH [$F(2, 103) = 4.786$, $p = 0.0103$, $\eta^2 = 6.218$] and an interaction between LVH and stress [$F(2, 103) = 3.148$, $p = 0.0471$, $\eta^2 = 4.09$]. Young active coping, represented as swimming during FST, did not significantly impact LVH. However, analysis did show main effects of sex [$F(1, 103) = 17.82$, $p < 0.0001$, $\eta^2 = 12.88$] and stress [$F(1, 103) = 10.04$, $p = 0.002$, $\eta^2 = 7.258$] with the high LVH no CVS males showing significantly more active coping than their CVS counterparts ($p = 0.0462$).

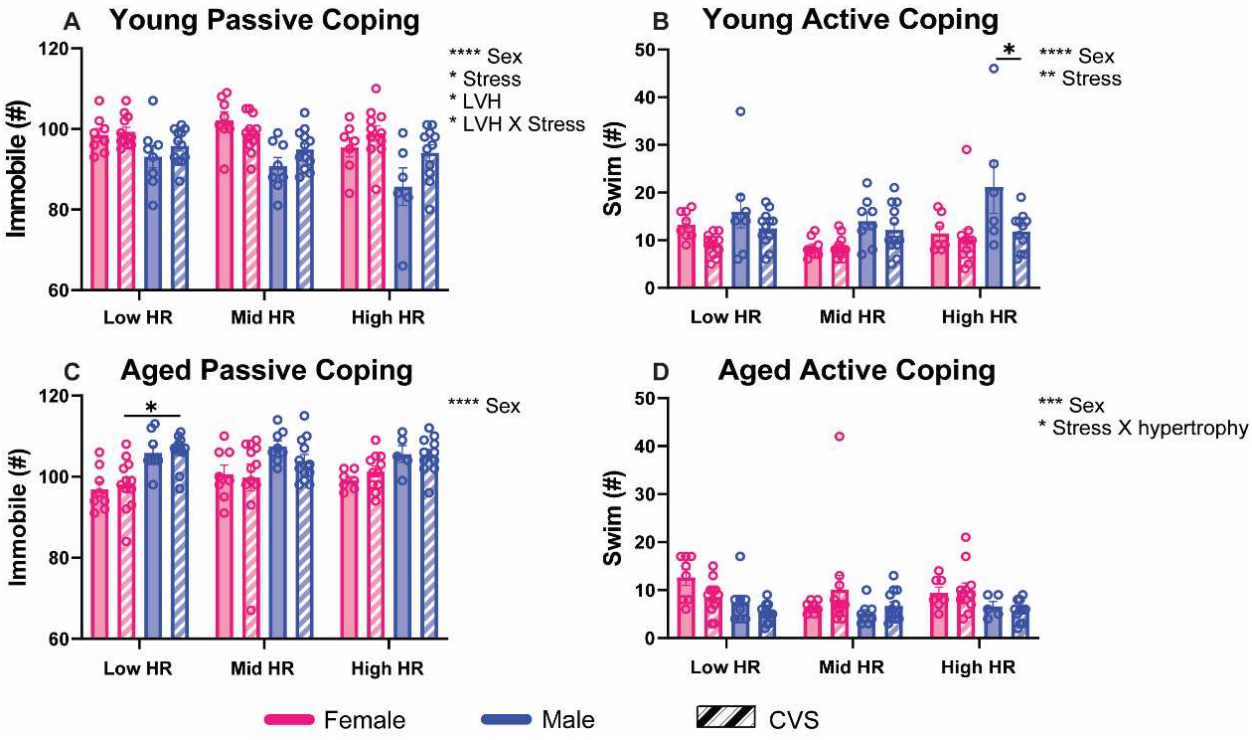

Figure 12. Behavioral analysis. Animals were challenged with a forced swim test immediately following chronic stress and after aging. Coping style was assessed as passive (A, C) or active (B, D). These were then ranked and compared across hypertrophy subpopulation. Data are expressed as mean ± SEM. * $p<0.05$, ** $p<0.01$, *** $p<0.001$, **** $p<0.0001$.

Interestingly in aged animals, immobility did not significantly impact LVH but maintained a main sex effect [$F(1, 102) = 30.75$, $p < 0.0001$, $\eta^2 = 22.15$]. However, within the low LVH animals, stressed males show significantly more active coping than stressed females ($p = 0.0467$). Active coping in aged animals exhibited both a main of sex [$F(1, 102) = 14.52$, $p = 0.0002$, $\eta^2 = 11.36$] and an interaction between stress exposure and hypertrophy [$F(2, 102) = 3.565$, $p = 0.0319$, $\eta^2 = 5.583$].

3.3 Glucocorticoid responses to metabolic stress

Overall, glucocorticoid responses during FST in both young and aged animals and GTT responses in young animals did not impact LVH (see supplemental material). Glucocorticoid response to the metabolic stress of a glucose tolerance test impacted LVH in an age and sex

dependent manner (**Fig. 13**). Baseline corticosterone in aged animals showed a main sex effect [$F(1, 85) = 4.912$, $p = 0.0293$, $\eta^2 = 0.0293$] and an interaction between sex, stress, and LVH [$F(2, 85) = 3.283$, $p = 0.0423$, $\eta^2 = 0.0423$]. Interestingly, when looking at peak corticosterone levels 30 minutes following intraperitoneal injection of glucose aged animals show a main effect of sex [$F(1, 86) = 6.772$, $p = 0.0109$, $\eta^2 = 6.818$] on peak corticosterone levels. Similarly aged animals show an interaction between LVH and sex [$F(2, 35) = 5.042$, $p = 0.0119$, $\eta^2 = 20.66$]. There were no significant differences in the total glucose responses of young or aged animals. Importantly, on regressive analysis, left ventricular hypertrophy was significantly positively correlated to baseline corticosterone in aged unstressed male rats ($r = 0.449$, $p = 0.041$) (**Fig. 15A**).

3.4 Adiposity

Measures of both Peripheral (inguinal) and visceral (mesenteric) adiposity significantly impacted LVH (**Fig. 14**). Peripheral adiposity had a main effect of sex [$F(1, 100) = 94.98$, $p < 0.0001$, $\eta^2 = 41.97$] and an interaction effect between LVH, sex, and stress [$F(2, 100) = 3.09$, $p = 0.499$, $\eta^2 = 2.731$].

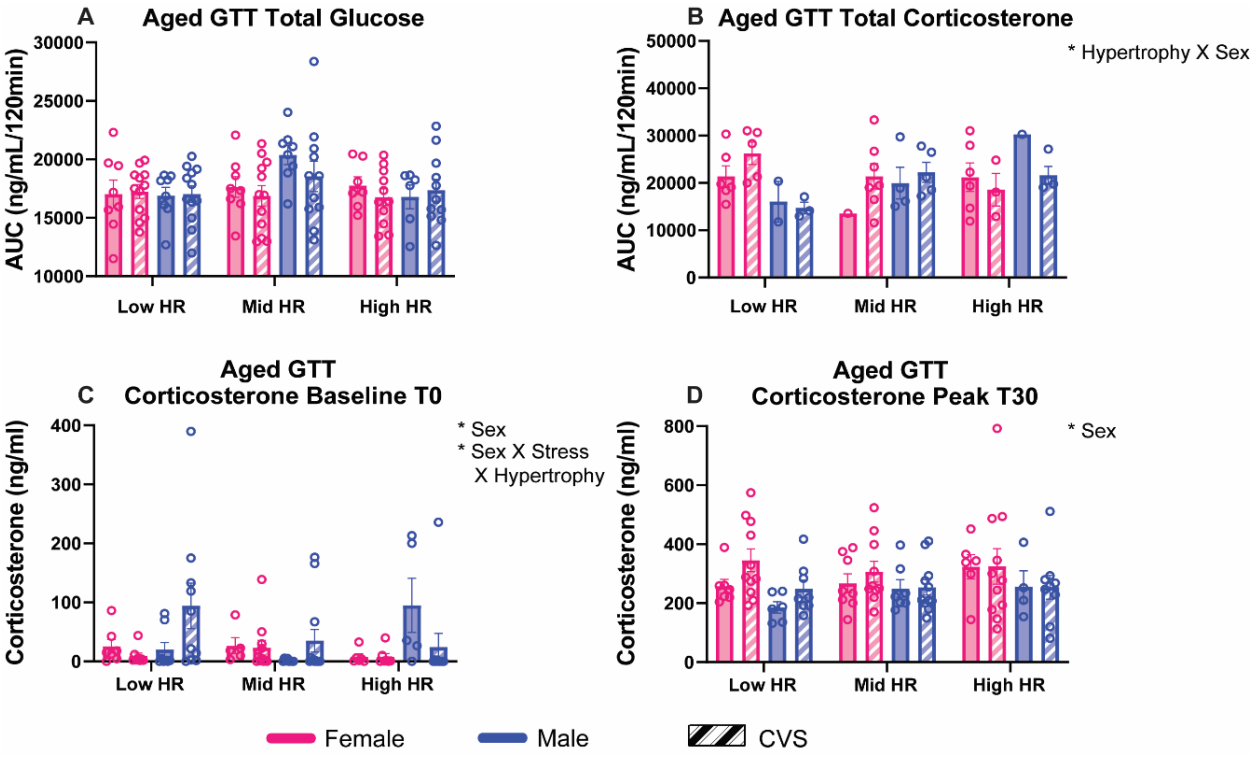

Figure 13. GTT glucocorticoid responses. Aged animals were metabolically challenged following chronic stress. Total blood glucose (A) and plasma corticosterone (B) were calculated from an AUC analysis. Baseline corticosterone was measured at T0 taken prior to glucose injection (C). Peak corticosterone response was measured 30 minutes following glucose injection (D). Groups were analyzed according to hypertrophy subpopulations. Data are expressed as mean ± SEM. * $p<0.05$.

Within the low LVH group, male CVS animals have greater peripheral adiposity than female CVS animals ($p = 0.0038$). Additionally, male animals in the mid LVH group have greater adiposity than females in both the CVS ($p = 0.0005$) and no CVS ($p < 0.0001$) groups. This is reflected in the high LVH group with the CVS males having higher adiposity than CVS females ($p < 0.0001$). Mesenteric adiposity reflected a main effect of LVH [$F(2, 101) = 3.916$, $p = 0.023$, $\eta^2 = 6.755$]. Regressive analysis showed LVH being positively correlated to mesenteric adiposity ($r = 0.387$, $p = 0.026$) in stress exposed aged males (**Fig. 15B**).

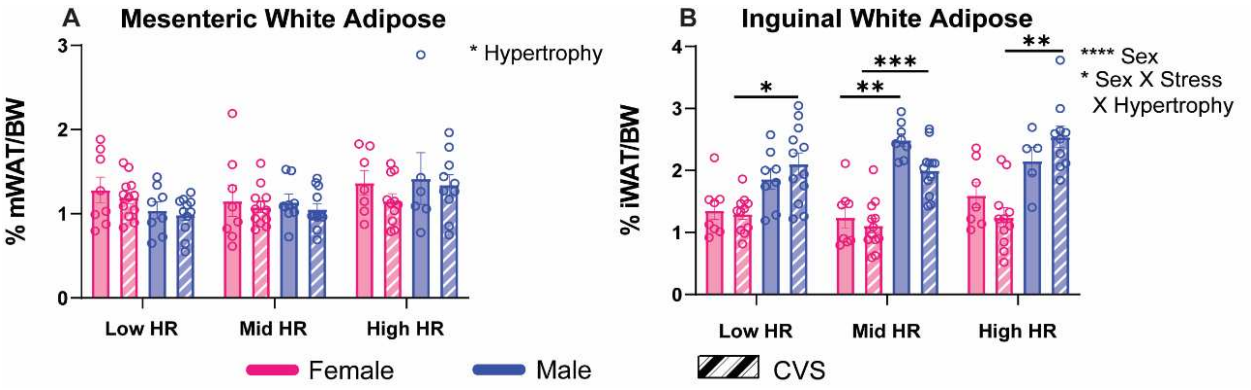

Figure 14. Adiposity following chronic stress. Following aging at euthanasia, mesenteric white adipose (A), inguinal white adipose (B). Groups were analyzed according to hypertrophy subpopulations. Data are expressed as mean ± SEM. * p<0.05, ** p<0.01, *** p<0.001, **** p<0.0001.

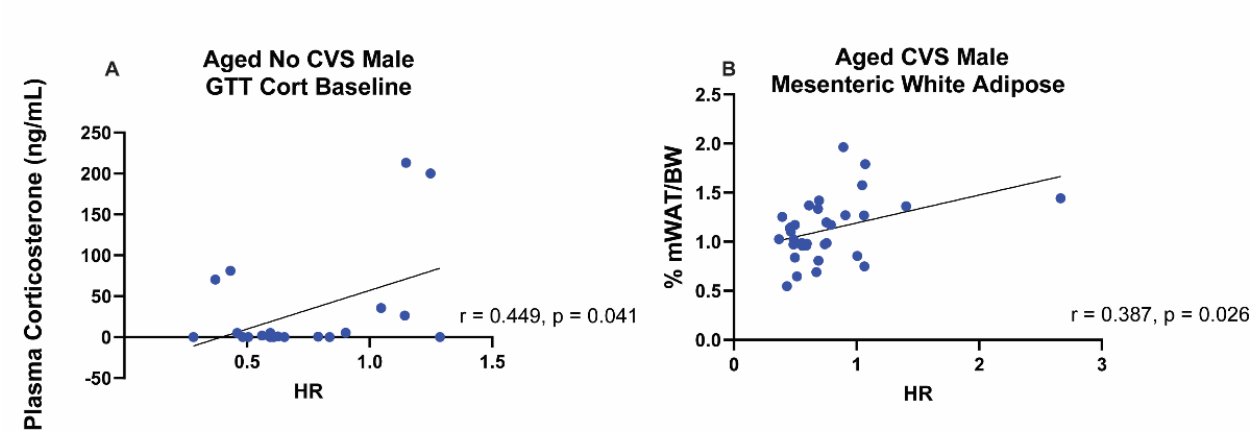

Figure 15. Correlations. Regressive analysis of aged No CVS male baseline corticosterone (A) and aged CVS male visceral adiposity (B).

4. Discussion

4.1 Sex-specific hypertrophy

Broadly, this study sought to expand on prior work and examine the effects of aging and stress on cardiac structure in male and female rats. While early life chronic stress appears to be a modulatory influence on cardiac structure later in life, these effects are broadly eclipsed by the aging process. The impact of these factors is largely sex dependent.

While heart size and LVH ratio indicate that females regardless of stress status have significant changes in cardiac structure, these changes are associated with fewer deleterious physiologic changes than in males. Importantly, this difference is likely due to these females being reproductively active. These results are in accordance with clinical data that show the rates of cardiovascular disease in cycling women are lower than that of age matched men (176). While the mechanism behind these clinical changes are not completely elucidated, our results support the consensus that female reproductive hormones have protective effects on the cardiovascular system (96, 177). It is likely that these females would experience greater dysfunction following reproductive senescence. Importantly, significantly increased left ventricular hypertrophy in females exposed to early chronic stress indicates that early life stress impacts cardiovascular structure throughout the lifespan in a sex-specific manner and is not dependent on the loss of reproductive hormones. These results may help to explain the clinical finding of female CVD rates rapidly overtaking and exceeding that of males following menopause if they are predisposed to structural changes that are masked prior to menopause.

4.2 Male susceptibility

It is known that exposure to chronic stress causes sex-specific cardiac remodeling immediately following stress exposure (156). However, this broader effect seems to resolve with age. While males did not experience overall higher rates of LVH, those animals with the highest amount of LVH showed evidence of higher cardiometabolic dysfunction in a stress specific manner. This susceptibility indicates that the long-term deleterious effects of chronic early life stress exposure differentially impacts individuals of the same population. Additionally, susceptible individuals show different behavioral responses to acute stress that then predict levels of LVH later in life.

Particularly, the interaction of LVH and stress within the young passive coping response indicates that, in males, later cardiac remodeling is predicted by coping response to acute stress

in a stress dependent manner. Further, unstressed males with the greatest LVH show significantly increased active coping compared to their CVS counterparts. The increase in active coping may be an adaptive response to acute stress in naïve animals that then increases susceptibility to cardiac remodeling. Chronic stress exposure appears to dampen these changes and adaptive responses. These results indicate that, in males, early life stress and consequent coping behavior predict later cardiac changes. Interestingly, coping style later in life does not correlate to cardiac remodeling and is instead primarily a function of sex.

While the metabolic analysis of the FST did not show the same male susceptibility in either young or aged animals, acute metabolic stress in aged animals again emphasized a stress and sex specific susceptibility in males. Particularly, baseline corticosterone measurements in aged animals showed an inverse relationship between stress condition and LVH. Additionally, regressive analysis shows a positive correlation of LVH and baseline corticosterone in unstressed males. These results suggest that increased glucocorticoid responsivity in chronic stress naïve males predicts greater cardiac remodeling and that chronic stress exposure changes these relationships. Further, the positive correlation in unstressed males implicates a deleterious association between metabolic responsivity and cardiac remodeling that becomes apparent with age.

The association between metabolic and cardiac changes with age is also apparent in somatic measures of peripheral and visceral adiposity. Visceral adiposity is strongly correlated with the development of multiple cardiometabolic diseases in humans (181). The correlation between peripheral adiposity and these disease processes is less clear. However, an overall increase in adiposity is persistently associated with increased risk for cardiometabolic disease (182). Interestingly, exposure to chronic stress leads to a positive correlation in visceral adiposity and LVH, indicating that early life chronic stress exposure may impact metabolic capacity and consequently cardiac remodeling. The effects of peripheral adiposity indicate that

an increase in overall adiposity that is not specific to the abdomen is likely still impacting left ventricular hypertrophy. However, it is interesting to note that the amount of LVH may be conversely impacting the adiposity of an individual through complex interactions of metabolism and behavior.

Interestingly more traditional measures of cardiovascular health, triglycerides and cholesterol (183), did not show significant associations with LVH regardless of sex or stress status. However, these measures were taken when the animals were young – immediately following chronic stress exposure. So while young measurements of these traditional markers did not predict later hypertrophy, they are not indicative of cardiac function at the time of hypertrophy measurement.

4.3 Bimodal dysfunction

Exposure to chronic stress and consequent repeated activation of the HPA axis and autonomic systems are likely impacting cardiac work (184). It is clear that in some animals this has led to increased left ventricular hypertrophy. However, the group of animals that present with low LVH may also show some level of dysfunctionality. This is apparent in stress specific changes in glucocorticoid release. Particularly, young females show an increase in total FST glucose mobilization within the mid LVH group, but a significant decrease when compared to the high LVH group. This stress specific bimodal change occurs in a number of metabolic markers and may be indicative of dysfunctionality in both extremes of LVH hypertrophy. This coincides with research indicating rats with low glucocorticoid responsiveness have similar sympathetic dysregulation to highly responsive animals following stress (185).

5. Conclusions

The results of this study indicate that while chronic stress exposure in adolescents impacts cardiometabolic physiology immediately following exposure, the effects of age have a greater impact particularly in female rats. However, in male rats, responses to acute stress are predictive of later cardiac hypertrophy, indicating the potential for susceptible subpopulations to be identified. Importantly, these results indicate sex-specific responses following chronic stress differentially impact later individual cardiac health. Thus, while some animals show resiliency, those that are susceptible may be at an increased risk for CVD. Consequently, responses to early life stress may predict later CVD risk in a sex-specific manner.

CHAPTER 4: PREFRONTAL-MEDULLARY CIRCUIT INHIBITION DYSREGULATES SEX-SPECIFIC ENDOCRINE RESPONSES TO METABOLIC STRESS

1. Introduction

Metabolic diseases, such as diabetes mellitus, increasingly impact mortality and years lived with disability (186). A greater population percentage also experiences symptoms of metabolic dysfunction, referred to as metabolic syndrome, at a subclinical level (187). Symptoms of metabolic syndrome increase subsequent disease risk and are characterized by abdominal obesity, hypertension, hyperlipidemia, and insulin resistance (21). While the etiology of metabolic diseases and metabolic syndrome is multifactorial (187–189), environmental factors, such as stress, strongly contribute to the pathogenesis of these conditions (20, 22, 190). Broadly defined, stress is any real or perceived threat to homeostasis and results from a variety of life events (7). Cumulative life stressors reduce organismal adaptive capacity (5). Importantly, these disease processes have sex-specific variations that are important for both prognosis and treatment outcomes (191, 192).

Exposure to chronic stress is strongly associated with deleterious changes across many physiologic systems that impact metabolic function (22, 193). Particularly in adolescents, chronic stress can impact cognitive and emotional development and contribute to abdominal obesity and metabolic syndrome (20, 23). Additionally, chronic stress has been shown to increase the risk of hypertension and myocardial infarction (25, 194), increase chronic pain (195) and inflammatory responsiveness (196), and alter circadian rhythmicity (14). These changes are part of a complex homeostatic dysregulation that impacts metabolic function and adaptive capacity.

While stress appraisal occurs in multiple brain regions, our understanding of the neurobiological basis of how stress impacts systemic physiology and subsequent disease pathogenesis is still largely unknown. The human ventromedial prefrontal cortex (vmPFC) and rodent homolog, the infralimbic cortex (IL), are important in limiting stress reactivity (68), influencing coping behavior (159), and have sex-specific impacts on motivational behaviors (73). However, this region does not directly innervate stress-reactive neuroendocrine cells – indicating more complex circuitry likely underlies these effects. Activation of projections to the rostral ventrolateral medulla (RVLM), an important regulator of sympathetic activity and glucoregulation (197, 198)), were recently shown to have sex-specific reductions in stress responsivity (199).

Therefore, to test the necessity of the IL-RVLM circuit in glucoregulation following chronic variable stress (CVS) in males and females, we used an intersectional genetic approach to selectively inhibit this circuit and then glycemically challenge animals with an acute metabolic stress test. Specifically, we hypothesized that the inhibition of this circuit will exacerbate the glucodysregulation associated with chronic stress with females showing greater susceptibility to metabolic dysfunction.

2. Methods

2.1 Subjects

Age-matched young adult (PND ~42) male and female rats were obtained from Charles River (Wilmington, MA). Animals were kept on a 12-hour light cycle with food and water *ad libitum*. Following stereotaxic surgery, rats were housed individually in a temperature- and humidity-controlled room. All experiments were approved by the Colorado State University Institutional Animal Care and Use Committee (Protocol:1392) and complied with the National

Institutes of Health Guidelines for the Care and Use of Laboratory Animals. All rats had daily welfare checks by veterinary and/or animal resource staff.

2.2 Design

Cohorts of young adult male and female rats (PND ~42, 2 cohorts/sex) were assigned to a 2X2 group of either CVS or No CVS and circuit-intact or circuit-inhibited (**Fig. 16**). These animals were randomly assigned to both viral group and CVS group within sex (n = 6-10/group/sex). CVS and No CVS groups within sex were weight-matched to ensure no significant differences in animal size. Male and female cohorts were run consecutively, preventing between-sex analyses. CVS began 5 weeks after viral injection (D0-D14). Fasted glucose tolerance testing (GTT) took place on day 15 followed by tissue collection on day 18.

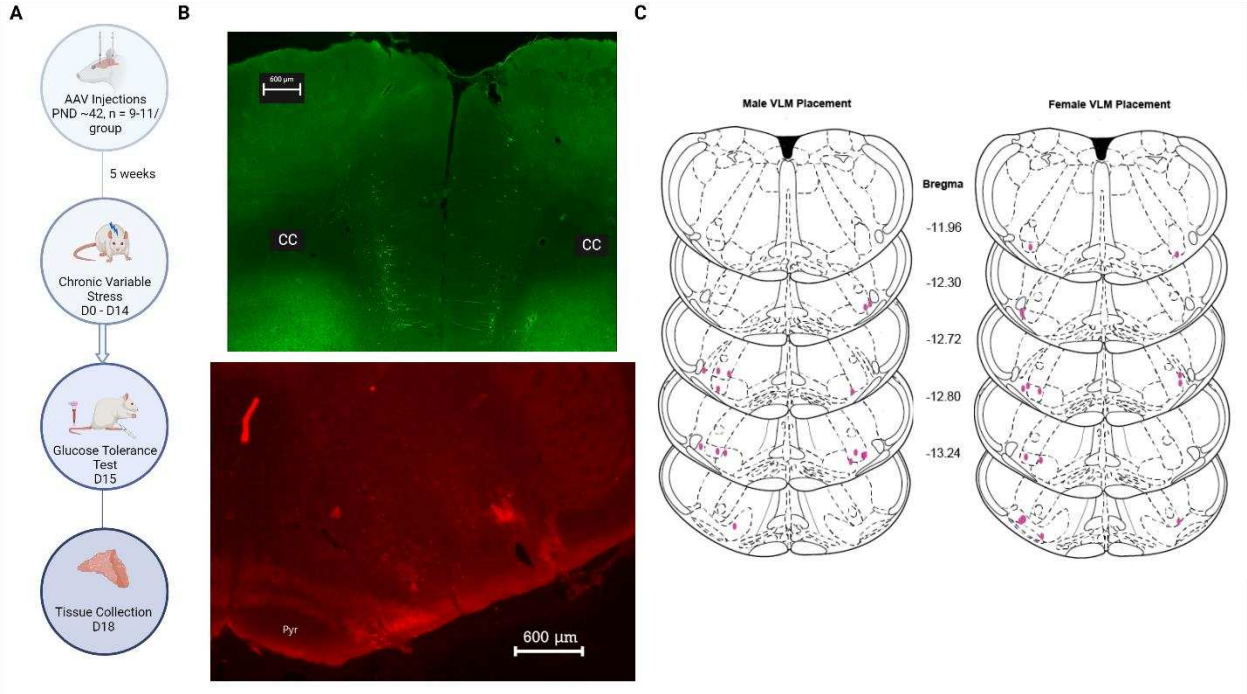

Figure 16. Experimental design and injection placement. Two distinct cohorts of male (n = 6-10/group) and female (n = 8-10/group) underwent viral injection followed by chronic stress exposure. Rats were then acutely challenged with GTT and tissue collected (A). Representative

images (B) of viral injection placement in both IL and VLM for males and females (C). Created with BioRender.

2.3 Microinjections

An intersectional genetic approach was used to selectively inhibit RVLM projecting IL neurons. Animals were first anesthetized with isoflurane (1-5%) followed by subcutaneous administrations of analgesic buprenorphine-SR (0.5 mg/kg). Unilateral RVLM injections (Female: 12.25 mm posterior to bregma, 1.9 mm lateral to midline, 9.95 mm ventral to skull; males: 12.25 mm posterior to bregma, 1.9 mm lateral to midline, 10.2 mm ventral to skull) were administered with a retrograde adeno-associated viral (AAV) Cre-construct (Female: 0.3 ul, male: 0.5ul) (Addgene, Watertown, MA). Injection lateralization was randomized and balanced among group and sex. Subsequently, bilateral IL injections (Female: 2.3 mm anterior to bregma, 0.5 mm lateral to midline, and 4 mm ventral from dura; males: 2.7 mm anterior to bregma, 0.6 mm lateral to midline, and 4.2 mm ventral from dura) of either a Cre-dependent Tetanus toxin Light Chain (TeLC) (Stanford Gene Vector and Virus Core, Stanford, CA) or Cre-dependent Green Fluorescent Protein (GFP) (Addgene, Watertown, MA) were administered (female: 0.6 ul, male: 0.8ul). TeLC acts to cleave synaptobrevin and inhibit neurotransmitter release, thereby inhibiting the IL-RVLM circuit (200, 201). Viral expression and recovery lasted for 5 weeks.

2.4 Stress Paradigm

Rats were exposed to CVS 5 weeks following viral injection. CVS lasted for 14 days and consisted of twice daily (AM and PM) randomized stressors and interspersed overnight stressors (4, 155, 156). Stressors included restraint (plexiglass tube, 1 h), shaker (100 rpm, 1), cold room (4˚ C, 1 h), brightly lit open field (1 m^2, 1 h), forced swim (23-27˚ C, 10 min), elevated platform (0.5 m, 1 h), predator odor (fox, coyote, 1 h), bright light exposure (overnight, 12 h),

and damp bedding (overnight, 12 h) (4, 156). All rats were fed *ad libitum* throughout CVS. Food was removed the morning of day 15 4 h prior to GTT.

2.5 Glucose tolerance testing

Following chronic stress on the morning of day 15, endocrine metabolic reactivity and glucose homeostasis was assessed using a 4h fasted GTT (4, 161). GTT was completed more than 12 h following the final stressor and took place between hours 3 - 6 of the light phase. A baseline blood sample was taken via tail clip prior to glucose injection (1.5 g/kg, 25% glucose, i.p.). Blood was then collected at 15, 30, 45, and 90 min. post injection and placed in tubes with 10 µl of 100 mmol/L ethylenediamine tetraacetate. Blood glucose was quantified in duplicate with Bayer Contour Next Glucometers and test strips (Ascensia, Parsippany, NJ). Blood was centrifuged at 3000 x g for 15 min at 4˚ C and stored at -20˚ C until analysis. Plasma corticosterone (C. V. = 6.6 – 8,0 %; ENZO Life Sciences, Farmingdale, NY), plasma glucagon (C. V. < 10 %; Crystal Chem, Elk Grove Village, IL), and plasma insulin (C. V. ≤ 10 %; Crystal Chem, Elk Grove Village, IL) were determined by ELISA. Vaginal swabs were taken for estrous analysis in females.

2.6 Tissue collection

Two days day following GTT, animals were injected with sodium pentobarbital (100 mg/Kg) and perfused transcardially with 0.9% saline followed by 4.0% paraformaldehyde in 0.1 M phosphate buffer solution. Brain tissue was collected for technical validation. Tissue was post-fixed in 4.0% paraformaldehyde for 24 hours at room temperature before storage in 30% sucrose at 4˚ C. Adrenal glands were collected and weighed. Vaginal swabs were taken for estrous analysis in females.

2.7 Statistical analyses

All data are presented as mean ± standard error of the mean (SEM). Animals were excluded from analyses if injection placement was determined to be greater than 0.5 mm from region boundary. All data were analyzed using Prism 10 (GraphPad, San Diego, CA), with a significance of $p < 0.05$ for all tests. All analyses were completed within sex. Body weight during CVS was analyzed by 3-way repeated measures ANOVA within sex with stress, viral condition, and time as conditions. Food intake and adrenal weight were compared via 2-way ANOVA with stress and viral condition. Hormones analyses were completed via 2-way ANOVA within stress with viral condition and time (repeated measure) as conditions. Tukey post-hoc analysis was used for within group comparisons. Correlative measures were determined by Pearson's r two-tailed analyses. See supplemental table (**S.2**) for all ANOVA analysis results.

3. Results

3.1 Body weight, food intake, and adrenal weight

Body weight analysis over the course of CVS (**Fig. 17**) showed main effects in females of day [$F(4, 132) = 6.825$, $p < 0.0001$] and stress [$F(1, 33) = 6.641$, $p = 0.0146$] and an interaction of day and stress [$F(4, 132) = 23.80$, $p < 0.0001$]. In females, food intake also reflected a main effect of stress [$F(1, 33) = 13.58$, $p = 0.0008$] where TeLC CVS females had significantly decreased food intake compared to TeLC No CVS females ($p = 0.0402$). When corrected for body weight, there were no significant differences in adrenal weight in females.

The body weights of male animals over the course of CVS showed a main effect of day [$F(4, 124) = 44.01$, $p < 0.0001$] and an interaction of day and stress [$F(4, 124) = 49.58$, $p < 0.0001$]. There were no significant differences in food intake over CVS. There was a main effect of stress on adrenal weight [$F(1, 28) = 20.32$, $p = 0.0001$]. Both GFP CVS males ($p = 0.0469$)

and TeLC CVS males (p = 0.0069) had significantly increased adrenal weights compared to their unstressed counterparts.

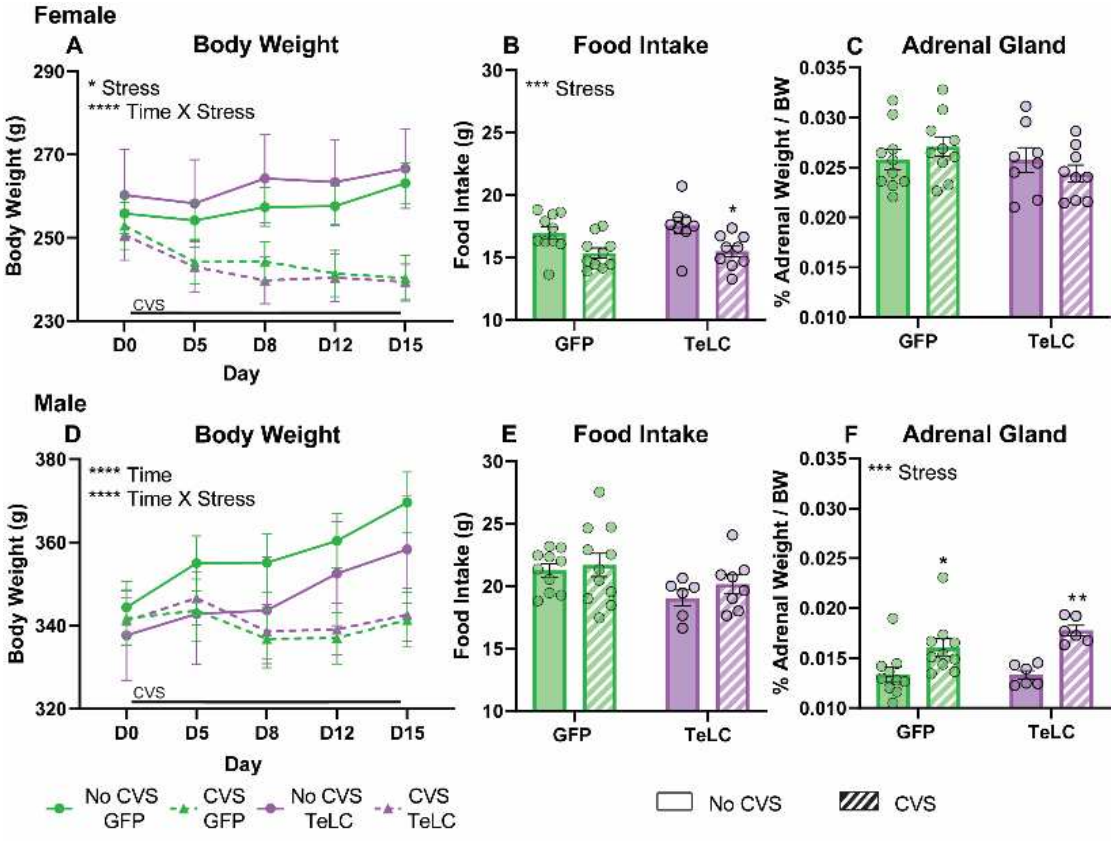

Figure. 17. Somatic measures following CVS. Female and male (n = 6-10/group/sex) body weight (A, D) and food intake (B, E) were measured over the course of CVS. Adrenal weight corrected for body weight (C, F) were measured at tissue collection. Data are expressed as mean ± SEM. * p<0.05, ** p<0.01, *** p<0.001, **** p<0.0001.

3.2 Hormone responses to GTT

Acute responses to metabolic challenge varied greatly between sex, stress, and viral condition. In females, the impacts of IL-RVLM (TeLC) inhibition mirrored chronic stress-induced glucocorticoid hypersecretion (**Fig. 18**) but had diverging impacts on metabolic reactivity when coincident with chronic stress. Unstressed TeLC females both decreased glucose clearance [F(1, 79) = 10.36, p = 0.0019] and increased corticosterone secretion [F(1, 79) = 14.41, p =

0.0003] compared to circuit-intact GFP controls with corticosterone being significantly increased 45 minutes after glucose injection (p = 0.0083). Interestingly, these animals showed no differences in plasma insulin or glucagon following GTT.

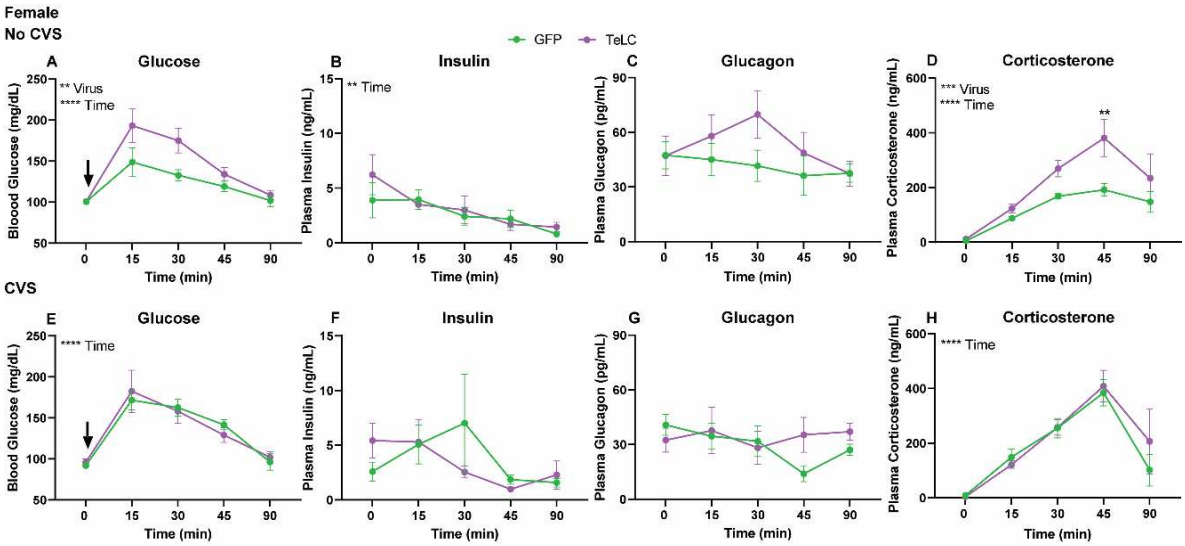

Figure 18. Female GTT hormonal responses. Following CVS, animals were challenged with GTT (n = 6-10/group/sex). Animals were compared within stress history: No CVS GFP (n = 10), No CVS TeLC (n = 8), CVS GFP (n= 10), CVS TeLC (n = 9). Blood was taken at 0, 15, 30, 45, and 90 min. At each time point total blood glucose (A, E), plasma insulin (B, F), plasma glucagon (C, G), and plasma corticosterone (D, H) were quantified over the 90-minute time course. Data are expressed as mean ± SEM. ↓ represents glucose bolus. ** p<0.01, *** p<0.001, **** p<0.0001.

The effects of chronic stress in female GFP rats corroborate our previously reported effects of dysfunctional glucoregulation (4). Interestingly, TeLC CVS females showed no significant differences from CVS GFP female blood glucose, plasma corticosterone, insulin, or glucagon. However, these animals still show glucodysregulation with high blood glucose and corticosterone values. This indicates that IL-RVLM inhibition does not interact with CVS to exacerbate the deleterious metabolic effects of chronic stress in females.

In No CVS males, circuit inhibition did not overtly change glucose tolerance or corticosterone responses to GTT (**Fig. 19**). However, these animals did have differences in the

underlying metabolic regulation that are reflected in their metabolic responsivity. No CVS TeLC males showed significantly increased glucagon compared to GFP controls [F(1, 63) = 4.015, p = 0.0494]. There were no significant differences in plasma insulin across the time course.

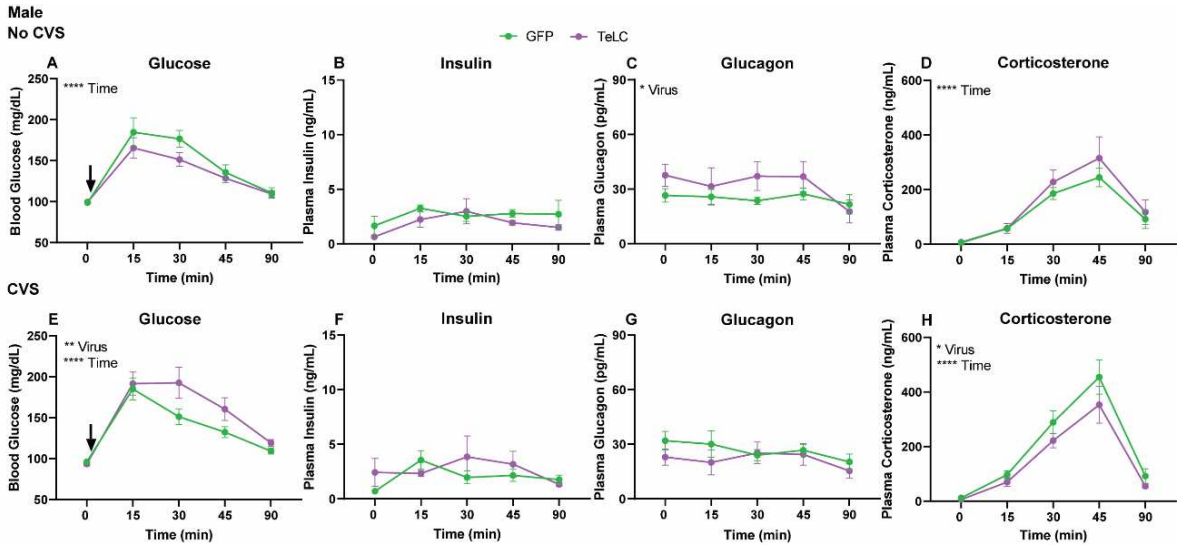

Figure 19. Male GTT hormonal responses. Following CVS, animals were challenged with GTT (n = 6-10/group/sex). Animals were compared within stress history: No CVS GFP (n = 10), No CVS TeLC (n = 6), CVS GFP (n= 11), CVS TeLC (n = 7). Blood was taken at 0, 15, 30, 45, and 90 min. At each time point total blood glucose (A, E), plasma insulin (B, F), plasma glucagon (C, G), and plasma corticosterone (D, H) were quantified over the 90 minute time course. Data are expressed as mean ± SEM. ↓ represents glucose bolus. * $p<0.05$, ** $p<0.01$, **** $p<0.0001$.

Following chronic stress, TeLC males showed significant deviations from the metabolic profile usually seen following chronic stress where males seem to have improved metabolic responses (4). TeLC males both significantly decreased glucose clearance [F(1, 81) = 7.018, p = 0.0097) and decreased corticosterone [F(1, 80) = 4.078, p = 0.0468]. There were no significant differences in insulin or glucagon across the time course.

3.3 Metabolic responsivity: females

To examine metabolic responsivity, we looked at relative pancreatic islet cell responsivity using a ratio of plasma insulin:plasma glucacon (I:G). This measure provides relative

sympathetic:parasympathetic input to the endocrine cells of the pancreas, which is vital for downstream glucoregulation and homeostatic adaptation (202). Additionally, we used regressive correlations to examine associations between glucoregulation and hormone efficacy over the course of the GTT. These combined analyses give insight into relative metabolic responsivity and pathway relationships.

In females, there were no significant differences in I:G between the unstressed TeLC and GFP animals (**Fig. 20A)**. However following chronic stress, GFP females showed a main effect of time X virus interaction on I:G [$F(4, 77) = 2.57$, $p = 0.0444$]. The TeLC CVS females more closely represented the unstressed females (**Fig. 20B**).

These pathway differences are reflected in correlative data (**Fig. 21**). In unstressed GFP females, plasma insulin at 90 min. is negatively correlated to blood glucose at 15 min. ($r = -0.92$, $p = 0.009$), 45 min. ($r = -0.896$, $p = 0.016$), and 90 min. ($r = -0.85$, $p = 0.032$) post-injection. Baseline glucagon is positively correlated to blood glucose at 45 min ($r = 0.72$, $p = 0.019$) and glucagon 15 min. post-injection is negatively correlated to glucose 15 min. post-injection ($r = -0.853$, $p = 0.003$). Glucose levels at 15 min. positively correlated to plasma corticosterone at 30 min. ($r = 0.644$, $p = 0.044$).

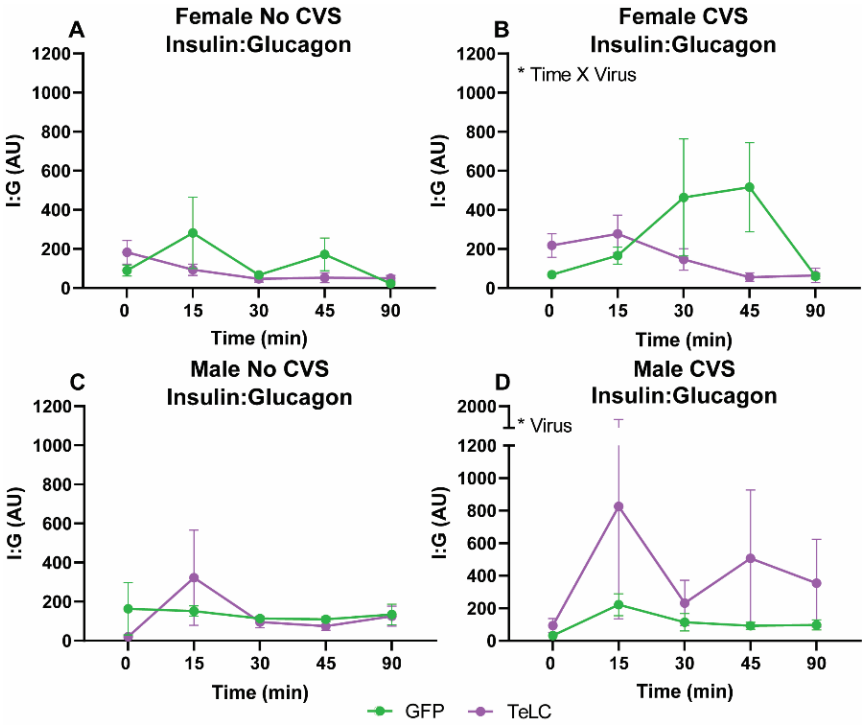

Figure 20. Insulin:Glucagon ratio over GTT. The ratio of I:G was quantified at each time point for both females (A, B) and males (C, D) by stress history (n = 6-10/group/sex). Data are expressed as mean ± SEM. * p<0.05.

Following CVS, these relationships change dramatically. Importantly, baseline plasma insulin is positively correlated to blood glucose at 15 min. ($r = 0.75$, $p = 0.032$) indicating changes in glucoregulation are associated with insulin insensitivity. Additionally, glucagon levels 15 min. post-injection are positively correlated to baseline glucose ($r = 0.699$, $p = 0.024$) and corticosterone at 15 min. ($r = 0.927$, $p < 0.0001$) and 30 min. ($r = 0.756$, $p = 0.018$) positively correlated to blood glucose at 15 min.

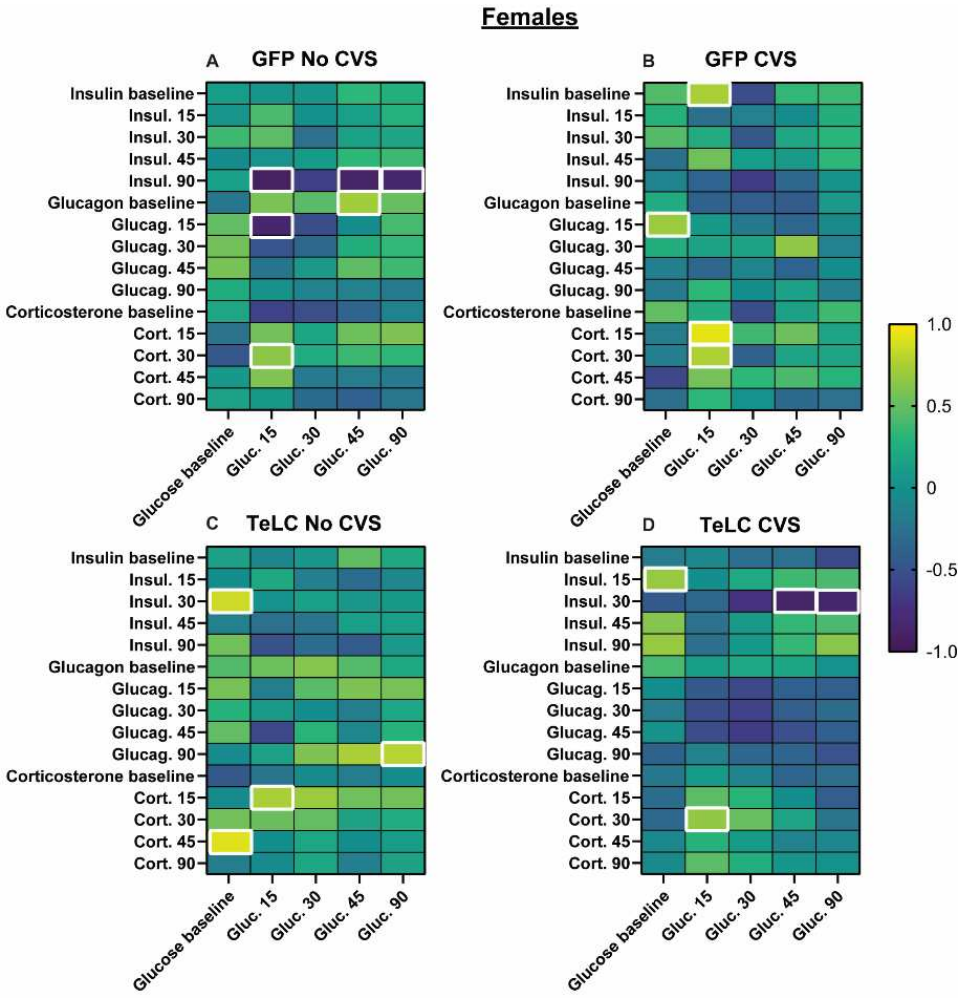

Figure 21. Regressive analysis: females. Pearson correlations were run within each group to examine the relationship between glucose and insulin, glucagon, and corticosterone. Significant associations ($p < 0.05$) are bolded.

IL-RVLM inhibition in unstressed females leads to a positive correlation between baseline glucose levels and insulin at 30 min. ($r = 0.853$, $p = 0.007$). Following the GTT, glucagon levels at 90 min. positively correlated to blood glucose at 90 min. ($r = 0.791$, $p = 0.034$). Interestingly, baseline glucose positively correlated to corticosterone at 45 min. ($r = 0.908$, $p = 0.002$) and glucose at 15 min. correlates to corticosterone at 15 min. ($r = 0.745$, $p = 0.034$).

In chronically stressed females, circuit inhibition again changes the metabolic profile. Baseline glucose correlated to insulin levels at 15 min. post-injection ($r = 0.681$, $p = 0.043$). Insulin levels at 30 minutes then negatively correlated to blood glucose at 45 min. ($r = -0.886$, $p = 0.008$) and 90 min. ($r = -0.854$, $p = 0.014$). There were no major correlations between glucagon and blood glucose. Blood glucose at 15 min. correlated to corticosterone at 30 min. ($r = 0.666$, p 0.05).

3.4 Metabolic responsivity: males

Male metabolic reactivity was vastly different from their female counterparts. While there was no difference in the I:G ratio between the unstressed GFP and TeLC males (**Fig. 20C**), TeLC males that have undergone chronic stress have a significantly increased I:G ratio compared to GFP animals [$F(1, 76) = 5.048$, $p = 0.0276$] (**Fig 20D**). This is in opposition to the effect on I:G seen in their female counterparts.

There were fewer endocrine correlations across all male groups (**Fig. 22**). In No CVS male GFP rats, baseline glucose positively correlated to insulin 45 min. post-injection ($r = 0.71$, $p = 0.031$). Baseline glucose also correlated to glucagon at 45 min. ($r = 0.79$, $p = 0.021$). Additionally, baseline glucagon correlated to glucose at 30 min. ($r = 0.61$, $p = 0.031$) and glucagon levels at 45 min. correlate to glucose 90 min. post-injection ($r = 0.74$, $p = 0.036$). There were no significant correlations with corticosterone. Additionally, in chronically stressed GFP males there were no correlations with insulin, glucagon, or corticosterone. However, in TeLC unstressed males, insulin levels at 15 min. post-injection positively correlate to glucose levels at 30 min. ($r = 0.83$, $p = 0.04$). There were no significant correlations with glucagon or corticosterone. TeLC chronically stressed males had no significant correlations with either insulin or corticosterone. Importantly, baseline glucose was negatively correlated to baseline glucagon ($r = -0.08$, $p = 0.032$) and glucagon levels at 45 min. ($r = -0.81$, $p = 0.026$).

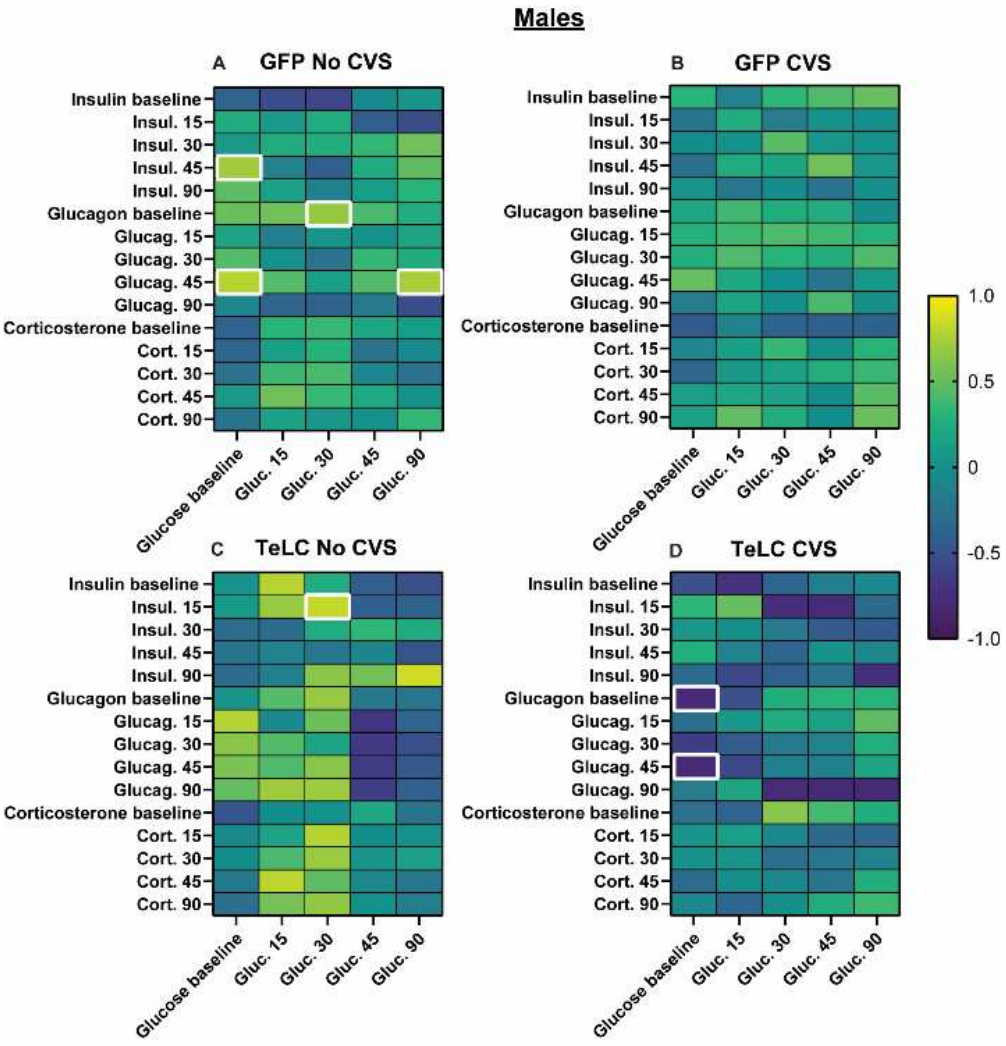

Figure 22. Regressive analysis: males. Pearson correlations were run within each group to examine the relationship between glucose and insulin, glucagon, and corticosterone. Significant associations ($p < 0.05$) are bolded.

3.5 Estrous cycle cytology

Vaginal cytology was done to determine estrous phase following GTT and at tissue collection (**Table 3**). These animals were allowed to free cycle and were not staged across group to prevent bias toward one reproductive hormone profile.

Table 3: Estrous stage at GTT and tissue collection.

	GTT				Tissue Collection			
	Proestrus (%)	Estrus (%)	Metestrus (%)	Diestrus (%)	Proestrus (%)	Estrus (%)	Metestrus (%)	Diestrus (%)
GFP No CVS	20	20	10	50	0	30	40	30
GFP CVS	40	20	40	0	10	50	20	20
TeLC No CVS	63.63	9.09	27.27	0	9.09	54.54	9.09	27.27
TeLC CVS	54.54	18.18	18.18	9.09	18.18	27.27	36.36	18.18

4. Discussion

4.1 IL-RVLM sympathetic dysregulation: females

Glucoregulation is a complex and dynamic process that is impacted by sex and prior stress history. These data indicate that IL-RVLM circuitry is necessary for glucoregulation in females. Circuit inhibition in these animals lead to decreased glucose clearance and increased corticosterone secretion regardless of stress history, further supporting the evidence that the IL-RVLM acts as a sympathetic inhibitor. Loss of this input leads to broad sympathetic dysregulation that stimulates hypothalamic-pituitary-adrenal axis activation. Further, this activation likely leads to the upregulation of gluconeogenic process that are reflected in the positive correlation of glucose to both corticosterone and glucagon in the TeLC No CVS females. In unstressed females, these changes are impacting metabolic regulatory systems, and consequently glucose regulation, seemly without changing pancreatic activity. This collateral effect on homeostatic function potentially acts as a detriment to adaptive capacity.

Interestingly, when IL-RVLM inhibition is combined with chronic stress exposure in females, gross glucodysregulation does not seem to be exacerbated. While these animals also show decreased glucose clearance and increased corticosterone release, it is not significantly

worse following chronic stress. However, pancreatic activation in these animals indicates an increase in gluconeogenic processes compared to GFP CVS females. This is further reflected in the positive correlative relations between glucose and insulin. Initially, the positive correlation between baseline glucose and the 15 min insulin response is indicative of an early compensatory response. However, the inverse correlation at 45 and 90 min with higher glucose relating to lower insulin indicates that this compensatory response is likely overridden by gluconeogenesis.

4.2 Insulin sensitivity following chronic stress

While glucodysregulation in females following chronic stress has been previously shown (4), the underlying mechanisms driving these changes has not been investigated. In these CVS GFP females, the increase in insulin over the GTT combined with the positive correlation between baseline insulin and glucose indicate that there is an insulin-resistant glucose intolerance in these animals. Therefore, chronic stress in females leads to dysregulation of counterregulatory mechanisms that maintain glucose homeostasis. Consequently, these results support clinical data indicating early life stress predisposes females to metabolic syndrome that can lead to further metabolic disease (23).

4.3 IL-RVLM homeostatic dysregulation: males

In male rats, the impact of inhibiting the IL-RVLM circuit is reduced. Unstressed animals do not show glucose intolerance or corticosterone hypersecretion. However, these animals do show increased glucagon throughout the GTT indicating an increase in gluconeogenic processes. This increase in gluconeogenesis is likely reflective of an increase in sympathetic activation, similar to their female counterparts. However, the lack of corresponding changes in glucoregulation could be indicative of increased metabolic homeostatic capacity.

Interestingly, when coincident with chronic stress Il-RVLM inhibition in males decreases glucose clearance. However, these animals show an increased I:G ratio and decreased corticosterone secretion. The positive correlation between glucagon and glucose in these animals indicates that circuit inhibition is still leading to sympathetic disinhibition. However, the shift in pancreatic activation toward insulin production and the decrease in corticosterone release may be characteristic of an adaptive response to metabolic stress. This complex interplay of homeostatic processes and sympathetic dysregulation in these animals suggests they may have a wider metabolic homeostatic range.

4.4 Sex-dependent homeostatic function

The relationships between glucoregulatory hormones and glucose vary immensely based on sex, stress history, and circuit disruption. Interestingly, these relationships were less pronounced in males, with GFP CVS males showing no significant relationships. One potential explanation of this phenomena is each counterregulatory mechanism is acting to dampen each individual mechanism. These interactions are vital in maintaining glucoregulation but act to mask statistical relationships. This is emphasized in the circuit-inhibited males where very few correlations present as significant. This further supports the idea that as homeostatic perturbations increase, the influence of counterregulatory mechanisms is altered. In females, these mechanisms become dysregulated and as feedback becomes uncoupled more relationships become statistically significant. It is important to note that in control animals, these relationships are present because of a lack of homeostatic challenge. Interestingly, these control relationships are different between males and females indicating that baseline metabolic responses are sex dependent. This suggests that sex plays an important role in determining metabolic function (192).

The current study aimed to examine the necessity of the IL-RVLM circuit in metabolic stress responding following chronic stress exposure. These data support the hypothesis that the

IL-RVLM is necessary for appropriate metabolic homeostasis and the inhibition of the circuit leads to sex-dependent glucodysregulation and the impingement of homeostatic regulation. While the analysis of these results is limited to within sex, further experiments to directly compare male and female function could elucidate specific metabolic changes that lead to dysfunction. Additionally, further analysis of metabolic function by protein analysis of peripheral insulin signaling may reveal downstream effects of metabolic dysfunction. Overall, this study provides novel insight into the glucoregulatory function of the RVLM and how chronic stress interacts in a sex-specific manner to change metabolic function. This understanding is vital to developing a foundation for sex-specific prevention and treatment of metabolic disease.

CHAPTER 5: PREFRONTAL-MEDULLARY INHIBITION LEADS TO SEX-SPECIFIC CARDIAC AND MICROVASCULAR DYSFUNCTION FOLLOWING CHRONIC STRESS

1. Introduction

Cardiovascular disease (CVD) is the leading cause of death worldwide (176) and is the leading cause of death in women (175). The development of CVD has multiple etiologies and is characterized by a range of physiologic changes across multiple organ systems that influence cardiac and vascular function (1, 26, 183). Many of these changes precede pathologic progression and additionally contribute to the development of comorbid conditions such as diabetes mellitus and hypertension (26). Therefore, understanding how these pathways are regulated and the mechanistic changes they undergo is essential to better understanding and mitigating CVD progression.

Chronic stress is a precipitating factor in the development of CVD, with detrimental changes to both cardiovascular structure and function (184). Particularly, exposure to chronic stress leads to left ventricular hypertrophy, decreased aortic compliance, and fibrotic changes (203, 204), as well as atherosclerotic change (205) and diastolic dysfunction (206, 207), an early predictor of cardiac disease. Importantly, vascular and microvascular function following stress exposure is an emerging area of CVD treatment. Stress exposure is known to contribute to systemic cardiovascular dysfunctionality that indirectly impacts endothelial function, such as hypertension and peripheral resistance (208), as well as having direct action on vascular function (209). The mechanisms through which chronic stress leads to vascular dysfunction are likely varied and multifaceted. However, evidence suggests these changes may be mediated by alterations in vasoactive receptors that impact oxidative mediators like nitric oxide (NO) (209, 210). It is important to note that this vascular dysfunction is largely considered through the lens of large conducting vasculature. However, microvascular dysfunction, that is often characterized

by reduced endothelium-dependent relaxation and exaggerated vasoconstriction (211, 212), likely preempts wider dysfunction. Therefore, elucidating the effects of chronic stress on microvascular function and the neurobiologic basis for these changes is vital.

While there are several brain regions responsible for cardiovascular regulation and stress appraisal, how these regions interact to regulate and mitigate deleterious changes is largely unknown. The prefrontal infralimbic (IL) cortex, which is known to sex-specifically impact stress reactivity (155, 159), to rostral ventrolateral medullary (RVLM) circuit likely plays an important role in the autonomic regulation of the cardiovascular system through the actions of catecholaminergic neurons (198, 199). Therefore, we sought to isolate the impact of the IL-RVLM circuit in the autonomic regulation of cardiovascular reactivity. To test the necessity of this circuit following chronic variable stress (CVS), we used a genetic approach to selectively inhibit the IL-RVLM circuit (199, 201) and examine *in vivo* and *ex vivo* measures of cardiac structure and vascular reactivity. Specifically, we hypothesized that IL-RVLM inhibition would lead to autonomic imbalance that alters microvascular reactivity and cardiac structure dependent on chronic stress exposure and sex.

2. Materials and methods

2.1 Subjects

Age matched young adult male and female rats (PND ~ 42) were obtained from Charles River (Wilmington, MA). Animals were housed with a 12 on-12 off light cycle, water *ad libitum,* and food *ad libitum* depending on experimental protocol. Following stereotaxic injection, animals were housed individually. All experiments were approved by the Colorado State University Institutional Animal Care and Use committee (protocol: 1392) and complied with the National

Institutes of Health Guidelines for the Care and Use of Laboratory Animals. All animals had daily welfare checks by veterinarian and/or animal resource staff.

2.2 Experimental design

2.2.1 Experiment 1: Cardiac analysis

Cohorts of young adult male and female rats (PND ~42, 2 cohorts/group) were randomly assigned to a 2x2 group of either CVS or No CVS and circuit intact or circuit inhibited (n = 6 - 11/group/sex) (**Fig. 23**). CVS and No CVS animals were weight matched to account for variability in body weight. All animals were fed *ad libitum* throughout the experiment. Male and female cohorts were run consecutively, preventing comparison directly between sex. CVS began 5 weeks post viral injection (D0-D14), metabolic analyses were run on day 15 as previously reported (Chapter 4), echocardiogram and aortic velocity analysis were completed (D16-17), followed by tissue collection on day 18.

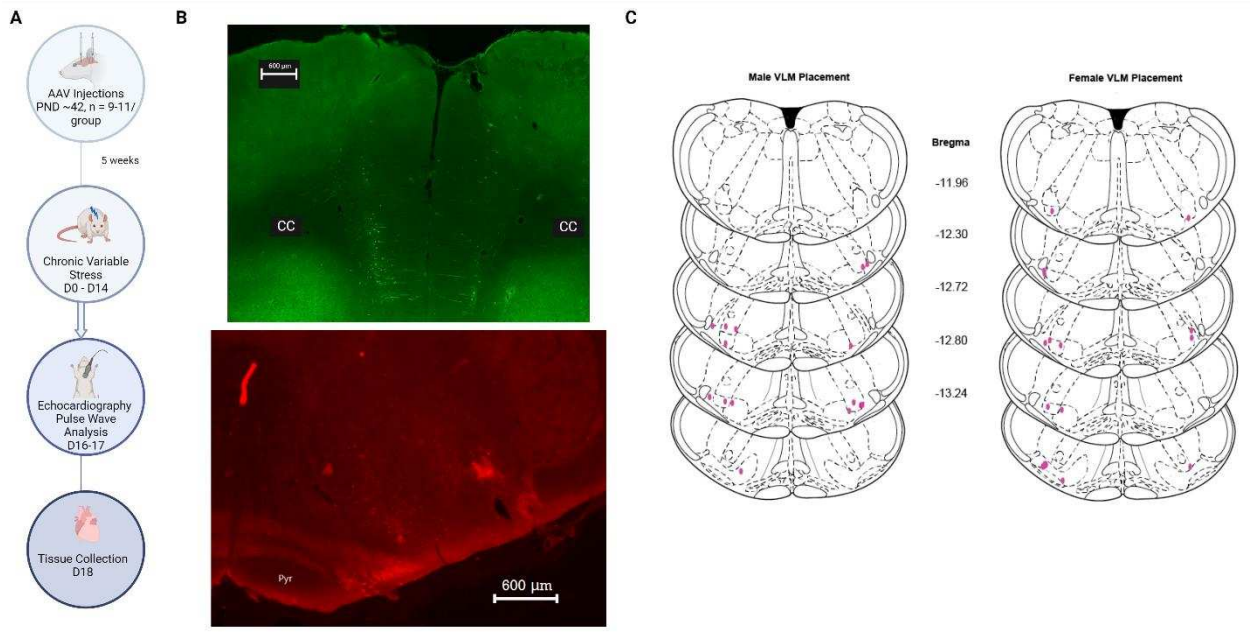

Figure 23. Experiment 1 design and injection placement. Two distinct cohorts of male (n = 6-10/group) and female rats (n = 8-10/group) underwent viral injection followed by chronic stress exposure. *In vivo* measures of cardiac function, echocardiography and pulse wave analysis,

were then completed prior to tissue collection (A). Representative images (B) of viral injection placement in both IL and VLM for males and females (C). Created with BioRender.

2.2.2 Experiment 2: Vascular analysis

Staggered cohorts of young adult male and female rats (PND ~42) were randomly assigned to the 2x2 organization above (n = 4 – 6/group/sex) (**Fig. 24**). Each cohort was evenly distributed between groups and was sex-specific. Animals were randomly assigned within each cohort. CVS and No CVS animals were weight matched prior to the start of CVS. However, No CVS animals were food restricted at a 10% reduction of the average control food intake for each sex during experiment 1 over the course CVS (M: 19.13 g/day, F: 15.29 g/day) to account the impact of body composition on vascular function (156, 213). CVS animals had *ad libitum* food access. Because of the running nature of this design, some weight differences between CVS and No CVS animals remained. CVS began 5 weeks post viral injection (D0 – D14). Pressure myography, non-invasive hemodynamics, and tissue collection occurred on day 15, immediately following the completion of CVS.

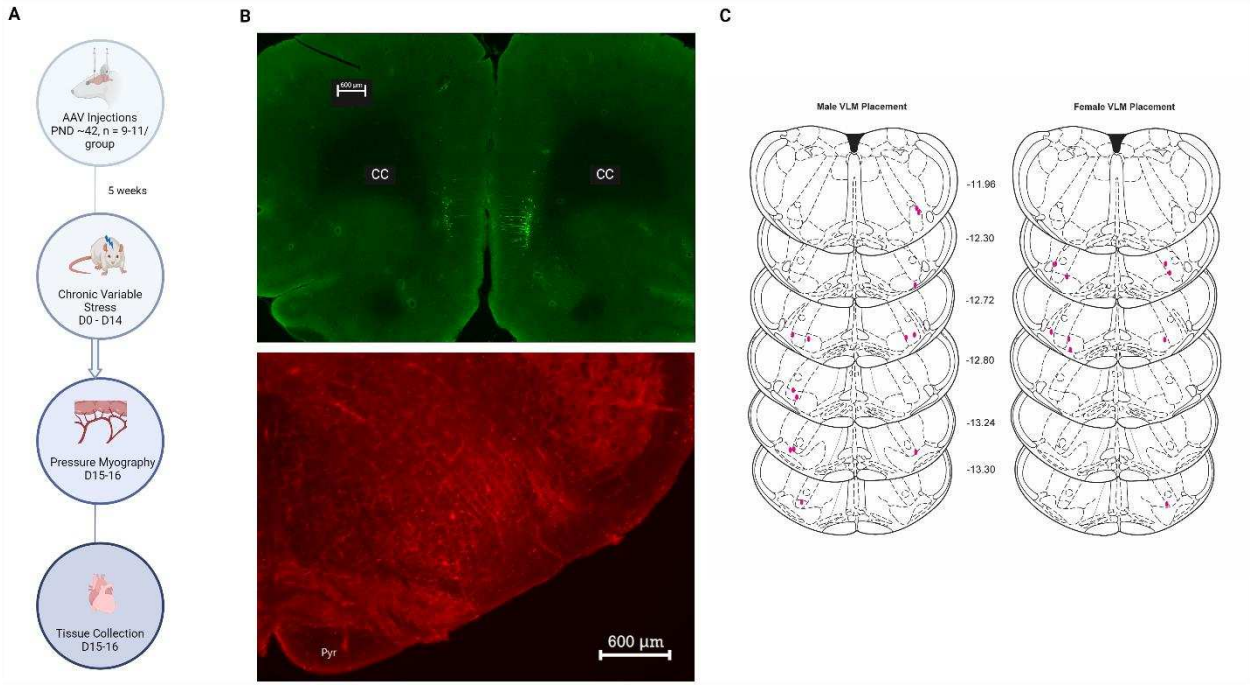

Figure 24. Experiment 2 design and injection placement. Cohorts of male and female (n = 4-6/group/sex) underwent viral injection followed by chronic stress. The day following stress exposure (D15), blood pressure was measured, tissue collected, and mesenteric arterioles used in pressure myography (A). Representative images (B) of viral injection placement in both IL and VLM for males and females (C). Created with BioRender.

2.3 Microinjections

An intersectional genetic approach was used in both experiments to selectively inhibit RVLM projecting IL neurons (199). In both experiments, animals were anesthetized (isoflurane, 1-5%) and given subcutaneous analgesic (buprenorphine-SR, 0.5 mg/Kg). Animals then received a unilateral RVLM microinjection (Female: 12.25 mm posterior to bregma, 1.9 mm lateral to midline, 9.95 mm ventral to skull; males: 12.25 mm posterior to bregma, 1.9 mm lateral to midline, 10.2 mm ventral to skull) with a retrograde adeno-associated viral (AAV) Cre-construct (Female: 0.3 ul, male: 0.5ul) (Addgene, Watertown, MA). Subsequently, bilateral IL injections (Female: 2.3 mm anterior to bregma, 0.5 mm lateral to midline, and 4 mm ventral from dura; males: 2.7 mm anterior to bregma, 0.6 mm lateral to midline, and 4.2 mm ventral from dura) of either a Cre-dependent Tetanus toxin Light Chain (TeLC) (Stanford Gene Vector and Virus Core, Stanford, CA) or Cre-dependent Green Fluorescent Protein (GFP) (Addgene, Watertown, MA) were administered (female: 0.6 ul, male: 0.8ul). Lateralization of RVLM injections were randomly alternated to reduce bias. TeLC acts to cleave synaptobrevin and to inhibit neurotransmitter release, thereby inhibiting the IL-RVLM circuit (200, 201). Viral expression and recovery lasted for 5 weeks.

2.4 Chronic stress paradigm

In both experiments (as described in Chapter 4), male and female CVS animals were exposed to twice daily (AM and PM) randomized stressors with intermittent overnight stressors (4, 155, 156). Stressors included (plexiglass tube, 1 h), shaker (100 rpm, 1), cold room (4˚ C, 1 h), brightly lit open field (1 m^2, 1 h), forced swim (23-27˚ C, 10 min), elevated platform (0.5 m, 1

h), predator odor (fox, coyote, 1 h), bright light exposure (overnight, 12 h), and damp bedding (overnight, 12 h) (4, 156).

2.5 Echocardiography, pulse wave velocity

In experiment 1, two days following CVS animals were anesthetized with 5% isoflurane and maintained at 1.5% isoflurane. A transverse echocardiogram was used to assess left ventricular functional and structural measures. Within 5 minutes of induction, a Phillips XD11 ultrasound system with a pediatric transducer was used to image 4-chamber angles in addition to M-mode measures of left ventricular diameter and wall thickness (73).

The following day, rats were again anesthetized with isoflurane (5% induction, 2% maintenance) and aortic flow velocity was measured using a 10 Hz pulse wave doppler. Velocity was determined from doppler measures of the right carotid and femoral artery. Each trial was completed within 15 minutes of induction with n = 6-8 biologic replicates/animal. Diastolic wall strain was calculated as [$\frac{(Posterior\ wall\ thickness(systole) - Posterior\ wall\ thickness\ (diastole))}{Posterior\ wall\ thickness\ (systole)}$] (217). Analysis was completed with DSPW doppler software (Indus Instruments, Houston, Tx).

2.6 Pressure myography and non-invasive hemodynamics

The day following CVS in experiment 2, animals were anesthetized with 5% isoflurane. Systolic and diastolic blood pressure was measured using a CODA tail cuff monitor (Kent Scientific, Torrington, CT). These measures were taken within 5-7 minutes of induction and maintenance at 1.5% isoflurane. 3-5 repeated measurements were taken per animal to reduce variability (201).

Following blood pressure measurements while under 5% isoflurane, animals were rapidly decapitated. The mesentery was then removed and placed in warm physiologic saline solution (PSS). 3rd order mesenteric arterioles were then dissected and returned to 37 ˚ C PSS. One

vessel was then mounted into a single chamber blind-ended pressure myography system (Living Systems, Fairfax, VT) (214, 215).

Following acclimation, the vessel was pressurized to 70 mmHg and function was tested using an endothelial-independent constrictor, Phenylephrine (PE), ranging from [1E-9] to [1E-5], an endothelial-independent dilator, Sodium Nitroprusside (SNP), from [1E-10] to [1E-4], and an endothelial-dependent dilator, Acetylcholine (ACh), from [1E-9] to [1E-5]. The vessel diameter was measured and averaged across the 30 seconds following equilibrium. The vessel was then pressurized to 120 mmHg, mimicking higher blood pressures recorded following stress, and the pharmacology was repeated to examine vascular function (216). Myogenic tone was also calculated as [$\frac{(Vessel\ Diameter\ (Ca^{2+}-free\ PSS)-Vessel\ Diameter\ (Ca^{2+}\ PSS))}{Vessel\ Diameter\ (Ca^{2+}-free\ PSS)} X100$] from vessel diameters measured across 20 to 120 mmHg in both PSS (active tone) and Calcium free PSS (passive tone).

2.7 Tissue Collection

In experiment 1 following acute measurements, animals were injected with sodium pentobarbital (100 mg/Kg) and perfused transcardially with 0.9% saline followed by 4.0% paraformaldehyde in 0.1 M phosphate buffer solution. Brain tissue was collected for technical validation. Hearts and adrenals were collected and weighed. Female vaginal cytology was completed. Tissue was post-fixed in 4.0% paraformaldehyde for 24 hours at room temperature before storing in 30% sucrose at 4˚ C.

Prior to and following CVS, whole blood was collected via a tail clip, placed in an EDTA tube, and plasma removed and stored following centrifugation at -20˚ C. Plasma Angiotensin II was determined via ELISA (C.V = 4.7-7.3 %; ENZO Life Sciences, Farmingdale, NY).

For experiment 2 following CVS, animals were anesthetized with 5% isoflurane. Following rapid decapitation and myography preparation, brain tissue was collected for technical

validation. Hearts and adrenals were collected and weighed. Tissue was post-fixed in 4.0% paraformaldehyde for 24 hours at room temperature, followed by paraformaldehyde for 48 hours at 4˚ C, and storage in 30% sucrose at 4˚ C. Mesenteric arteries not used in Myography prep were post-fixed in paraformaldehyde for 24 hours at room temperature prior to storage in 30% sucrose at 4˚ C. In females, vaginal cytology was taken for estrous staging.

2.8 Statistical analysis

Data are expressed as mean ± standard error of the mean (SEM). In both experiments, analyses were completed within sex due to the nature of the experimental designs. Body weight was analyzed via 3-way ANOVA with time (repeated), stress, and virus as conditions. Somatic data, echocardiography, and hemodynamics were analyzed by 2-way ANOVA with stress and virus as conditions. Myography was analyzed by 2-way ANOVA within stress condition using virus and either pressure or concentration as conditions. Post-hoc analysis was done with a Tukey correction. See supplemental table (**S.3**) for all ANOVA analysis results. Myography data were sorted using a Savitzky-Golay FIR filter and GESD outlier test to remove noise and tracking error.

3. Results

3.1 Experiment 1: Somatic measures

As previously reported (Chapter 4), somatic measures (**Fig. 25**) of body weight in females over the course of CVS showed main effects of time [$F(4, 132) = 6.825$, $p < 0.0001$], stress [$F(1, 33) = 6.641$, $p = 0.0146$], an interaction of time and CVS [$F(4, 132) = 23.80$, $p < 0.0001$]. Food intake reflected a main effect of stress [$F(1, 33) = 13.58$, $p = 0.0008$] with TeLC CVS females having significantly decreased food intake compared to TeLC No CVS females ($p = 0.0402$). While females showed no differences in adrenal weight, there was a main viral effect on heart

index [F(1, 31) = 7.554, p = 0.0099] with No CVS TeLC females having significantly larger hearts than their GFP counterparts (p = 0.0468) (**Fig. 26)**. Additionally, females showed no difference in plasma angiotensin II levels or aortic pulse wave velocity.

Male animals over the course of CVS showed no differences in food intake and changes in body weight reflected a main effect of day [F(4, 124) = 44.01, p < 0.0001] and an interaction of day and stress [F(4, 124) = 49.58, p < 0.0001]. Following CVS, males showed a main effect of stress on adrenal weight [F(1, 28) = 20.32, p = 0.0001] with GFP CVS males (p = 0.0469) and TeLC CVS males (p = 0.0069) having significantly increased adrenal weights compared to their unstressed counterparts. A main effect of stress was also seen in male plasma angiotensin II [F(1, 48) = 5.321, p = 0.0254]. These animals showed no differences in heart index or aortic pulse wave velocity following chronic stress.

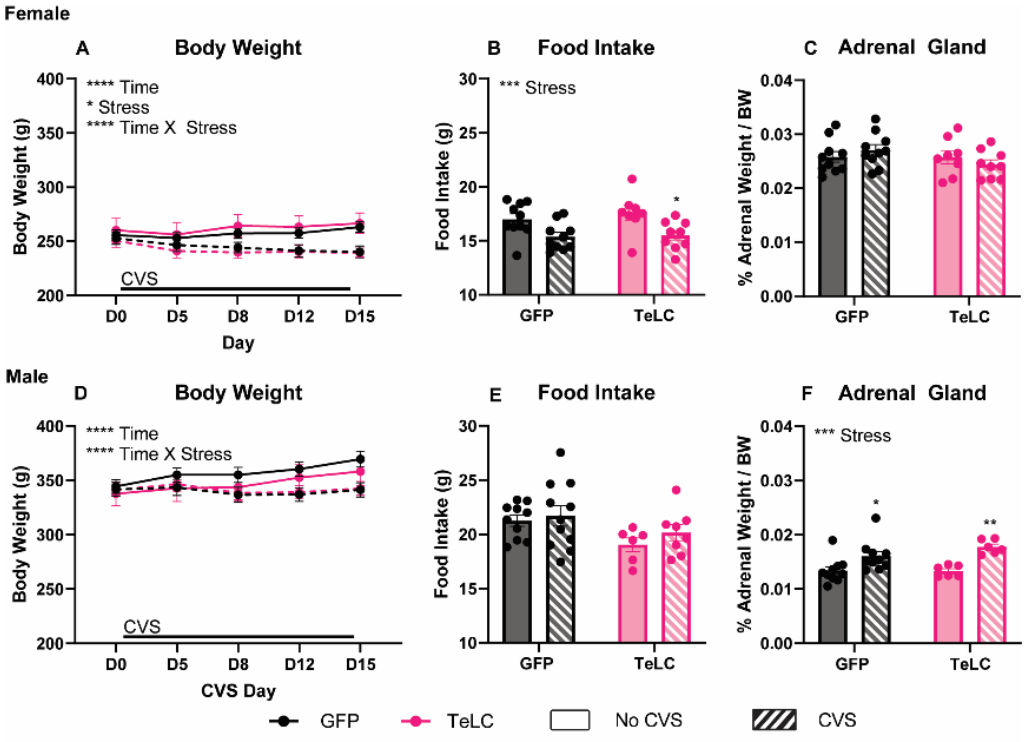

Figure 25. Somatic measures following CVS in experiment 1. Female and male body weight (A, D) and food intake (B, F) (n = 6-11/group/sex) were measured over the course of CVS.

Adrenal weight (C, G) corrected for bodyweight was measured at tissue collection. Data are expressed as mean ± SEM. * p<0.05, *** p<0.001, **** p<0.0001.

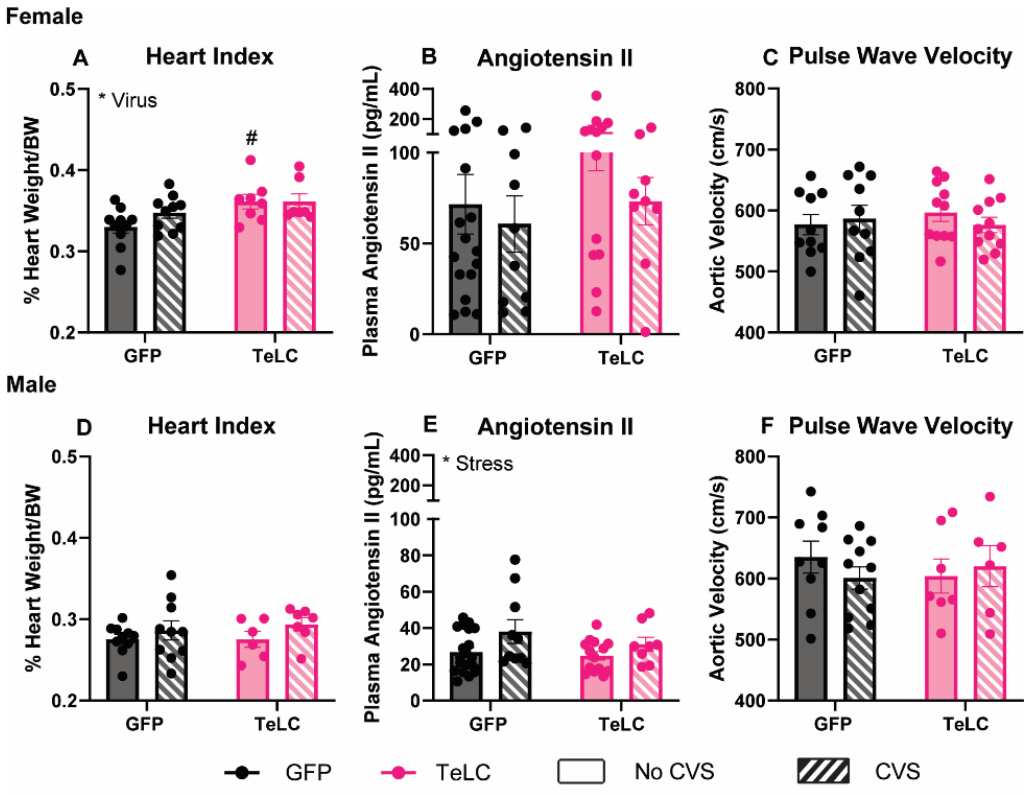

Figure 26. Cardiac measures. Female and male heart weight corrected for body weight (A, D) was measured at tissue collection (n = 6-11/group/sex). Plasma angiotensin II was quantified before and after CVS (B, D) (n = 6-17/group/sex). Aortic velocity (C, F) was quantified via pulse wave doppler. Data are expressed as mean ± SEM. # Effect of virus. * p<0.05.

3.2 Echocardiography

Interestingly, echocardiographic analysis of left ventricular structure and function following chronic stress showed sex-specific changes that were primarily represented in TeLC animals (**Fig. 27**). There were no significant differences in left ventricular diameter during systole or diastole in males or females. However, female animals showed a main interaction of stress and circuit in the thickness of the left ventricular posterior wall during systole [$F(1, 33) = 4.422$, $p = 0.0432$] that is also present in a calculation of diastolic wall strain [$F(1, 33) = 4.710$, p

= 0.0373] (217). TeLC males showed a decrease in left ventricular wall thickness in both systole and diastole with a main effect of [F(1, 29) = 4.460, p = 0.0434] and [F(1, 29) = 4.943, p =0.0341] respectively. Importantly, these males showed no significant differences in diastolic wall strain. Additionally, no differences were seen in fractional shortening or ventricular filling in any group.

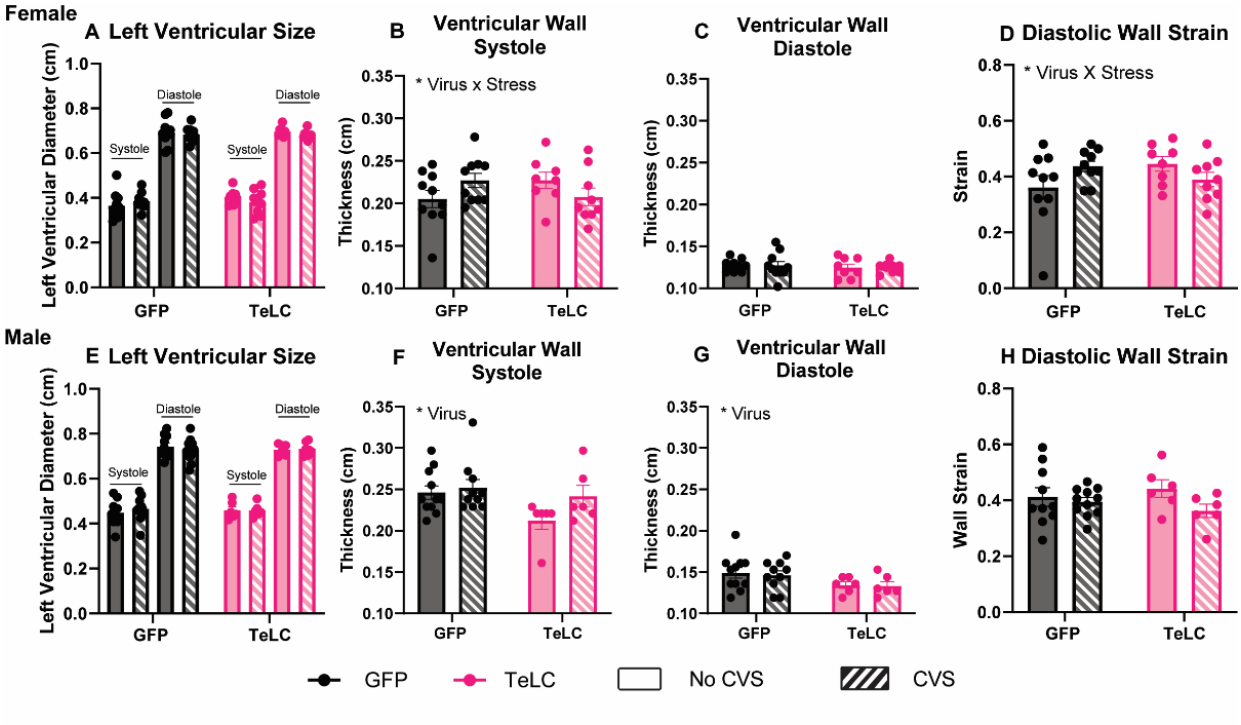

Figure 27. Echocardiography measures. Following CVS, left ventricular structure and function were quantified by echocardiography in males and females (n = 6-11/group/sex). Left ventricular diameter (A, E), left ventricular posterior wall thickness in systole (B, F), and diastole (C, G) were measured. Diastolic wall strain, a measure of diastolic function, was quantified (D, H). Data are expressed as mean ± SEM. * p<0.05.

3.3 Experiment 2: Somatic Measures

Over the course of CVS, the body weight of female animals did show main effects of time [F(5, 80) = 5.470, p = 0.0002], virus [F(1, 16) = 5.958, p = 0.0267], and an interaction of

time and stress [F(5, 80) = 3.126, p = 0.0125) despite food restriction of the CVS animals (**Fig. 28)**. These differences were likely due to the small sample size between these groups. Male body weight over the course of CVS showed only a main effect of time [F(5, 94) = 6.889, p< 0.0001).

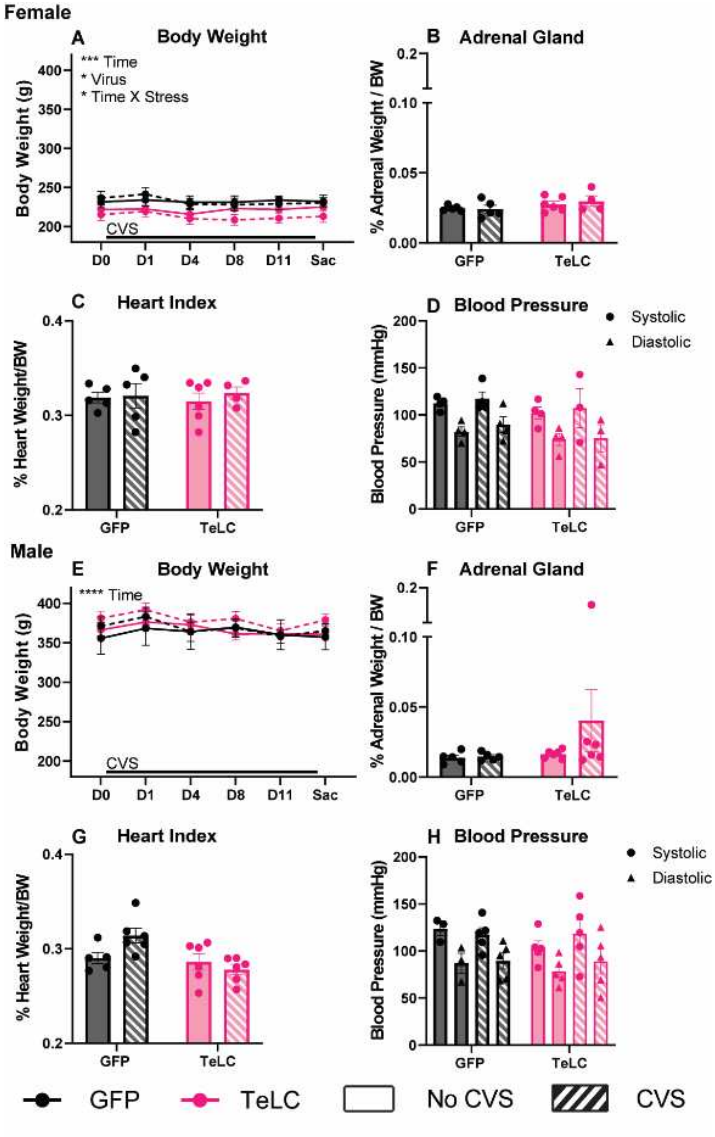

Figure 28. Somatic measures following CVS in experiment 2. Female and male body weight (A, E) were measured over the course of CVS. Adrenal weight (B, F) and heart weight (C, G) corrected for bodyweight were measured at tissue collection (n = 4-6/group/sex). Systolic and Diastolic blood pressure were measured prior to myography prep (D, H). Data are expressed as mean ± SEM. * p<0.05, *** p<0.001, **** p<0.0001.

There were no significant effects between any group when analyzing both adrenal weight and heart index. The absence of these effects may, again, be due to a small sample size, differences in body composition, or food intake. Anesthetized blood pressure measurements taken prior to myography preparation did not yield any significant differences in systolic or diastolic pressure. However, the mean systolic pressures in each group of 110-130 mmHg while anesthetized support testing vascular reactivity across a range of pressures.

3.4 Pressure myography myogenic tone

The myogenic tone of mesenteric resistance arterioles was calculated across of range of pressures from 20-120 mmHg (**Fig. 29)**. In No CVS females, TeLC increased myogenic tone with a main effect of virus [$F(1, 52) = 7.717$, $p = 0.0076$) while TeLC No CVS females had significantly higher myogenic tone at 120 mmHg ($p = 0.0304$). This result was mirrored in the CVS animals. TeLC females had increased myogenic tone with a main effect of virus [$F(1, 36) = 13.02$, $p = 0.0009$].

Interestingly, vessels from male animals did not resemble the females. In No CVS males, there were no differences between the TeLC animals and the GFP controls. However, in the CVS groups, TeLC animals showed reduced myogenic tone with a main effect of virus [$F(1, 42) = 5.147$, $p = 0.0285$.

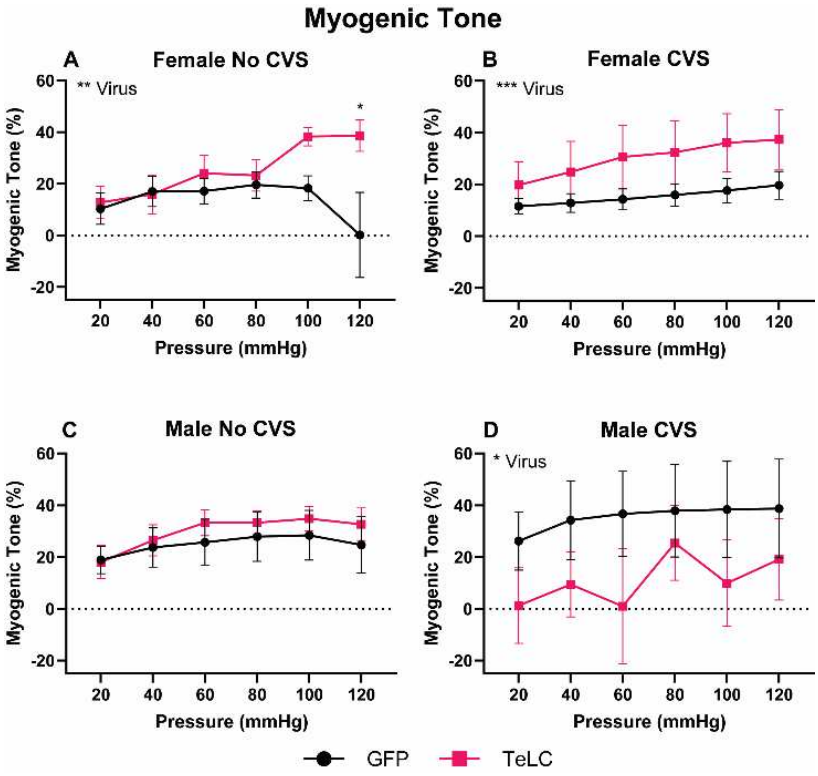

Figure 29. Myogenic tone. Female and male myogenic tone was quantified from active and passive vessel diameter within both the No CVS (A, C) and CVS (B, D) groups (n = 4-6/group/sex). Data are expressed as mean ± SEM. * $p<0.05$, ** $p<0.01$, *** $p<0.001$.

3.5 Pressure myography pharmacology: females

At 70 mmHg, females responded to PE constriction with main effects of concentration in both the No CVS animals [$F(4, 45) = 33.09$, $p < 0.0001$] and CVS females [$F(4,35) = 17.64$, $p < 0.0001$] (**Fig. 30)**. However, there were no effects of either stress or circuit on endothelial-independent constriction. During endothelial-independent relaxation with SNP, No CVS females showed concentration-dependent dilation [$F(6, 63) = 3.383$, $p = 0.0025$]. Interestingly, regardless of circuit inhibition, CVS females had no concentration-dependent SNP relaxation. Additionally, stress and circuit did not significantly affect SNP relaxation at 70 mmHg.

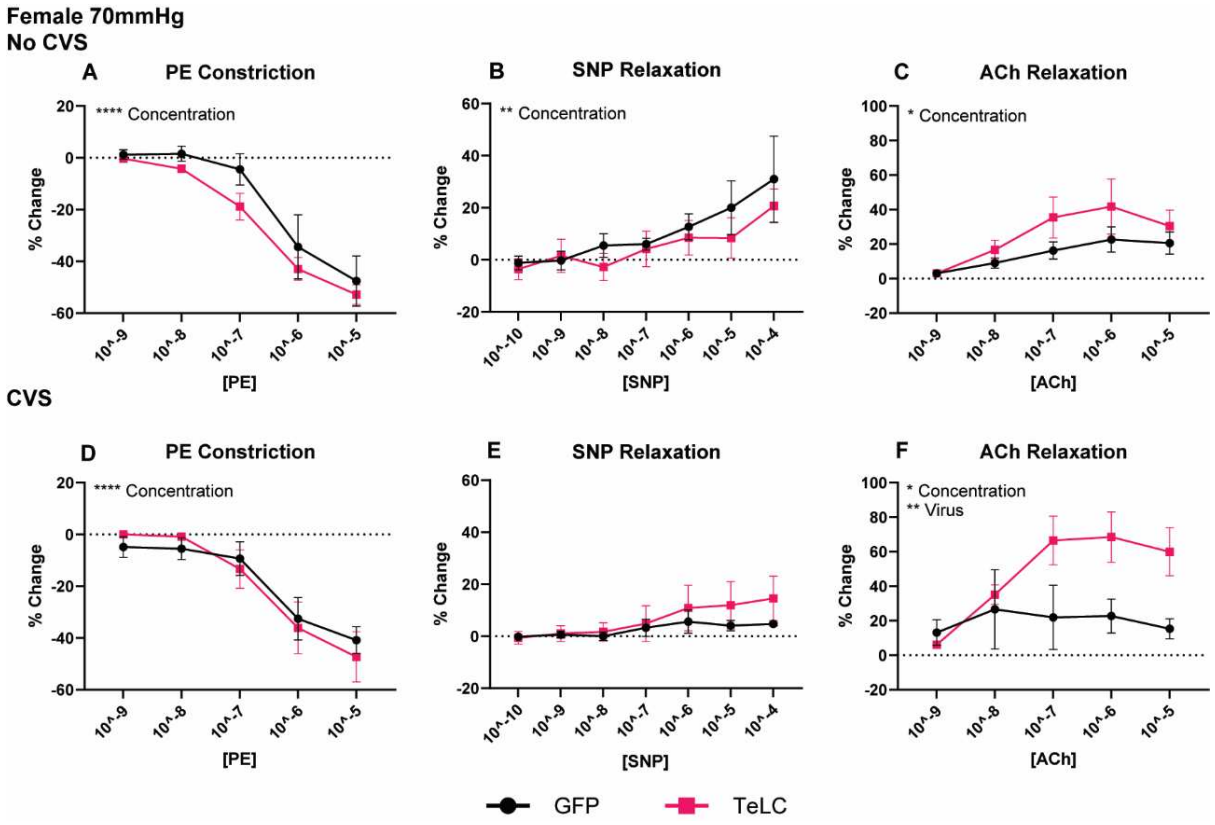

Figure 30. Female pressure myography pharmacology at 70 mmHg. PE endothelial-independent constriction (A, D), SNP endothelial-independent relaxation (B, E), and ACh endothelial-dependent relaxation (C, F) of mesenteric arterioles were quantified (n = 4-6/group/sex). Maximal vessel diameter was measured at each concentration. Data are expressed as mean ± SEM. * p<0.05, ** p<0.01, **** p<0.0001.

Looking at endothelial function with ACh, both No CVS [F(4,40) = 3.101, p = 0.0259] and CVS females [F(4,32) = 3.198, p= 0.0257] showed dilation responses to increasing concentrations. Circuit inhibition had no effect on this response in No CVS animals. However, in CVS females, TeLC had a main effect on dilation [F(1, 32) = 13.06, p = 0.001] with circuit inhibited animals having increased relaxation.

These responses are altered by increasing the pressure on the vessel to 120 mmHg (**Fig. 31**). PE-dependent constriction still resulted in a concentration dependent response in both No CVS females [F(4,40) = 15.19, p < 0.0001] and CVS females [F(4, 35) = 18.38, p < 0.0001].

Similar to 70 mmHg, there was no effect on PE constriction with CVS or circuit inhibition. SNP endothelial-independent relaxation again showed a concentration response in No CVS animals [F(6, 56) = 3.369, p = 0.0066]. Interestingly, while there was significant concentration response in the CVS animals, circuit inhibition reduced dilation with a main effect of virus [F(1, 42) = 5.352, p = 0.0257].

Acetylcholine relaxation was reduced in all groups. The No CVS animals showed no significant response at the higher pressure. Similarly, the CVS animals also showed no significant response to increasing ACh concentration. However, in opposition to the SNP relaxation, TeLC animals showed increased ACh relaxation with a main effect of virus [F(1, 30) = 12.32, p = 0.0014].

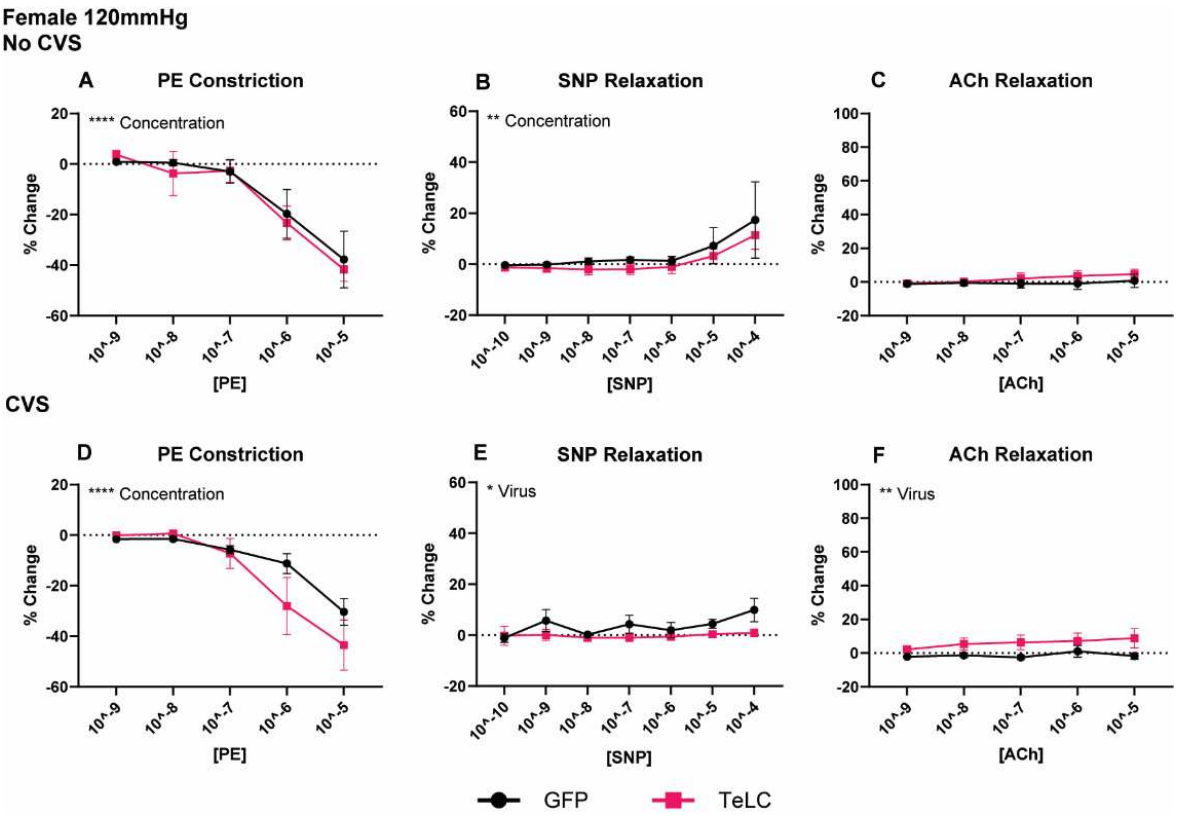

Figure 31. Female pressure myography pharmacology at 120 mmHg. PE endothelial-independent constriction (A, D), SNP endothelial-independent relaxation (B, E), and ACh endothelial-dependent relaxation (C, F) of mesenteric arterioles were quantified (n = 4-

6/group/sex). Maximal vessel diameter was measured at each concentration. Data are expressed as mean ± SEM. * p<0.05, ** p<0.01, **** p<0.0001.

3.6 Pressure myography pharmacology: males

Vascular reactivity in males was impacted less by both stress exposure and circuit inhibition. At 70 mmHg, PE constriction showed a concentration response in both the No CVS [F(4, 45) = 36.19, p <0.0001] and CVS animals [F(4, 25) = 18.42, p < 0.0001] (**Fig. 32**). Additionally, No CVS and CVS animals showed a concentration response to SNP with main effects of concentration [F(6, 55) = 2.835, p = 0.0178] and [F(6, 35) = 5.115, p = 0.0007] respectively. The endothelial-independent responses in these males at 70 mmHg were not significantly impacted by either stress exposure or circuit inhibition. Endothelial-independent ACh relaxation in these animals was reduced with no effects of concentration, stress, or circuit inhibition at 70 mmHg.

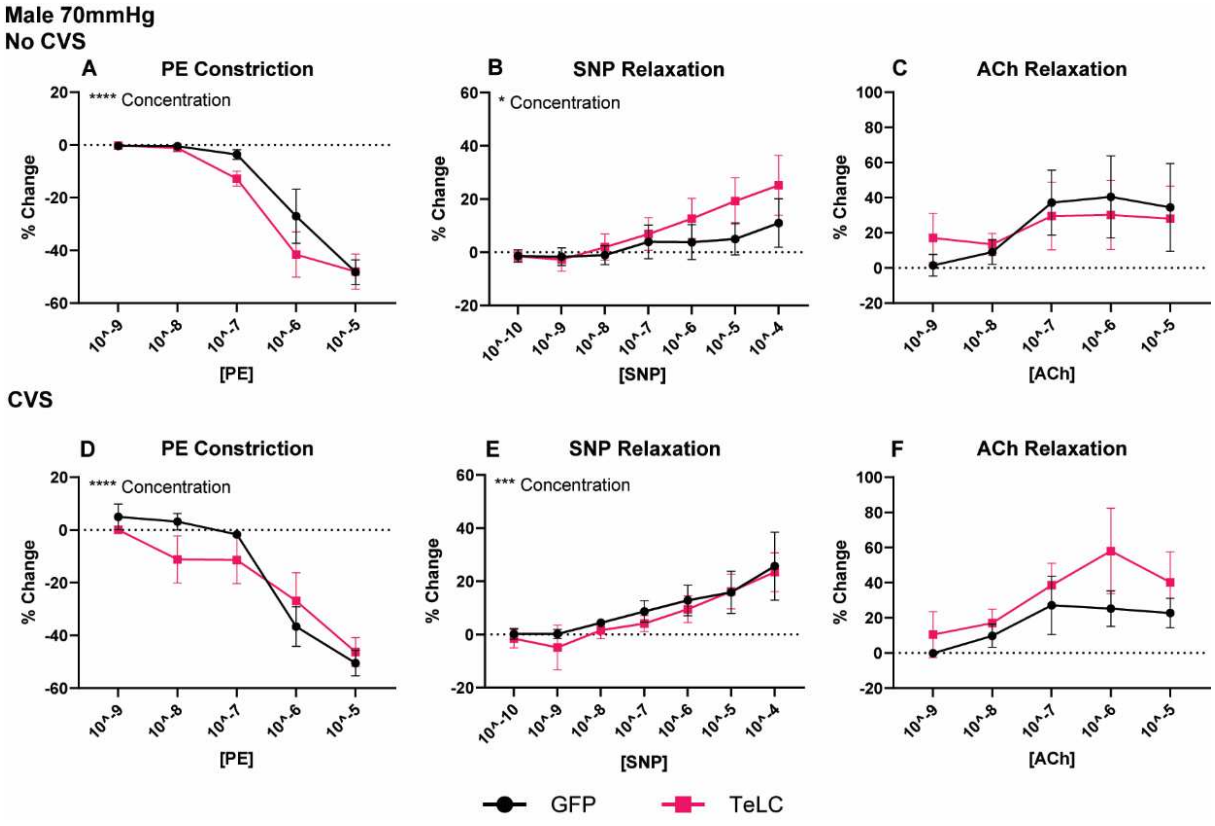

Figure 32. Male pressure myography pharmacology at 70 mmHg. PE endothelial-independent constriction (A, D), SNP endothelial-independent relaxation (B, E), and ACh endothelial-dependent relaxation (C, F) of mesenteric arterioles were quantified (n = 4-6/group/sex). Maximal vessel diameter was measured at each concentration. Data are expressed as mean ± SEM. * p<0.05, *** p<0.001, **** p<0.0001.

When pressure was increased to 120 mmHg, endothelial-independent responses were reduced (**Fig. 33**). Interestingly, the PE constriction maintained a significant response to increasing concentration in both the No CVS [F(4, 45) = 11.14, p < 0.0001] and CVS animals [F(4, 25) = 14.98, p < 0.0001]. However, stress and circuit inhibition had no significant effect. While there were no main effects of concentration following SNP administration, within the No CVS animals there was main effect of circuit inhibition [F(1, 63) = 6.051, p = 0.0167] with TeLC animals showing increased relaxation. This effect was eliminated in the CVS animals with no significant differences between circuit intact and inhibited animals.

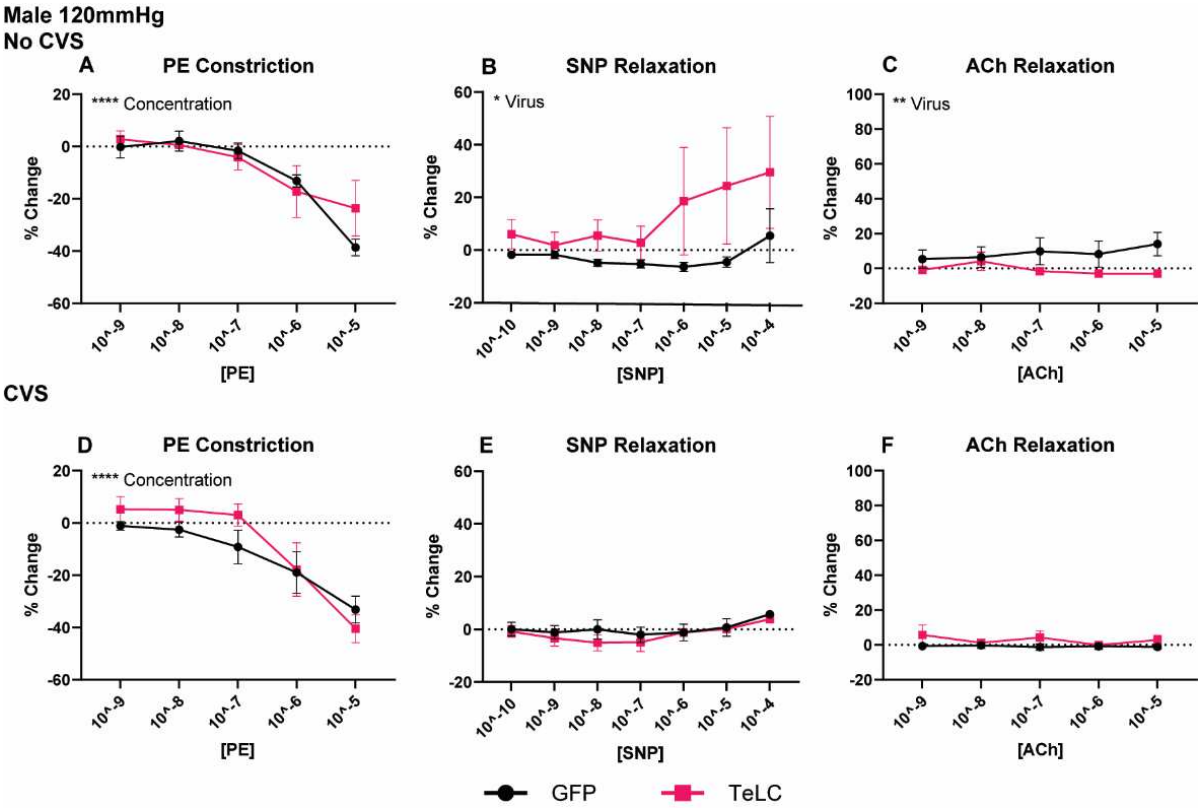

Figure 33. Male pressure myography pharmacology at 120 mmHg. PE endothelial-independent constriction (A, D), SNP endothelial-independent relaxation (B, E), and ACh endothelial-dependent relaxation (C, F) of mesenteric arterioles were quantified (n = 4-6/group/sex). Maximal vessel diameter was measured at each concentration. Data are expressed as mean ± SEM. * $p<0.05$, ** $p<0.01$, **** $p<0.0001$.

These results were similar in the endothelial-independent ACh responses. There were no significant concentration responses in any group. Within the No CVS animals, there was a main circuit effect [$F(1, 45) = 10.09$, $p = 0.002$]; however, circuit-inhibited animals showed less relaxation than GFP controls. Similarly, CVS animals did not show this effect with no difference between circuit groups.

3.7 Estrous cycle cytology

Vaginal cytology was done to determine estrous phase at myography preparation (**Table 4**). These animals were allowed to free cycle and were not staged across group to prevent bias toward one reproductive hormone profile. However, due to the small sample size not all estrus stages are present.

Table 4: Estrous stage at myography preparation.

	Myography preparation			
	Proestrus (%)	Estrus (%)	Metestrus (%)	Diestrus (%)
GFP No CVS	40	20	40	0
GFP CVS	20	60	20	0
TeLC No CVS	60	40	0	0
TeLC CVS	50	25	0	0

4. Discussion

4.1 Sympathetic tone alters female peripheral resistance

Total peripheral resistance is often characterized as the force exerted by vasculature on blood and is vital for the regulation and maintenance of blood pressure. An increase in peripheral resistance is considered to be characteristic of hypertension and cardiac dysfunction. While these studies do not directly measure total peripheral resistance, many of the reported measures are indicative of changes in peripheral resistance following circuit inhibition and may telegraph dysregulation (218).

In circuit-inhibited females, mesenteric arterioles show increased endothelial-dependent relaxation following acetylcholine administration as well as overall increased myogenic tone following chronic stress. This increase in vascular reactivity may lead to an increase in cardiac afterload that is then reflected in the changes in diastolic wall strain seen in the female counterparts of experiment 1. Additionally, the circuit-inhibited females in experiment 1 show an increase in heart index, which is likely reflective of increased ventricular wall thickness during systole and increased afterload.

While the changes in afterload in circuit-inhibited females are subtle, the changes in diastolic wall strain are indicative of a change in diastolic function. This is an important shift because diastolic dysfunction is often the first indicator of cardiovascular dysfunction in people (219). While typical measures of systolic function, namely fractional shortening and ventricular filling velocity, did not indicate gross systolic dysfunction, the changes in afterload and diastolic function signify changes in the autonomic regulation of flow and cardiac output in circuit-inhibited females. The IL-RVLM circuit seems to act as a sympathetic regulator (199) and its inhibition allows for an increase in sympathetic output that may account for these changes in females. This is further supported by the reduction in endothelial-independent relaxation at higher pressures.

While the mechanism underlying these changes is unknown, the disturbances in autonomic regulation of both cardiac and vascular function as well as changes in hematology

could lead to receptor expression changes in the endothelium and vascular smooth muscle. Interestingly, there were no differences in endothelial-independent, or smooth muscle dependent, vascular constriction or relaxation. Consequently, the changes may be reflected in an upregulation of endothelial muscarinic M3 receptors or a change in the sensitivity of L-type calcium channels in the smooth muscle. Either of these changes would result in greater reactivity to acetylcholine in both enhanced relaxation and increased tone.

However, when circuit-inhibition interacts with chronic stress exposure many of the cardiac-specific effects seem to diminish. This may be because animals in experiment 1 were not food restricted. The energy deficit experienced by animals undergoing CVS has been shown to mask the cardiovascular impact of chronic stress because of the decrease in body composition that lessens overall cardiac work (156, 213).

4.2 Adaptive dysregulation of male cardiac function

The effects of circuit-inhibition in males indicates an adaptive response that is further impacted by chronic stress exposure. Namely, while circuit-inhibition reduces ventricular wall thickness during both systole and diastole, diastolic wall strain is not impacted. Interestingly, plasma angiotensin II is increased following chronic stress in these animals. While angiotensin II acts through numerous mechanisms to increase blood pressure and alter autonomic function, the increase is not strongly reflected in overall cardiac function and may represent an angiotensin II-mediated reduction in sympathetic input to the heart (209, 220). This is supported by the reduction in vascular tone seen in circuit-inhibited males exposed to chronic stress.

This response is further supported in the pharmacologic data that shows at high pressure, circuit-inhibited males show increased endothelial-independent relaxation that is dependent on NO action. Endothelial-independent relaxation through the action of SNP, and subsequently NO, alters vasodilation through the increase of cGMP and protein kinase

activation (221). Upregulating cGMP may cause an increase in β2 adrenergic receptor activation through crosstalk with cAMP (222, 223), consequently further promoting relaxation. Conversely, this vasculature has reduced endothelial-dependent relaxation that is acetylcholine mediated. This may reflect moderate endothelial dysfunction at higher pressures. Importantly, the mechanism driving these changes may occur at receptor, cellular, and system level to alter vascular reactivity in response to autonomic dysregulation.

4.3 IL-RVLM influence on sex-specific cardiovascular function

Overall, cardiac function and vascular reactivity are impacted by IL-RVLM inhibition, indicating that its function is necessary for normal cardiovascular function. Additionally, the regulatory changes seen with circuit-inhibition are sex-dependent. While changes in female physiologic responses reflect an overall increase in sympathetic activation that is consistent with data indicating that the IL-RVLM circuit acts to inhibit sympathetic activation, males show broader disorganization of autonomic regulation and endothelial function that is stress history-dependent. Many of the responses indicate males exhibit cardiovascular compensation for autonomic imbalance. However, the oppositional responses that are underlied by chronic stress exposure indicate an uncoordinated homeostatic microvascular response. Consequently, the impact of IL-RVLM function in the maintenance of cardiovascular activity is both sex- and stress-dependent. The necessity of this circuit in maintaining cardiovascular autonomic balance is a vital part of understanding how autonomic dysregulation leads to CVD progression.

CHAPTER 6: THE IMPLICATIONS OF STRESS REGULATION ON SYSTEMIC PHYSIOLOGIC FUNCTION

1. Chronic stress as a precipitating factor in disease

Broadly, this research supports the tenet of chronic stress having deleterious effects on physiology and that these changes play an important role in the etiology of cardiometabolic disease. Importantly, these studies elucidate sex-differences in the effects of early-life chronic stress, both in early adulthood and following aging, and how the regulation of these stress responses is both sex and physiologic system dependent.

Early-life chronic stress exposure affected both physiologic responses and behavioral stress responses in often opposing directions in males and females. Then in late life, females show dysregulated glucocorticoid responses, increased hypertrophic remodeling, and sex-specific behavioral responses to acute stress, but none of these changes indicate gross individual susceptibility to pathologic changes. However, these animals may not reflect the individual susceptibility of reproductively senescent women, because the rats were still reproductively active. Reproductive hormones are known to impact cardiovascular and metabolic function and their absence is associated with changes in female CVD rates. Our studies were not statistically powered to elucidate cycle specific effects.

The overall impact of chronic stress on cardiometabolic function in males seems to be smaller than in females. As a group, chronic stress leads to fewer changes in cardiac structure and glucocorticoid responsivity after aging. However, these males show individual susceptibility or resiliency to cardiac remodeling. Interestingly, the positive correlation seen between passive coping and glucose responses in aged males likely relates to cardiac susceptibility. The

interplay between behavioral, metabolic, and cardiovascular function is both individual and stress history dependent.

The adaptive capacity of an individual is determined by a vast number of factors. Here we focus on sex and age, but in practice, the impact of stress on an individual is mediated by their entire history. Therefore, it is difficult to say that males or females as a group are better or worse at adapting to chronic stress exposure. However, the impact of sex and age on these responses is prominent. These factors should consequently be accounted for in the risk assessment of and treatment plan for cardiometabolic disease. Considering stress history, lifestyle, reproductive status, and glucocorticoid responsivity in an individual care plan will improve long term outcomes and reduce the burden of cardiometabolic disease.

2. Sex-specific stress regulation

When the IL-RVLM circuit is inhibited in females, stress responses are further dysregulated; however, the physiologic consequences of circuit inhibition and chronic stress exposure are not consistently additive. In females, the patterns of dysregulation indicate a broad increase in sympathetic inputs to cardiovascular and metabolic function. Particularly in the measures of cardiovascular function, IL-RVLM inhibition promoted cardiovascular dysfunction and resulted in increased afterload and diastolic dysfunction. In measures of metabolic function, the inhibition of this circuit altered glucoregulatory pathways. While metabolic dysfunction did not drastically worsen with inhibition and chronic stress, the influence of sympathetically-mediated gluconeogenic processes overcame the insulin-resistant changes seen in animals exposed to chronic stress.

These results support the data indicating this circuit is a sympathetic regulator and that, in females, its inhibition reduces the adaptive capacity of the animal to respond to chronic stress

exposure. This sex-specific response is essential in understanding how stress differentially impacts the overall health and disease risk of individuals.

Interestingly, inhibiting this circuit in male rats does not consistently alter physiology to indicate changes in sympathetic regulation. More broadly, male responses indicate a dysregulation of autonomic function and potentially disjointed regulatory mechanisms. While the initial data in males showed a greater ability to adaptively respond to stress, when stress exposure is combined with circuit inhibition, these animals show both adaptive and maladaptive metabolic and cardiovascular responses. This may indicate that functional responses and adaptive capacity are system dependent. There are signs that this circuit still acts as a sympathetic regulator in males, with inhibition increasing gluconeogenic processes in males. However, either the regulatory function of this circuit or the response to its loss in males leads to complex interactions that confound physiologic function.

The sex-specific nature of these physiologic responses may be mediated by cell-specific responses in the RVLM. Changes in both excitatory and inhibitory signaling that are potentially caused by stress-induced transcriptional alterations may underlie the broad changes seen with circuit-inhibition. Particularly, changes in glutamatergic signaling that is altered transcriptionally may result in functional differences of IL-RVLM output that consequently influence physiologic responding to chronic stress.

Overall, the impact of IL-RVLM function on cardiometabolic physiologic is vital to appropriate stress responding and influences both glucoregulation and vascular function in males and females. While the results of IL-RVLM inhibition are sex- and stress history-dependent, the overarching function of autonomic homeostasis is essential to system regulation. More research into the cell-specific protein expression and activation during stress would need to be done to determine if RVLM catecholaminergic neurons could be a viable drug target for sympathetic control. However, it is unlikely that this brain region could be specifically targeted with minimal

non-specific action. Therefore, increasing treatment capabilities for the impacts of chronic stress are more likely to be successful systemically.

Further research in understanding the systemic implications of chronic stress should focus on sex-specific changes in autonomic and endocrine receptor expression that result in end-organ functional changes. Particular to this research, understanding how autonomic receptor expression in the endothelium changes with chronic stress exposure could provide a mechanistic explanation of endothelial dysfunction. Further, investigating how chronic stress influences blood flow dynamics as an integrator across cardiovascular and microvascular function would improve our ability to moderate the negative cardiovascular consequences of chronic stress through multiple treatment avenues. It would also be beneficial to examine metabolic end-organ receptor expression and activation, such as insulin receptor and insulin receptor substrate activation or other metabolic mediators, to examine how stress is impacting both downstream regulators and initial endocrine activation as described above. Being able to tease apart the where the most significant changes in metabolic function occur with chronic stress would improve treatment plans by increasing the number of treatment targets. Importantly, understanding the downstream receptor effects in both the autonomic and endocrine systems following chronic stress would further allow for multi-system integration in treatment because of the broad systemic effects seen with many pharmacologic interventions. Current understanding of chronic stress impacts on individual physiologic systems deters broadly acting treatments because of the potential of unintended dysfunction. Integrating across systems and end-organs would overcome many of these challenges.

Understanding how the IL-RVLM circuit influences the autonomic regulation of stress responses increases our capability to influence autonomic dysregulation in disease. While this circuit is not a viable treatment target with current technology, understanding its activation and influence on physiology provides a basis for altering individual care plans and creating

regiments that will improve health outcomes and mitigate the deleterious changes associated chronic stress.

REFERENCES

1. **Anand SS**, **Yi Q**, **Gerstein H**, **Lonn E**, **Jacobs R**, **Vuksan V**, **Teo K**, **Davis B**, **Montague P**, **Yusuf S**. Relationship of metabolic syndrome and fibrinolytic dysfunction to cardiovascular disease. *Circulation* 108: 420–425, 2003. doi: 10.1161/01.CIR.0000080884.27358.49.
2. **Isfort M**, **Stevens SCW**, **Schaffer S**, **Jong CJ**, **Wold LE**. Metabolic dysfunction in diabetic cardiomyopathy. *Heart Fail Rev* 19: 35–48, 2014. doi: 10.1007/s10741-013-9377-8.
3. **McIntyre RS**, **Rasgon NL**, **Kemp DE**, **Nguyen HT**, **Law CWY**, **Taylor VH**, **Woldeyohannes HO**, **Alsuwaidan MT**, **Soczynska JK**, **Kim B**, **Lourenco MT**, **Kahn LS**, **Goldstein BI**. Metabolic syndrome and major depressive disorder: Co-occurrence and pathophysiologic overlap. *Curr Diab Rep* 9: 51–59, 2009. doi: 10.1007/s11892-009-0010-0.
4. **Dearing C**, **Morano R**, **Ptaskiewicz E**, **Mahbod P**, **Scheimann JR**, **Franco-Villanueva A**, **Wulsin L**, **Myers B**. Glucoregulation and coping behavior after chronic stress in rats: Sex differences across the lifespan. *Horm Behav* 136: 105060, 2021. doi: 10.1016/j.yhbeh.2021.105060.
5. **Myers B**, **McKlveen JM**, **Herman JP**. Glucocorticoid actions on synapses, circuits, and behavior: Implications for the energetics of stress. *Front Neuroendocrinol* 35: 180–196, 2014. doi: 10.1016/j.yfrne.2013.12.003.
6. **Dhabhar FS**. The power of positive stress–a complementary commentary. *Stress* 22: 526–529, 2019. doi: 10.1080/10253890.2019.1634049.
7. **Chrousos G**, **Gold P**. The concepts of stress and stress system disorders. Overview of physical and behavioral homeostasis. *JAMA J Am Med Assoc* 267: 1244–1252, 1992.

doi: 10.1001/jama.267.9.1244.

8. **Sudheimer K**, **Keller J**, **Gomez R**, **Tennakoon L**, **Reiss A**, **Garrett A**, **Kenna H**, **O'Hara R**, **Schatzberg AF**. Decreased hypothalamic functional connectivity with subgenual cortex in psychotic major depression. *Neuropsychopharmacology* 40: 849–860, 2015. doi: 10.1038/npp.2014.259.

9. **Herman JP**, **Mcklveen JM**, **Ghosal S**, **Kopp B**, **Wulsin A**, **Makinson R**, **Scheimann J**, **Myers B**. Regulation of the hypothalamic-pituitary-adrenocortical stress response. *Compr Physiol* 6: 603–621, 2016. doi: 10.1002/cphy.c150015.Regulation.

10. **Langellier BA**, **Fleming PJ**, **Kemmick Pintor JB**, **Stimpson JP**. Allostatic Load Among U.S.- and Foreign-Born Whites, Blacks, and Latinx. *Am J Prev Med* 60: 159–168, 2021. doi: 10.1016/j.amepre.2020.08.022.

11. **Algren MH**, **Ekholm O**, **Nielsen L**, **Ersbøll AK**, **Bak CK**, **Andersen PT**. Associations between perceived stress, socioeconomic status, and health-risk behaviour in deprived neighbourhoods in Denmark: A cross-sectional study. *BMC Public Health* 18: 1–12, 2018. doi: 10.1186/s12889-018-5170-x.

12. **Ursache A**, **Merz E**, **Melvin S**, **Meyer J**, **Noble K**. Socioeconomic Status, Hair Cortisol and Internalizing Symptoms in Parents and Children. *Psychoneuroendocrinology* 78: 142–150, 2017. doi: 10.1016/j.psyneuen.2017.01.020.Socioeconomic.

13. **Graves KY**, **Nowakowski ACH**. Childhood Socioeconomic Status and Stress in Late Adulthood: A Longitudinal Approach to Measuring Allostatic Load. *Glob Pediatr Heal* 4: 1–12, 2017. doi: 10.1177/2333794x17744950.

14. **Cohen S**, **Schwartz JE**, **Epel E**, **Kirschbaum C**, **Sidney S**, **Seeman T**. Socioeconomic status, race, and diurnal cortisol decline in the Coronary Artery Risk Development in Young Adults (CARDIA) Study. *Psychosom Med* 68: 41–50, 2006. doi: 10.1097/01.psy.0000195967.51768.ea.

15. **Schmeer K**, **Yoon A**. SES Inequalities in Low-Grade Inflammation during Childhood.

Arch Dis child 101: 1043–1047, 2016. doi: 10.1136/archdischild-2016-310837.SES.

16. **Stringhini S**, **Polidoro S**, **Sacerdote C**, **Kelly RS**, **Van Veldhoven K**, **Agnoli C**, **Grioni S**, **Tumino R**, **Giurdanella MC**, **Panico S**, **Mattiello A**, **Palli D**, **Masala G**, **Gallo V**, **Castagné R**, **Paccaud F**, **Campanella G**, **Chadeau-Hyam M**, **Vineis P**. Life-course socioeconomic status and DNA methylation of genes regulating inflammation. *Int J Epidemiol* 44: 1320–1330, 2015. doi: 10.1093/ije/dyv060.

17. **Sullivan AD**, **Benoit R**, **Breslend NL**, **Vreeland A**, **Compas B**, **Forehand R**. Cumulative socioeconomic status risk and observations of parent depression: Are there associations with child outcomes? *J Fam Psychol* 33: 883–893, 2019. doi: 10.1037/fam0000567.

18. **Avan A**, **Digaleh H**, **Di Napoli M**, **Stranges S**, **Behrouz R**, **Shojaeianbabaei G**, **Amiri A**, **Tabrizi R**, **Mokhber N**, **Spence JD**, **Azarpazhooh MR**. Socioeconomic status and stroke incidence, prevalence, mortality, and worldwide burden: An ecological analysis from the Global Burden of Disease Study 2017. *BMC Med* 17, 2019. doi: 10.1186/s12916-019-1397-3.

19. **Williams J**, **Allen L**, **Wickramasinghe K**, **Mikkelsen B**, **Roberts N**, **Townsend N**. A systematic review of associations between non-communicable diseases and socioeconomic status within low- and lower-middle-income countries. *J Glob Health* 8, 2018. doi: 10.7189/jogh.08.020409.

20. **Hostinar C**, **Ross K**, **Chen E**, **Miller G**. Early-life Socioeconomic Disadvantage and Metabolic Health Disparities. *Psychosom Med* 79: 514–523, 2017. doi: 10.1097/PSY.0000000000000455.Early-life.

21. **Saklayen M**. The Global Epidemic of the Metabolic Syndrome. *Curr Hypertens Rep* 20, 2018.

22. **Picard M**, **Juster RP**, **McEwen BS**. Mitochondrial allostatic load puts the “gluc” back in glucocorticoids. *Nat Rev Endocrinol* 10: 303–310, 2014. doi: 10.1038/nrendo.2014.22.

23. **Pervanidou P**, **Chrousos GP**. Stress and obesity/metabolic syndrome in childhood and

adolescence. *Int J Pediatr Obes* 6: 21–28, 2011. doi: 10.3109/17477166.2011.615996.

24. **Chandola T**, **Brunner E**, **Marmot M**. Chronic stress at work and the metabolic syndrome: Prospective study. *Br Med J* 332: 521–524, 2006. doi: 10.1136/bmj.38693.435301.80.

25. **Yusef S**, **Haken S**, **Ounpuu S**, **Dans T**, **Avesum A**, **Lanas F**, **McQueen M**, **Budaj A**, **Pais P**, **Varigos J**, **Lisheng L**. Effect of potentially modifiable risk factors associated with myocardial infarction in 52 countries (the INTERHEART study): case-control study. *Lancet* 364: 937–952, 2004.

26. **Petrie JR**, **Guzik TJ**, **Touyz RM**. Diabetes, Hypertension, and Cardiovascular Disease: Clinical Insights and Vascular Mechanisms. *Can J Cardiol* 34: 575–584, 2018. doi: 10.1016/j.cjca.2017.12.005.

27. **Fiksdal A**, **Hanlin L**, **Kuras Y**, **Gianferante D**, **Chen X**, **Thoma M V**, **Rohleder N**. Associations Between Symptoms of Depression and Anxiety and Cortisol Responses to and Recovery from Acute Stress. *Psychoneuroendocrinology* 102: 44–52, 2019. doi: 10.1016/j.psyneuen.2018.11.035.Associations.

28. **Kohler O**, **Krogh J**, **Mors O**, **Benros ME**. Inflammation in Depression and the Potential for Anti-Inflammatory Treatment. *Curr Neuropharmacol* 14: 732–742, 2016. doi: 10.2174/1570159X14666151208113.

29. **Leonard BE**. Inflammation and depression: A causal or coincidental link to the pathophysiology? *Acta Neuropsychiatr* 30: 1–16, 2018. doi: 10.1017/neu.2016.69.

30. **Goldstein JM**, **Hale T**, **Foster SL**, **Tobet SA**. Sex differences in major depression and comorbidity of cardiometabolic disorders : impact of prenatal stress and immune exposures. *Neuropsychopharmacology* , 2020. doi: 10.1038/s41386-018-0146-1.

31. **McCorry LK**. Physiology of the autonomic nervous system. *Am J Pharm Educ* 71: 78, 2007. doi: 10.5688/aj710478.

32. **Tank AW**, **Lee Wong D**. Peripheral and central effects of circulating catecholamines.

Compr Physiol 5: 1–15, 2015. doi: 10.1002/cphy.c140007.

33. **Myers B**, **McKlveen JM**, **Herman JP**. Neural regulation of the stress response: The many faces of feedback. *Cell Mol Neurobiol* 32: 683–694, 2012. doi: 10.1007/s10571-012-9801-y.

34. **vom Berg-Maurer CM**, **Trivedi CA**, **Bollmann JH**, **De Marco RJ**, **Ryu S**. The severity of acute stress is represented by increased synchronous activity and recruitment of hypothalamic CRH neurons. *J Neurosci* 36: 3350–3362, 2016. doi: 10.1523/JNEUROSCI.3390-15.2016.

35. **Focke CMB**, **Iremonger KJ**. Rhythmicity matters: Circadian and ultradian patterns of HPA axis activity. *Mol Cell Endocrinol* 501: 110652, 2020. doi: 10.1016/j.mce.2019.110652.

36. **Firmino EMS**, **Kuntze LB**, **Lagatta DC**, **Dias DPM**, **Resstel LBM**. Effect of chronic stress on cardiovascular and ventilatory responses activated by both chemoreflex and baroreflex in rats. *J Exp Biol* 222, 2019. doi: 10.1242/jeb.204883.

37. **Sgoifo A**, **Carnevali L**, **Grippo AJ**. The socially stressed heart. Insights from studies in rodents. *Neurosci Biobehav Rev* 39: 51–60, 2014. doi: 10.1016/j.neubiorev.2013.12.005.

38. **Farah VMA**, **Joaquim LF**, **Bernatova I**, **Morris M**. Acute and chronic stress influence blood pressure variability in mice. *Physiol Behav* 83: 135–142, 2004. doi: 10.1016/j.physbeh.2004.08.004.

39. **Han K**, **Min J**, **Lee M**, **Kang BM**, **Park T**, **Hahn J**, **Yei J**, **Lee J**, **Woo J**, **Lee CJ**, **Kim SG**, **Suh M**. Neurovascular Coupling under Chronic Stress Is Modified by Altered GABAergic Interneuron Activity. *J Neurosci* 39: 10081–10095, 2019. doi: 10.1523/JNEUROSCI.1357-19.2019.

40. **Oliveira LA**, **Gomes-de-Souza L**, **Benini R**, **Wood SK**, **Crestani CC**. Both CRF1 and CRF2 receptors in the bed nucleus of stria terminalis are involved in baroreflex impairment evoked by chronic stress in rats. *Prog Neuro-Psychopharmacology Biol*

Psychiatry 105, 2021. doi: 10.1016/j.pnpbp.2020.110009.

41. **Ulrich-Lai YM**, **Figueiredo HF**, **Ostrander MM**, **Choi DC**, **Engeland WC**, **Herman JP**. Chronic stress induces adrenal hyperplasia and hypertrophy in a subregion-specific manner. *Am J Physiol - Endocrinol Metab* 291: 965–973, 2006. doi: 10.1152/ajpendo.00070.2006.

42. **Adam EK**, **Quinn ME**, **Tavernier R**, **McQuillan MT**, **Dahlke KA**, **Gilbert KE**. Diurnal cortisol slopes and mental and physical health outcomes: A systematic review and meta-analysis. *Psychoneuroendocrinology* 83: 25–41, 2017. doi: 10.1016/j.psyneuen.2017.05.018.

43. **Starr LR**, **Dienes K**, **Li YI**, **Shaw ZA**. Chronic stress exposure, diurnal cortisol slope, and implications for mood and fatigue: Moderation by multilocus HPA-Axis genetic variation. *Psychoneuroendocrinology* 100: 156–163, 2019. doi: 10.1016/j.psyneuen.2018.10.003.

44. **Ford ES**, **Giles WH**, **Dietz W**. Prevalence of the metabolic syndrome among U.S. adults. *Diabetes Care* 287, 2002. doi: 10.2337/diacare.27.10.2444.

45. **Rodgers JL**, **Jones J**, **Bolleddu SI**, **Vanthenapalli S**, **Rodgers LE**, **Shah K**, **Karia K**, **Panguluri SK**. Cardiovascular risks associated with gender and aging. *J Cardiovasc Dev Dis* 6, 2019. doi: 10.3390/jcdd6020019.

46. **Burt VK**, **Stein K**. Epidemiology of depression throughout the female life cycle. *J Clin Psychiatry* 63: 9–15, 2002.

47. **Rosamond W**, **Flegal K**, **Friday G**, **Furie K**, **Go A**, **Greenlund K**, **Haase N**, **Ho M**, **Howard V**, **Kissela B**, **Kittner S**, **Lloyd-Jones D**, **McDermott M**, **Meigs J**, **Moy C**, **Nichol G**, **O'Donnell CJ**, **Roger V**, **Rumsfeld J**, **Sorlie P**, **Steinberger J**, **Thom T**, **Wasserthiel-Smoller S**, **Hong Y**. Heart disease and stroke statistics - 2007 Update: A report from the American Heart Association Statistics Committee and Stroke Statistics Subcommittee. 2007.

48. **Kessler RC**, **Berglund P**, **Demler O**, **Jin R**, **Koretz D**, **Merikangas KR**, **Rush AJ**,

Walters EE, **Wang A**, **Rovner B**, **Casten R**. The epidemiology of major depressive disorder: results from the National Comorbidity Survey Replication (NCS-R). *JAMA J Am Med Assoc* 289: 3095–105, 2003. doi: 10.1097/00132578-200310000-00002.

49. **Zeng X**, **Xie Y jie**, **Liu Y ting**, **Long S lian**, **Mo Z cheng**. Polycystic ovarian syndrome: Correlation between hyperandrogenism, insulin resistance and obesity. *Clin Chim Acta* 502: 214–221, 2020. doi: 10.1016/j.cca.2019.11.003.

50. **Viau V**, **Meaney MJ**. Variations in the hypothalamic-pituitary-adrenal response to stress during the estrous cycle in the rat. *Endocrinology* 129: 2503–2511, 1991. doi: 10.1210/endo-129-5-2503.

51. **Davis SR**, **Martinez-Garcia A**, **Robinson PJ**, **Handelsman DJ**, **Desai R**, **Wolfe R**, **Bell RJ**. Estrone is a strong predictor of circulating estradiol in women age 70 years and older. *J Clin Endocrinol Metab* 105: E3348–E3354, 2020. doi: 10.1210/clinem/dgaa429.

52. **Ikeda K**, **Horie-Inoue K**, **Inoue S**. Functions of estrogen and estrogen receptor signaling on skeletal muscle. *J Steroid Biochem Mol Biol* 191: 105375, 2019. doi: 10.1016/j.jsbmb.2019.105375.

53. **Chen C**, **Gong X**, **Yang X**, **Shang X**, **Du Q**, **Liao Q**, **Xie R**, **Chen Y**, **Jingyu XU**. The roles of estrogen and estrogen receptors in gastrointestinal disease (Review). *Oncol Lett* 18: 5673–5680, 2019. doi: 10.3892/ol.2019.10983.

54. **Hutson DD**, **Gurrala R**, **Ogola BO**, **Zimmerman MA**, **Mostany R**, **Satou R**, **Lindsey SH**. Estrogen receptor profiles across tissues from male and female Rattus norvegicus. *Biol Sex Differ* 10(1): 1–13, 2019. doi: 10.1186/s13293-019-0219-9.

55. **Arias-Loza PA**, **Jazbutyte V**, **Pelzer T**. Genetic and pharmacologic strategies to determine the function of estrogen receptor α and estrogen receptor β in cardiovascular system. *Gend Med* 5: 34–45, 2008. doi: 10.1016/j.genm.2008.03.005.

56. **Taraborrelli S**. Physiology, production and action of progesterone. *Acta Obstet Gynecol Scand* 94: 8–16, 2015. doi: 10.1111/aogs.12771.

57. **Li W**, **Li D**, **Sun L**, **Li Z**, **Yu L**, **Wu S**. The protective effects of estrogen on hepatic ischemia-reperfusion injury in rats by downregulating the Ang II/AT1R pathway. *Biochem Biophys Res Commun* 503: 2543–2548, 2018. doi: 10.1016/j.bbrc.2018.07.013.

58. **Liu S bing**, **Zhao M gao**. Neuroprotective effect of estrogen: Role of nonsynaptic NR2B-containing NMDA receptors. *Brain Res Bull* 93: 27–31, 2013. doi: 10.1016/j.brainresbull.2012.10.004.

59. **Liu R**, **Yang SH**. Window of opportunity: Estrogen as a treatment for ischemic stroke. *Brain Res* 1514: 83–90, 2013. doi: 10.1016/j.brainres.2013.01.023.

60. **Zhao Z**, **Mai Z**, **Ou L**, **Duan X**, **Zeng G**. Serum Estradiol and Testosterone Levels in Kidney Stones Disease with and without Calcium Oxalate Components in Naturally Postmenopausal Women. *PLoS One* 8: 1–6, 2013. doi: 10.1371/journal.pone.0075513.

61. **Lagranha CJ**, **Silva TLA**, **Silva SCA**, **Braz GRF**, **da Silva AI**, **Fernandes MP**, **Sellitti DF**. Protective effects of estrogen against cardiovascular disease mediated via oxidative stress in the brain. *Life Sci* 192: 190–198, 2018. doi: 10.1016/j.lfs.2017.11.043.

62. **Zhou Z**, **Ribas V**, **Rajbhandari P**, **Drew BG**, **Moore TM**, **Fluitt AH**, **Reddish BR**, **Whitney KA**, **Georgia S**, **Vergnes L**, **Reue K**, **Liesa M**, **Shirihai O**, **Van Der Bliek AM**, **Chi NW**, **Mahata SK**, **Tiano JP**, **Hewitt SC**, **Tontonoz P**, **Korach KS**, **Mauvais-Jarvis F**, **Hevener AL**. Estrogen receptor alpha protects pancreatic beta cells from apoptosis by preserving mitochondrial function and suppressing endoplasmic reticulum stress. *J Biol Chem* 293: 4735–4751, 2018. doi: 10.1074/jbc.M117.805069.

63. **Steagall RJ**, **Yao F**, **Shaikh SR**, **Abdel-Rahman AA**. Estrogen receptor α activation enhances its cell surface localization and improves myocardial redox status in ovariectomized rats. *Life Sci* 182: 41–49, 2017. doi: 10.1016/j.lfs.2017.06.005.

64. **Mann V**, **Huber C**, **Kogianni G**, **Collins F**, **Noble B**. The antioxidant effect of estrogen and Selective Estrogen Receptor Modulators in the inhibition of osteocyte apoptosis in vitro. *Bone* 40: 674–684, 2007. doi: 10.1016/j.bone.2006.10.014.

65. **Cho JJ**, **Cadet P**, **Salamon E**, **Mantione KJ**, **Stefano GB**. The nongenomic protective effects of estrogen on the male cardiovascular system: Clinical and therapeutic implications in aging men. *Med Sci Monit* 9: 63–68, 2003.

66. **Ghimire A**, **Howlett SE**. An acute estrogen receptor agonist enhances protective effects of cardioplegia in hearts from aging male and female mice. *Exp Gerontol* 141, 2020. doi: 10.1016/j.exger.2020.111093.

67. **Sheng JA**, **Bales NJ**, **Myers SA**, **Bautista AI**, **Roueinfar M**, **Hale TM**, **Handa RJ**. The Hypothalamic-Pituitary-Adrenal Axis: Development, Programming Actions of Hormones, and Maternal-Fetal Interactions. *Front Behav Neurosci* 14: 1–21, 2021. doi: 10.3389/fnbeh.2020.601939.

68. **Myers B**. Corticolimbic regulation of cardiovascular responses to stress. *Physiol Behav* 172: 49–59, 2017. doi: 10.1016/j.physbeh.2016.10.015.

69. **Handa RJ**, **Weiser MJ**. Gonadal steroid hormones and the hypothalamo-pituitary-adrenal axis. *Front Neuroendocrinol* 35: 197–220, 2014. doi: 10.1016/j.yfrne.2013.11.001.

70. **Handa RJ**, **Mani SK**, **Uht RM**. Estrogen receptors and the regulation of neural stress responses. *Neuroendocrinology* 96: 111–118, 2012. doi: 10.1159/000338397.

71. **Garrett JE**, **Wellman CL**. Chronic stress effects on dendritic morphology in medial prefrontal cortex: sex differences and estrogen dependence. *Neuroscience* 162: 195–207, 2009. doi: 10.1016/j.neuroscience.2009.04.057.

72. **Karisetty BC**, **Joshi PC**, **Kumar A**, **Chakravarty S**. Sex differences in the effect of chronic mild stress on mouse prefrontal cortical BDNF levels: A role of major ovarian hormones. *Neuroscience* 356: 89–101, 2017. doi: 10.1016/j.neuroscience.2017.05.020.

73. **Wallace T**, **Schaeuble D**, **Pace SA**, **Schackmuth MK**, **Hentges ST**, **Chicco AJ**, **Myers B**. Sexually divergent cortical control of affective-autonomic integration. *Psychoneuroendocrinology* 129: 105238, 2021. doi: 10.1016/j.psyneuen.2021.105238.

74. **Guo L**, **Chen YX**, **Hu YT**, **Wu XY**, **He Y**, **Wu JL**, **Huang ML**, **Mason M**, **Bao AM**. Sex

hormones affect acute and chronic stress responses in sexually dimorphic patterns: Consequences for depression models. *Psychoneuroendocrinology* 95: 34–42, 2018. doi: 10.1016/j.psyneuen.2018.05.016.

75. **Wei J**, **Yuen EY**, **Liu W**, **Li X**, **Zhong P**, **Karatsoreos IN**, **McEwen BS**, **Yan Z**. Estrogen protects against the detrimental effects of repeated stress on glutamatergic transmission and cognition. *Mol Psychiatry* 19: 588–598, 2014. doi: 10.1038/mp.2013.83.

76. **Contoreggi NH**, **Mazid S**, **Goldstein LB**, **Park J**, **Ovalles AC**, **Waters EM**, **Glass MJ**, **Milner TA**. Sex and age influence gonadal steroid hormone receptor distributions relative to estrogen receptor β-containing neurons in the mouse hypothalamic paraventricular nucleus. *J Comp Neurol* 529: 2283–2310, 2021. doi: 10.1002/cne.25093.

77. **Bao AM**, **Fischer DF**, **Wu YH**, **Hol EM**, **Balesar R**, **Unmehopa UA**, **Zhou JN**, **Swaab DF**. A direct androgenic involvement in the expression of human corticotropin-releasing hormone. *Mol Psychiatry* 11: 567–576, 2006. doi: 10.1038/sj.mp.4001800.

78. **Evans AN**, **Liu Y**, **MacGregor R**, **Huang V**, **Aguilera G**. Regulation of hypothalamic corticotropin-releasing hormone transcription by elevated glucocorticoids. *Mol Endocrinol* 27: 1796–1807, 2013. doi: 10.1210/me.2013-1095.

79. **Han F**, **Ozawa H**, **Matsuda KI**, **Nishi M**, **Kawata M**. Colocalization of mineralocorticoid receptor and glucocorticoid receptor in the hippocampus and hypothalamus. *Neurosci Res* 51: 371–381, 2005. doi: 10.1016/j.neures.2004.12.013.

80. **Manoranjan B**, **Salehi F**, **Scheithauer BW**, **Rotondo F**, **Kovacs K**, **Cusimano MD**. Estrogen receptors α and β immunohistochemical expression: Clinicopathological correlations in pituitary adenomas. *Anticancer Res* 30: 2897–2904, 2010.

81. **Hu P**, **Liu J**, **Yasrebi A**, **Gotthardt JD**, **Bello NT**, **Pang ZP**, **Roepke TA**. Gq Protein-Coupled membrane-Initiated estrogen signaling rapidly excites corticotropin-releasing hormone neurons in the hypothalamic paraventricular nucleus in female mice. *Endocrinology* 157: 3604–3620, 2016. doi: 10.1210/en.2016-1191.

82. **Maejima Y**, **Aoyama M**, **Ookawara S**, **Hirao A**, **Sugita S**. Distribution of the androgen receptor in the diencephalon and the pituitary gland in goats: Co-localisation with corticotrophin releasing hormone, arginine vasopressin and corticotrophs. *Vet J* 181: 193–199, 2009. doi: 10.1016/j.tvjl.2008.02.021.

83. **Keller-Wood M**. Hypothalamic-pituitary-adrenal axis-feedback control. *Compr Physiol* 5: 1161–1182, 2015. doi: 10.1002/cphy.c140065.

84. **Trejter M**, **Jopek K**, **Celichowski P**, **Tyczewska M**, **Malendowicz LK**, **Rucinski M**. Expression of estrogen, estrogen related and androgen receptors in adrenal cortex of intact adult male and female rats. *Folia Histochem Cytobiol* 53: 133–144, 2015. doi: 10.5603/FHC.a2015.0012.

85. **VanderHorst VGJM**, **Terasawa E**, **Ralston HJ**. Estrogen receptor-α immunoreactive neurons in the brainstem and spinal cord of the female rhesus monkey: Species-specific characteristics. *Neuroscience* 158: 798–810, 2009. doi: 10.1016/j.neuroscience.2008.10.017.

86. **Coolen RL**, **Cambier JC**, **Spantidea PI**, **van Asselt E**, **Blok BFM**. Androgen receptors in areas of the spinal cord and brainstem: A study in adult male cats. *J Anat* : 1–11, 2021. doi: 10.1111/joa.13407.

87. **Schlenker EH**, **Hansen SN**. Sex-specific densities of estrogen receptors alpha and beta in the subnuclei of the nucleus tractus solitarius, hypoglossal nucleus and dorsal vagal motor nucleus weanling rats. *Brain Res* 1123: 89–100, 2006. doi: 10.1016/j.brainres.2006.09.035.

88. **Brailoiu E**, **Dun SL**, **Brailoiu GC**, **Mizuo K**, **Sklar LA**, **Oprea TI**, **Prossnitz ER**, **Dun NJ**. Distribution and characterization of estrogen receptor G protein-coupled receptor 30 in the rat central nervous system. *J Endocrinol* 193: 311–321, 2007. doi: 10.1677/JOE-07-0017.

89. **Zoubina E V.**, **Smith PG**. Distributions of estrogen receptors alpha and beta in

sympathetic neurons of female rats: Enriched expression by uterine innervation. *J Neurobiol* 52: 14–23, 2002. doi: 10.1002/neu.10064.

90. **Young WJ**, **Chang C**. Ontogeny and autoregulation of androgen receptor mRNA expression in the nervous system. *Endocrine* 9: 79–88, 1998. doi: 10.1385/ENDO:9:1:79.

91. **Mahmoodzadeh S**, **Dworatzek E**. The role of 17β-estradiol and estrogen receptors in regulation of Ca2+ channels and mitochondrial function in Cardio myocytes. *Front Endocrinol (Lausanne)* 10: 1–15, 2019. doi: 10.3389/fendo.2019.00310.

92. **Lizotte E**, **Grandy SA**, **Tremblay A**, **Allen BG**, **Fiset C**. Cellular Physiology Biochemistry and Biochemistr y Expression , Distribution and Regulation of Sex Steroid Hormone Receptors in Mouse Heart. *Cell Physiol Biochem* 8: 75–86, 2009.

93. **Oakley RH**, **Cruz-Topete D**, **He B**, **Foley JF**, **Myers PH**, **Xu X**, **Gomez-Sanchez CE**, **Chambon P**, **Willis MS**, **Cidlowski JA**. Cardiomyocyte glucocorticoid and mineralocorticoid receptors directly and antagonistically regulate heart disease in mice. *Sci Signal* 12, 2019. doi: 10.1126/scisignal.aau9685.

94. **Gros R**, **Ding Q**, **Liu B**, **Chorazyczewski J**, **Feldman RD**. Aldosterone mediates its rapid effects in vascular endothelial cells through GPER activation. *Am J Physiol - Cell Physiol* 304: 532–540, 2013. doi: 10.1152/ajpcell.00203.2012.

95. **Yeap BB**. Androgens and cardiovascular disease. *Curr Opin Endocrinol Diabetes Obes* 17: 269–276, 2010. doi: 10.1097/MED.0b013e3283383031.

96. **Mendelsohn ME**, **Karas RH**. The Protective Effects of Estrogen on the Cardiovascular System. *N Engl J Med* 340: 1801–1811, 1999.

97. **Faulkner JL**, **Belin de Chantemèle EJ**. Mineralocorticoid Receptor and Endothelial Dysfunction in Hypertension. *Curr Hypertens Rep* 21, 2019. doi: 10.1007/s11906-019-0981-4.

98. **Kornel L**, **Nelson WA**, **Manisundaram B**, **Chigurupati R**, **Hayashi T**. Mechanism of the effects of glucocorticoids and mineralocorticoids on vascular smooth muscle contractility.

Steroids 58: 580–587, 1993. doi: 10.1016/0039-128X(93)90099-9.

99. **Joseph V**, **Doan VD**, **Morency CE**, **Lajeunesse Y**, **Bairam A**. Expression of sex-steroid receptors and steroidogenic enzymes in the carotid body of adult and newborn male rats. *Brain Res* 1073–1074: 71–82, 2006. doi: 10.1016/j.brainres.2005.12.075.

100. **Broughton BRS**, **Miller AA**, **Sobey CG**. Endothelium-dependent relaxation by G protein-coupled receptor 30 agonists in rat carotid arteries. *Am J Physiol - Hear Circ Physiol* 298: 1055–1061, 2010. doi: 10.1152/ajpheart.00878.2009.

101. **Falvey A**, **Duprat F**, **Simon T**, **Hugues-Ascery S**, **Conde S V.**, **Glaichenhaus N**, **Blancou P**. Electrostimulation of the carotid sinus nerve in mice attenuates inflammation via glucocorticoid receptor on myeloid immune cells. *J Neuroinflammation* 17: 1–12, 2020. doi: 10.1186/s12974-020-02016-8.

102. **Lombès M**, **Oblin ME**, **Gasc JM**, **Baulieu EE**, **Farman N**, **Bonvalet JP**. Immunohistochemical and biochemical evidence for a cardiovascular mineralocorticoid receptor. *Circ Res* 71: 503–510, 1992. doi: 10.1161/01.res.71.3.503.

103. **Jacobson L**, **Sapolsky R**. The role of the hippocampus in feedback regulation of the hypothalamic-pituitary-adrenocortical axis. *Endocr Rev* 12: 118–134, 1991. doi: 10.1210/edrv-12-2-118.

104. **Qu N**, **Wang X-M**, **Zhang T**, **Zhang S-F**, **Li Y**, **Cao F-Y**, **Wang Q**, **Ning L-N**, **Tian Q**. Estrogen Receptor α Agonist is Beneficial for Young Female Rats Against Chronic Unpredicted Mild Stress-Induced Depressive Behavior and Cognitive Deficits. *J Alzheimer's Dis* 77: 1077–1093, 2020. doi: 10.3233/jad-200486.

105. **Rosinger Z**, **Jacobskind J**, **Bulanchuk N**, **Malone M**, **Fico D**, **Justice N**, **Zuloaga D**. Characterization and gonadal hormone regulation of a sexually dimorphic corticotropin releasing factor receptor 1 cell group. *J Comp Neurol* 527: 1056–1069, 2019. doi: 10.1002/cne.24588.Characterization.

106. **Saleh MC**, **Connell BJ**, **Saleh TM**. Autonomic and cardiovascular reflex responses to

central estrogen injection in ovariectomized female rats. *Brain Res* 879: 105–114, 2000. doi: 10.1016/S0006-8993(00)02757-8.

107. **Xue B**, **Zhang Z**, **Beltz TG**, **Johnson RF**, **Guo F**, **Hay M**, **Johnson AK**. Estrogen receptor-β in the paraventricular nucleus and rostroventrolateral medulla plays an essential protective role in aldosterone/salt-induced hypertension in female rats. *Hypertension* 61: 1255–1262, 2013. doi: 10.1161/HYPERTENSIONAHA.111.00903.

108. **Sabbatini AR**, **Kararigas G**. Estrogen-related mechanisms in sex differences of hypertension and target organ damage. *Biol Sex Differ* 11: 1–17, 2020. doi: 10.1186/s13293-020-00306-7.

109. **Brahmbhatt Y**, **Gupta M**, **Hamrahian S**. Hypertension in Premenopausal and Postmenopausal Women. *Curr Hypertens Rep* 21: 1–10, 2019. doi: 10.1007/s11906-019-0979-y.

110. **Brooks SD**, **Hileman SM**, **Chantler PD**, **Milde SA**, **Lemaster KA**, **Frisbee SJ**, **Shoemaker JK**, **Jackson DN**, **Frisbee JC**. Protection from vascular dysfunction in female rats with chronic stress and depressive symptoms. *Am J Physiol - Hear Circ Physiol* 314: H1070–H1084, 2018. doi: 10.1152/ajpheart.00647.2017.

111. **Morford J**, **Mauvais-jarvis F**. Sex differences in the effects of androgens acting in the central nervous system on metabolism. *Dialogues Clin Neurosci* 18: 415–424, 2016.

112. **Perusquía M**, **Contreras D**, **Herrera N**. Hypotestosteronemia is an important factor for the development of hypertension: elevated blood pressure in orchidectomized conscious rats is reversed by different androgens. *Endocrine* 65: 416–425, 2019. doi: 10.1007/s12020-019-01978-x.

113. **Hanson AE**, **Perusquia M**, **Stallone JN**. Hypogonadal hypertension in male Sprague-Dawley rats is renin-angiotensin system-dependent: Role of endogenous androgens. *Biol Sex Differ* 11: 1–13, 2020. doi: 10.1186/s13293-020-00324-5.

114. **Moretti C**, **Lanzolla G**, **Moretti M**, **Gnessi L**, **Carmina E**. Androgens and Hypertension

in Men and Women: a Unifying View. *Curr Hypertens Rep* 19, 2017. doi: 10.1007/s11906-017-0740-3.

115. **Wainwright SR**, **Workman JL**, **Tehrani A**, **Hamson DK**, **Chow C**, **Lieblich SE**, **Galea LAM**. Testosterone has antidepressant-like efficacy and facilitates imipramine-induced neuroplasticity in male rats exposed to chronic unpredictable stress. *Horm Behav* 79: 58–69, 2016. doi: 10.1016/j.yhbeh.2016.01.001.

116. **Arun S**, **Burawat J**, **Sukhorum W**, **Sampannang A**, **Maneenin C**, **Iamsaard S**. Chronic restraint stress induces sperm acrosome reaction and changes in testicular tyrosine phosphorylated proteins in rats. *Int J Reprod Biomed* 14: 443–452, 2016. doi: 10.29252/ijrm.14.7.2.

117. **Viau V**, **Meaney MJ**. The inhibitory effect of testosterone on hypothalamic-pituitary-adrenal responses to stress is mediated by the medial preoptic area. *J Neurosci* 16: 1866–1876, 1996. doi: 10.1523/jneurosci.16-05-01866.1996.

118. **Joyner MJ**, **Wallin BG**, **Charkoudian N**. Sex differences and blood pressure regulation in humans. *Exp Physiol* 101: 349–355, 2016. doi: 10.1113/EP085146.

119. **Kappus RM**, **Ranadive SM**, **Yan H**, **Lane-cordova AD**, **Cook MD**, **Sun P**, **Harvey IS**, **Wilund KR**, **Woods JA**, **Fernhall B**. Sex differences in autonomic function following maximal exercise. *Biol Sex Differ* 6: 4–11, 2015. doi: 10.1186/s13293-015-0046-6.

120. **Nahman-averbuch H**, **Dayan L**, **Sprecher E**, **Hochberg U**, **Brill S**, **Yarnitsky D**, **Jacob G**. Physiology & Behavior Sex differences in the relationships between parasympathetic activity and pain modulation. *Physiol Behav* 154: 40–48, 2016. doi: 10.1016/j.physbeh.2015.11.004.

121. **Ferreira MJ**, **Sanches IC**, **Jorge L**, **Llesuy SF**, **Irigoyen MC**, **De Angelis K**. Ovarian status modulates cardiovascular autonomic control and oxidative stress in target organs. *Biol Sex Differ* 11: 1–10, 2020. doi: 10.1186/s13293-020-00290-y.

122. **Yang SG**, **Mlček M**, **Kittnar O**. Estrogen can modulate menopausalwomen's heart rate

variability. *Physiol Res* 62, 2013. doi: 10.33549/physiolres.932612.

123. **Brockbank CL**, **Chatterjee F**, **Bruce SA**, **Woledge RC**. Heart rate and its variability change after the menopause. *Exp Physiol* 85: 327–330, 2000. doi: 10.1111/j.1469-445X.2000.01902.x.

124. **Virtanen I**, **Polo O**, **Polo-Kantola P**, **Kuusela T**, **Ekholm E**. The effect of estrogen replacement therapy on cardiac autonomic regulation. *Maturitas* 37: 45–51, 2000. doi: 10.1016/S0378-5122(00)00162-6.

125. **Shen H**, **Fuchino Y**, **Miyamoto D**, **Nomura H**, **Matsuki N**. Vagus nerve stimulation enhances perforant path-CA3 synaptic transmission via the activation of β-adrenergic receptors and the locus coeruleus. *Int J Neuropsychopharmacol* 15: 523–530, 2012. doi: 10.1017/S1461145711000708.

126. **Vieira JO**, **Duarte JO**, **Costa-Ferreira W**, **Morais-Silva G**, **Marin MT**, **Crestani CC**. Sex differences in cardiovascular, neuroendocrine and behavioral changes evoked by chronic stressors in rats. *Prog Neuro-Psychopharmacology Biol Psychiatry* 81: 426–437, 2018. doi: 10.1016/j.pnpbp.2017.08.014.

127. **Stanley SC**, **Brooks SD**, **Butcher JT**, **D'Audiffret AC**, **Frisbee SJ**, **Frisbee JC**. Protective effect of sex on chronic stress- and depressive behavior-induced vascular dysfunction in BALB/cJ mice. *J Appl Physiol* 117: 959–970, 2014. doi: 10.1152/japplphysiol.00537.2014.

128. **Finnell JE**, **Wood SK**. Neuroinflammation at the interface of depression and cardiovascular disease: Evidence from rodent models of social stress. *Neurobiol Stress* 4: 1–14, 2016. doi: 10.1016/j.ynstr.2016.04.001.

129. **Goshen I**, **Kreisel T**, **Ben-Menachem-Zidon O**, **Licht T**, **Weidenfeld J**, **Ben-Hur T**, **Yirmiya R**. Brain interleukin-1 mediates chronic stress-induced depression in mice via adrenocortical activation and hippocampal neurogenesis suppression. *Mol Psychiatry* 13: 717–728, 2008. doi: 10.1038/sj.mp.4002055.

130. **Wang YL**, **Han QQ**, **Gong WQ**, **Pan DH**, **Wang LZ**, **Hu W**, **Yang M**, **Li B**, **Yu J**, **Liu Q**. Microglial activation mediates chronic mild stress-induced depressive- and anxiety-like behavior in adult rats. *J Neuroinflammation* 15: 1–14, 2018. doi: 10.1186/s12974-018-1054-3.

131. **Barnard DF**, **Gabella KM**, **Kulp AC**, **Parker AD**, **Dugan PB**, **Johnson JD**. Sex differences in the regulation of brain IL-1β in response to chronic stress. *Psychoneuroendocrinology* 103: 203–211, 2019. doi: 10.1016/j.psyneuen.2019.01.026.

132. **Bekhbat M**, **Howell PA**, **Rowson SA**, **Kelly SD**, **Tansey MG**, **Neigh GN**. Chronic adolescent stress sex-specifically alters central and peripheral neuro-immune reactivity in rats. *Brain Behav Immun* 76: 248–257, 2019. doi: 10.1016/j.bbi.2018.12.005.

133. **Finnell JE**, **Muniz BL**, **Padi AR**, **Lombard CM**, **Moffitt CM**, **Wood CS**, **Wilson LB**, **Reagan LP**, **Wilson MA**, **Wood SK**. Essential Role of Ovarian Hormones in Susceptibility to the Consequences of Witnessing Social Defeat in Female Rats. *Biol Psychiatry* 84: 372–382, 2018. doi: 10.1016/j.biopsych.2018.01.013.

134. **Cotella EM**, **Morano RL**, **Wulsin AC**, **Martelle SM**, **Lemen P**, **Fitzgerald M**, **Packard BA**, **Moloney RD**, **Herman JP**. Lasting Impact of Chronic Adolescent Stress and Glucocorticoid Receptor Selective Modulation in Male and Female Rats. *Psychoneuroendocrinology* 112: 104490, 2020. doi: 10.1016/j.psyneuen.2019.104490.

135. **Wulsin AC**, **Wick-Carlson D**, **Packard BA**, **Morano R**, **Herman JP**. Adolescent chronic stress causes hypothalamo-pituitary-adrenocortical hypo-responsiveness and depression-like behavior in adult female rats. *Psychoneuroendocrinology* 65: 109–117, 2016. doi: 10.1016/j.psyneuen.2015.12.004.

136. **Yan Y**, **Dominguez S**, **Fisher DW**, **Dong H**. Sex differences in chronic stress responses and Alzheimer ’s disease. *Neurobiol Stress* 8: 120–126, 2018. doi: 10.1016/j.ynstr.2018.03.002.

137. **Kyrou I**, **Tsigos C**. Stress hormones : physiological stress and regulation of metabolism.

Curr Opin Pharmacol 9: 787–793, 2009. doi: 10.1016/j.coph.2009.08.007.

138. **Kaufman D**, **Banerji MA**, **Shorman I**, **Smith ELP**, **Coplan JD**, **Rosenblum LA**, **Kral JG**. Early-life stress and the development of obesity and insulin resistance in juvenile bonnet macaques. *Diabetes* 56: 1382–1386, 2007. doi: 10.2337/db06-1409.

139. **Vargas J**, **Junco M**, **Gomez C**, **Lajud N**. Early life stress increases metabolic risk, HPA axis reactivity, and depressive-like behavior when combined with postweaning social isolation in rats. *PLoS One* 11: 1–21, 2016. doi: 10.1371/journal.pone.0162665.

140. **Carr CP**, **Martins CMS**, **Stingel AM**, **Lemgruber VB**, **Juruena MF**. The role of early life stress in adult psychiatric disorders: A systematic review according to childhood trauma subtypes. *J Nerv Ment Dis* 201: 1007–1020, 2013. doi: 10.1097/NMD.0000000000000049.

141. **Enoch MA**. The role of early life stress as a predictor for alcohol and drug dependence. *Psychopharmacology (Berl)* 214: 17–31, 2011. doi: 10.1007/s00213-010-1916-6.

142. **Jankord R**, **Solomon MB**, **Albertz J**, **Flak JN**, **Zhang R**, **Herman JP**. Stress Vulnerability during Adolescent Development in Rats. *Endocrinology* 152: 629–638, 2011. doi: 10.1210/en.2010-0658.

143. **Naninck EFG**, **Hoeijmakers L**, **Kakava-Georgiadou N**, **Meesters A**, **Lazic SE**, **Lucassen PJ**, **Korosi A**. Chronic early life stress alters developmental and adult neurogenesis and impairs cognitive function in mice. *Hippocampus* 25: 309–328, 2015. doi: 10.1002/hipo.22374.

144. **Pereira VH**, **Marques F**, **Lages V**, **Pereira FG**, **Patchev A**, **Almeida OFX**, **Palha JA**, **Sousa N**, **Cerqueira JJ**. Glucose intolerance after chronic stress is related with downregulated PPAR - γ in adipose tissue. *Cardiovasc Diabetol* 15: 1–11, 2016. doi: 10.1186/s12933-016-0433-2.

145. **Brunson KL**, **Kramár E**, **Lin B**, **Chen Y**, **Colgin LL**, **Yanagihara TK**, **Lynch G**, **Baram TZ**. Mechanisms of late-onset cognitive decline after early-life stress. *J Neurosci* 25:

9328–9338, 2005. doi: 10.1523/JNEUROSCI.2281-05.2005.

146. **Pechtel P**, **Pizzagalli DA**. Effects of early life stress on cognitive and affective function: An integrated review of human literature. *Psychopharmacology (Berl)* 214: 55–70, 2011. doi: 10.1007/s00213-010-2009-2.

147. **Hedges DW**, **Woon FL**. Early-life stress and cognitive outcome. *Psychopharmacology (Berl)* 214: 121–130, 2011. doi: 10.1007/s00213-010-2090-6.

148. **Saleh A**, **Potter G**, **McQuoid D**, **Boyd B**, **Turner R**, **MacFall J**, **Taylor W**. Effects of Early Life Stress on Depression, Cognitive Performance, and Brain Morphology. *Psychol Med* 47: 171–181, 2017. doi: 10.1016/j.physbeh.2017.03.040.

149. **Bolton J**, **Molet J**, **Ivy A**, **Baram T**. New insights into early-life stress and behavioral outcomes. *Curr Opin Behav Sci* 14: 133–139, 2017. doi: 10.1038/s41395-018-0061-4.

150. **McEwen B**. Understanding the potency of stressful early life experiences on brain and body function. *Metabolism* 57: 1–8, 2009. doi: 10.1016/j.metabol.2008.07.006.Understanding.

151. **Loman MM**, **Gunnar MR**. Early experience and the development of stress reactivity and regulation in children. *Neurosci Biobehav Rev* 34: 867–876, 2010. doi: 10.1016/j.neubiorev.2009.05.007.

152. **Goldman-Mellor S**, **Hamer M**, **Steptoe A**. Early-life stress and recurrent psychological distress over the lifecourse predict divergent cortisol reactivity patterns in adulthood. *Psychoneuroendocrinology* 37: 1755–1768, 2012. doi: 10.1016/j.psyneuen.2012.03.010.

153. **Oliveira P**, **Coroa M**, **Madeira N**, **Santos V**. Sex differences in psychiatric inpatients: Demographics, psychiatric diagnoses and medical comorbidities. *Eur Psychiatry* 41: S698–S698, 2017. doi: 10.1016/j.eurpsy.2017.01.1231.

154. **Jalnapurkar I**, **Allen M**, **Pigott T**. Sex Differences in Anxiety Disorders: A Review. *Psychiatry, Depress Anxiety* 4, 2018. doi: 10.24966/pda-0150/100012.

155. **Myers B**, **McKlveen JM**, **Morano R**, **Ulrich-Lai YM**, **Solomon MB**, **Wilson SP**, **Herman**

JP. Vesicular glutamate transporter 1 knockdown in infralimbic prefrontal cortex augments neuroendocrine responses to chronic stress in male rats. *Endocrinology* 158: 3579–3591, 2017. doi: 10.1210/en.2017-00426.

156. **Schaeuble D**, **Packard AEB**, **McKlveen JM**, **Morano R**, **Fourman S**, **Smith BL**, **Scheimann JR**, **Packard BA**, **Wilson SP**, **James J**, **Hui DY**, **Ulrich-Lai YM**, **Herman JP**, **Myers B**. Prefrontal Cortex Regulates Chronic Stress-Induced Cardiovascular Susceptibility. *J Am Heart Assoc* 8: e014451, 2019. doi: 10.1161/JAHA.119.014451.
157. **Bekhbat M**, **Glasper E**, **Rowson S**, **Kelly S**, **Neigh G**. Measuring Corticosterone concentrations over a physiological dynamic range in female rats. *Physiol Behav* 194: 73–76, 2018.
158. **Molendijk ML**, **de Kloet ER**. Coping with the forced swim stressor: Current state-of-the-art. *Behav Brain Res* 364: 1–10, 2019. doi: 10.1016/j.bbr.2019.02.005.
159. **Pace SA**, **Christensen C**, **Schackmuth MK**, **Wallace T**, **Jessica M**, **Beischel W**, **Morano R**, **Scheimann JR**, **Wilson SP**, **Herman P**, **Myers B**. Infralimbic cortical glutamate output is necessary for the neural and behavioral consequences of chronic stress. .
160. **Smith EP**, **An Z**, **Wagner C**, **Lewis AG**, **Cohen EB**, **Li B**, **Mahbod P**, **Sandoval D**, **Perez-Tilve D**, **Tamarina N**, **Philipson LH**, **Stoffers DA**, **Seeley RJ**, **D'Alessio DA**. The role of β cell glucagon-like peptide-1 signaling in glucose regulation and response to diabetes drugs. *Cell Metab* 19: 1050–1057, 2014. doi: 10.1016/j.cmet.2014.04.005.
161. **Ghosal S**, **Nunley A**, **Mahbod P**, **Lewis AG**, **Smith EP**, **Tong J**, **D'Alessio DA**, **Herman JP**. Mouse handling limits the impact of stress on metabolic endpoints. *Physiol Behav* 150: 31–37, 2015. doi: 10.1016/j.physbeh.2015.06.021.
162. **Hill JL**, **Solomon MB**, **Nguyen ET**, **Caldwell JL**, **Wei Y**, **Foster MT**. Glucocorticoids regulate adipose tissue protein concentration in a depot- and sex-specific manner. *Stress* 23: 243–247, 2020. doi: 10.1080/10253890.2019.1658736.

163. **Nguyen ET**, **Berman S**, **Streicher J**, **Estrada CM**, **Caldwell JL**, **Ghisays V**, **Ulrich-Lai Y**, **Solomon MB**. Effects of combined glucocorticoid/mineralocorticoid receptor modulation (CORT118335) on energy balance, adiposity, and lipid metabolism in male rats. *Am J Physiol - Endocrinol Metab* 317: E337–E349, 2019. doi: 10.1152/ajpendo.00018.2019.

164. **Lin EE**, **Scott-Solomon E**, **Kuruvilla R**. Peripheral Innervation in the Regulation of Glucose Homeostasis. *Trends Neurosci* 44: 189–202, 2021. doi: 10.1016/j.tins.2020.10.015.

165. **Romeo RD**, **Karatsoreos IN**, **Ali FS**, **McEwen BS**. The effects of acute stress and pubertal development on metabolic hormones in the rat. *Stress* 10: 101–106, 2007. doi: 10.1080/10253890701204270.

166. **Foilb AR**, **Lui P**, **Romeo RD**. The transformation of hormonal stress responses throughout puberty and adolescence. *J Endocrinol* 210: 391–398, 2011. doi: 10.1530/JOE-11-0206.

167. **Romeo RD**, **Lee SJ**, **McEwen BS**. Differential stress reactivity in intact and ovariectomized prepubertal and adult female rats. *Neuroendocrinology* 80: 387–393, 2004. doi: 10.1159/000084203.

168. **Smith B**, **Morano R**, **Ulrich-Lai YM**, **Myers B**, **Solomon MB**, **Herman JP**. Adolescent environmental enrichment prevents behavioral and physiological sequelae of adolescent chronic stress in female (but not male) rats. *Stress* 21: 464–473, 2018. doi: 10.1016/j.physbeh.2017.03.040.

169. **Navarro G**, **Allard C**, **Xu W**, **Mauvais-Jarvis F**. The role of androgens in metabolism, obesity, and diabetes in males and females. *Obesity* 23: 713–719, 2015. doi: 10.1002/oby.21033.

170. **Frye CA**, **Wawrzycki JA**. Effect of prenatal stress and gonadal hormone condition on depressive behaviors of female and male rats. *Horm Behav* 44: 319–326, 2003. doi:

10.1016/S0018-506X(03)00159-4.

171. **Hodes GE**, **Epperson CN**. Sex Differences in Vulnerability and Resilience to Stress Across the Life Span. *Biol Psychiatry* 86: 421–432, 2019. doi: 10.1016/j.biopsych.2019.04.028.

172. **Hahn RG**, **Ljunggren S**, **Larsen F**, **Nyström T**. A simple intravenous glucose tolerance test for assessment of insulin sensitivity. *Theor Biol Med Model* 8: 1–10, 2011. doi: 10.1186/1742-4682-8-12.

173. **Brinton RD**. Minireview: Translational animal models of human menopause: Challenges and emerging opportunities. *Endocrinology* 153: 3571–3578, 2012. doi: 10.1210/en.2012-1340.

174. **Towfighi A**, **Zheng L**, **Ovbiagele B**. Sex-specific trends in midlife coronary heart disease risk and prevalence. *Arch Intern Med* 169: 1762–1766, 2009. doi: 10.1001/archinternmed.2009.318.

175. **Garcia M**, **Mulvagh SL**, **Merz CNB**, **Buring JE**, **Manson JAE**. Cardiovascular disease in women: Clinical perspectives. *Circ Res* 118: 1273–1293, 2016. doi: 10.1161/CIRCRESAHA.116.307547.

176. **Benjamin EJ**, **Muntner P**, **Alonso A**, **Bittencourt MS**, **Callaway CW**, **Carson AP**, **Chamberlain AM**, **Chang AR**, **Cheng S**, **Das SR**, **Delling FN**, **Djousse L**, **Elkind MSV**, **Ferguson JF**, **Fornage M**, **Jordan LC**, **Khan SS**, **Kissela BM**, **Knutson KL**, **Kwan TW**, **Lackland DT**, **Lewis TT**, **Lichtman JH**, **Longenecker CT**, **Loop MS**, **Lutsey PL**, **Martin SS**, **Matsushita K**, **Moran AE**, **Mussolino ME**, **O'Flaherty M**, **Pandey A**, **Perak AM**, **Rosamond WD**, **Roth GA**, **Sampson UKA**, **Satou GM**, **Schroeder EB**, **Shah SH**, **Spartano NL**, **Stokes A**, **Tirschwell DL**, **Tsao CW**, **Turakhia MP**, **VanWagner LB**, **Wilkins JT**, **Wong SS**, **Virani SS**. Heart Disease and Stroke Statistics-2019 Update: A Report From the American Heart Association. 2019.

177. **Boese AC**, **Kim SC**, **Yin K**, **Lee J**, **Hamblin MH**. Sex differences in vascular physiology

and pathophysiology : estrogen and androgen signaling in health and disease. *Heat Circ Physiol* 70112: 524–545, 2020. doi: 10.1152/ajpheart.00217.2016.

178. **El Khoudary SR**, **Aggarwal B**, **Beckie TM**, **Hodis HN**, **Johnson AE**, **Langer RD**, **Limacher MC**, **Manson JE**, **Stefanick ML**, **Allison MA**. Menopause Transition and Cardiovascular Disease Risk: Implications for Timing of Early Prevention: A Scientific Statement from the American Heart Association. *Circulation* 142: E506–E532, 2020. doi: 10.1161/CIR.0000000000000912.
179. **Akinboboye OO**, **Chou RL**, **Bergmann SR**. Myocardial blood flow and efficiency in concentric and eccentric left ventricular hypertrophy. *Am J Hypertens* 17: 433–438, 2004. doi: 10.1016/j.amjhyper.2004.02.006.
180. **Lazzeroni D**, **Rimoldi O**, **Camici PG**. From left ventricular hypertrophy to dysfunction and failure. *Circ J* 80: 555–564, 2016. doi: 10.1253/circj.CJ-16-0062.
181. **Piché ME**, **Tchernof A**, **Després JP**. Obesity Phenotypes, Diabetes, and Cardiovascular Diseases. *Circ Res* 126: 1477–1500, 2020. doi: 10.1161/CIRCRESAHA.120.316101.
182. **Goossens GH**. The Metabolic Phenotype in Obesity: Fat Mass, Body Fat Distribution, and Adipose Tissue Function. *Obes Facts* 10: 207–215, 2017. doi: 10.1159/000471488.
183. **Wadström BN**, **Pedersen KM**, **Wulff AB**, **Nordestgaard BG**. Elevated remnant cholesterol, plasma triglycerides, and cardiovascular and non-cardiovascular mortality. *Eur Heart J* 44: 1432–1445, 2023. doi: 10.1093/eurheartj/ehac822.
184. **Steptoe A**, **Kivimäki M**. Stress and cardiovascular disease. *Nat Rev Cardiol* 9: 360–370, 2012. doi: 10.1038/nrcardio.2012.45.
185. **Huzard D**, **Ghosal S**, **Grosse J**, **Carnevali L**, **Sgoifo A**, **Sandi C**. Low vagal tone in two rat models of psychopathology involving high or low corticosterone stress responses. *Psychoneuroendocrinology* 101: 101–110, 2019. doi: 10.1016/j.psyneuen.2018.11.003.
186. **Chew NWS**, **Ng CH**, **Tan DJH**, **Kong G**, **Lin C**, **Chin YH**, **Lim WH**, **Huang DQ**, **Quek J**, **Fu CE**, **Xiao J**, **Syn N**, **Foo R**, **Khoo CM**, **Wang JW**, **Dimitriadis GK**, **Young DY**,

Siddiqui MS, **Lam CSP**, **Wang Y**, **Figtree GA**, **Chan MY**, **Cummings DE**, **Noureddin M**, **Wong VWS**, **Ma RCW**, **Mantzoros CS**, **Sanyal A**, **Muthiah MD**. The global burden of metabolic disease: Data from 2000 to 2019. *Cell Metab* 35: 414-428.e3, 2023. doi: 10.1016/j.cmet.2023.02.003.

187. **Noubiap JJ**, **Nansseu JR**, **Lontchi-Yimagou E**, **Nkeck JR**, **Nyaga UF**, **Ngouo AT**, **Tounouga DN**, **Tianyi FL**, **Foka AJ**, **Ndoadoumgue AL**, **Bigna JJ**. Geographic distribution of metabolic syndrome and its components in the general adult population: A meta-analysis of global data from 28 million individuals. *Diabetes Res Clin Pract* 188: 1–9, 2022. doi: 10.1016/j.diabres.2022.109924.

188. **Silveira Rossi JL**, **Barbalho SM**, **Reverete de Araujo R**, **Bechara MD**, **Sloan KP**, **Sloan LA**. Metabolic syndrome and cardiovascular diseases: Going beyond traditional risk factors. *Diabetes Metab Res Rev* 38: 1–11, 2022. doi: 10.1002/dmrr.3502.

189. **McHill AW**, **Wright KP**. Role of sleep and circadian disruption on energy expenditure and in metabolic predisposition to human obesity and metabolic disease. *Obes Rev* 18: 15–24, 2017. doi: 10.1111/obr.12503.

190. **Stefanaki C**, **Pervanidou P**, **Boschiero D**, **Chrousos GP**. Chronic stress and body composition disorders : implications for health and disease. *Hormones (Athens)* 17: 33–43, 2018. doi: https://doi.org/10.1007/s42000-018-0023-7.

191. **Dearing C**, **Handa RJ**. Sex differences in autonomic responses to stress : implications for cardiometabolic physiology. *Am J Physiol - Endocrinol Metab* 323: E281–E289, 2022. doi: 10.1152/ajpendo.00058.2022.

192. **Contreras-zentella ML**, **Hern R**. Possible Gender Influence in the Mechanisms Underlying the Oxidative Stress , Inflammatory Response , and the Metabolic Alterations in Patients with Obesity and / or Type 2 Diabetes. *Antioxidants (Basel, Switzerland)* 1 0: 1729, 2021. doi: https://doi.org/10.3390/antiox10111729.

193. **Mcewen BS**. Central effects of stress hormones in health and disease : Understanding

the protective and damaging effects of stress and stress mediators. *Eur J Pharmacol* 583: 174–185, 2008. doi: 10.1016/j.ejphar.2007.11.071.

194. **Hamer M**, **Steptoe A**. Cortisol responses to mental stress and incident hypertension in healthy men and women. *J Clin Endocrinol Metab* 97: 29–34, 2012. doi: 10.1210/jc.2011-2132.

195. **Blackburn-Munro G**, **Blackburn-Munro RE**. Review Article Chronic Pain , Chronic Stress and Depression : Coincidence or Consequence ? *J Neuroendocrinol* 13: 1009–1023, 2001.

196. **Pace TWW**, **Ph D**, **Mletzko TC**, **Alagbe O**, **Musselman DL**, **Nemeroff CB**, **Ph D**, **Miller AH**, **Heim CM**, **Ph D**. Increased Stress-Induced Inflammatory Responses in Male Patients With Major Depression and Increased Early Life Stress. *Am J Psychiachtry* 163: 1630–1633, 2006.

197. **Kim A**, **Knudsen JG**, **Madara JC**, **Benrick A**, **Hill TG**, **Kadir LA**, **Kellard JA**, **Mellander L**, **Miranda C**, **Lin H**, **James T**, **Suba K**, **Spigelman AF**, **Wu Y**, **Macdonald PE**, **Asterholm IW**, **Magnussen T**, **Christensen M**, **Vilsbøll T**, **Salem V**, **Knop FK**, **Rorsman P**, **Endocrinology D**, **Deaconess BI**. vasopressin mediates counter- - regulatory glucagon release and is diminished in type 1 diabetes. *Elife* 10, 2021.

198. **Pace SA**, **Myers B**. Hindbrain Adrenergic / Noradrenergic Control of Integrated Endocrine and Autonomic Stress Responses. *Endocrinology* 165: 1–10, 2024. doi: 10.1210/endocr/bqad178.

199. **Pace S**. Cortical-brainstem circuitry attenuates physiological stress reactivity. .

200. **Sando R**, **Bushong E**, **Zhu Y**, **Uytiepo M**, **Ellisman M**, **Maximov A**, **Sando R**, **Bushong E**, **Zhu Y**, **Huang M**, **Considine C**, **Phan S**. Assembly of Excitatory Synapses in the Absence of Glutamatergic Neurotransmission. *Neuron* 94: 312-321.e3, 2017. doi: 10.1016/j.neuron.2017.03.047.

201. **Schaeuble D**, **Wallace T**, **Pace SA**, **Hentges ST**, **Myers B**. Sex-specific prefrontal-

hypothalamic control of behavior and stress responding. *Psychoneuroendocrinology* 159: 106413, 2024. doi: 10.1016/j.psyneuen.2023.106413.

202. **Kalra S**, **Gupta Y**. The Insulin : Glucagon Ratio and the Choice of Glucose-Lowering Drugs THE INSULIN : GLUCAGON BIPOLAR. *Diabetes Ther* 7: 1–9, 2016. doi: 10.1007/s13300-016-0160-4.

203. **Seldenrijk A**, **Hamer M**, **Lahiri A**, **Penninx BWJH**, **Steptoe A**. Psychological distress, cortisol stress response and subclinical coronary calcification. *Psychoneuroendocrinology* 37: 48–55, 2012. doi: 10.1016/j.psyneuen.2011.05.001.

204. **Hamer M**, **Endrighi R**, **Venuraju SM**, **Lahiri A**, **Steptoe A**. Cortisol responses to mental stress and the progression of coronary artery calcification in healthy men and women. *PLoS One* 7: 1–6, 2012. doi: 10.1371/journal.pone.0031356.

205. **Meng L**, **Zhang Y**, **Luo Y**, **Gong T**, **Liu D**. Chronic Stress A Potential Suspect Zero of Atherosclerosis : A Systematic Review. *Front Cardiovasc Med* 8: 1–12, 2021. doi: 10.3389/fcvm.2021.738654.

206. **Harris KM**, **Gottdiener JS**, **Gottlieb SS**, **Burg MM**, **Li S**, **Krantz DS**. Impact of Mental Stress and Anger on Indices of Diastolic Function in Patients With Heart Failure. *J Card Fail* 26: 1006–1010, 2020. doi: 10.1016/j.cardfail.2020.07.008.

207. **Hieda M**, **Yoo J**, **Badrov MB**, **Parker RS**, **Anderson EH**, **Wiblin JL**, **Kawalsky J**, **North CS**, **Suris A**, **Fu Q**. Reduced left ventricular diastolic function in women with posttraumatic stress disorder. *Am J Physiol - Regul Integr Comp Physiol* 317: 108–112, 2019. doi: 10.1152/ajpregu.00002.2019.

208. **Inderliter ALANLH**, **Carolina N**, **Sherwood A**. Endothelial Function and Hemodynamic Responses During Mental Stress. *Psychosom Med* 370: 365–370, 1999.

209. **Sher LD**, **Geddie H**, **Olivier L**, **Cairns XM**, **Truter N**, **Beselaar L**, **Essop XMF**. Chronic stress and endothelial dysfunction : mechanisms , experimental challenges , and the way ahead. *Am J Physiol - Hear Circ Physiol* 319: 488–506, 2020. doi:

10.1152/ajpheart.00244.2020.

210. **Rocha HNM**, **Batista GMS**, **Storch AS**, **Garcia VP**, **Teixeira GF**. Mental stress induces endothelial dysfunction by AT1R-mediated redox imbalance in overweight / obese men. *Brazilian Hournal Med Biol Res* 56: 1–10, 2023. doi: 10.1590/1414-431X2023e12547.

211. **Greaney JL**, **Darling AM**, **Mogle J**, **Saunders EFH**. Depressive Disorder. *Hypertension* 79: 1091–1100, 2022. doi: 10.1161/HYPERTENSIONAHA.122.18985.

212. **Greaney JL**, **Saunders EFH**, **Santhanam L**, **Alexander LM**. Oxidative Stress Contributes to Microvascular Endothelial Dysfunction in Men and Women With Major Depressive Disorder. *Circ Res* 124: 564–574, 2019. doi: 10.1161/CIRCRESAHA.118.313764.

213. **Flak JN**, **Jankord R**, **Solomon MB**, **Krause EG**, **Herman JP**. Physiology & Behavior Opposing effects of chronic stress and weight restriction on cardiovascular , neuroendocrine and metabolic function. *Physiol Behav* 104: 228–234, 2011. doi: 10.1016/j.physbeh.2011.03.002.

214. **Jadeja RN**, **Rachakonda V**, **Bagi Z**, **Khurana S**. Assessing Myogenic Response and Vasoactivity In Resistance Mesenteric Arteries Using Pressure Myography. *J Vis Exp* 101: 1–7, 2015. doi: 10.3791/50997.

215. **Schjørring OL**, **Carlsson R**, **Simonsen U**. Pressure Myography to Study the Function and Structure of Isolated Small Arteries. In: *Methods in Mouse Atherosclerosis*, edited by Andrés V, Dorado B. Springer New York, p. 277–295.

216. **Gunduz F**, **Baskurt OK**, **Meiselman HJ**. Vascular Dilation Responses of Rat Small Mesenteric Arteries at High Intravascular Pressure in Spontaneously Hypertensive Rats. *Circ J* 73: 2091–2097, 2009. doi: 10.1253/circj.CJ-09-0392.

217. **Selvaraj S**, **Aguilar FG**, **Martinez EE**, **Beussink L**, **Kim KA**, **Peng J**, **Lee DC**, **Patel A**, **Sha J**, **Irvin MR**, **Arnett DK**, **Shah SJ**. Diastolic wall strain : a simple marker of abnormal cardiac mechanics. *Cardiovasc Ultrasound* 12: 1–10, 2014.

218. **Jackson WF**, **Jackson WF**. Myogenic Tone in Peripheral Resistance Arteries and Arterioles : The Pressure Is On ! *Front Physiol* 12, 2021. doi: 10.3389/fphys.2021.699517.

219. **Kang M-K**, **Ju S**, **Mun H-S**, **Choi S**, **Cho JR**, **Lee N**. Decreased diastolic wall strain is associated with adverse left ventricular remodeling even in patients with normal left ventricular diastolic function. *J Echocardiogr* 13: 35–42, 2015. doi: 10.1007/s12574-014-0238-9.

220. **Lima AM**, **Xavier CH**, **Ferreira AJ**, **Raizada MK**, **Wallukat G**, **Velloso P**, **Augusto R**, **Antônio M**, **Fontes P**. Activation of angiotensin-converting enzyme 2 / angiotensin- (1 – 7)/ Mas axis attenuates the cardiac reactivity to acute emotional stress. *Am J Physiol - Hear Circ Physiol* 305: 1057–1067, 2013. doi: 10.1152/ajpheart.00433.2013.

221. **Krawutschke C**, **Koesling D**, **Russwurm M**. Cyclic GMP in Vascular Relaxation Export Is of Similar Importance as Degradation. *Arterioscler Thromb Vasc Biol* 35: 2011–2019, 2015. doi: 10.1161/ATVBAHA.115.306133.

222. **Rybalkin SD**, **Yan C**, **Bornfeldt KE**, **Beavo JA**. Cyclic GMP Phosphodiesterases and Regulation of Smooth Muscle Function. *Circ Res* 93: 280–291, 2003. doi: 10.1161/01.RES.0000087541.15600.2B.

223. **Takimoto E**, **Champion HC**, **Belardi D**, **Moslehi J**, **Mongillo M**, **Mergia E**, **Montrose DC**, **Isoda T**, **Aufiero K**, **Zaccolo M**, **Dostmann WR**, **Smith CJ**, **Kass DA**, **Pdea C**. cGMP Catabolism by Phosphodiesterase 5A Regulates Cardiac Adrenergic Stimulation by NOS3-Dependent Mechanism. *Circ Res* 96: 100–109, 2005. doi: 10.1161/01.RES.0000152262.22968.72.

APPENDIX

1. Chapter 2 supplemental material

1.1 Age effects: baseline

Age impacted body weight and baseline corticosterone (**Fig. S.1.1**). Specifically, ANOVA indicated an age effect on body weight [$F(7, 231) = 670.5$, $p < 0.0001$, $\eta_p^2 = 0.953$] with post-hoc analysis finding that aged rats, regardless of group, weighed significantly more ($p < 0.0001$). There was also an age effect on baseline corticosterone [$F(7, 228) = 8.681$, $p < 0.0001$, $\eta_p^2 = 0.210$] with unstressed females having significantly higher corticosterone after aging ($p < 0.001$), indicating a sex-specific change in glucocorticoid tone.

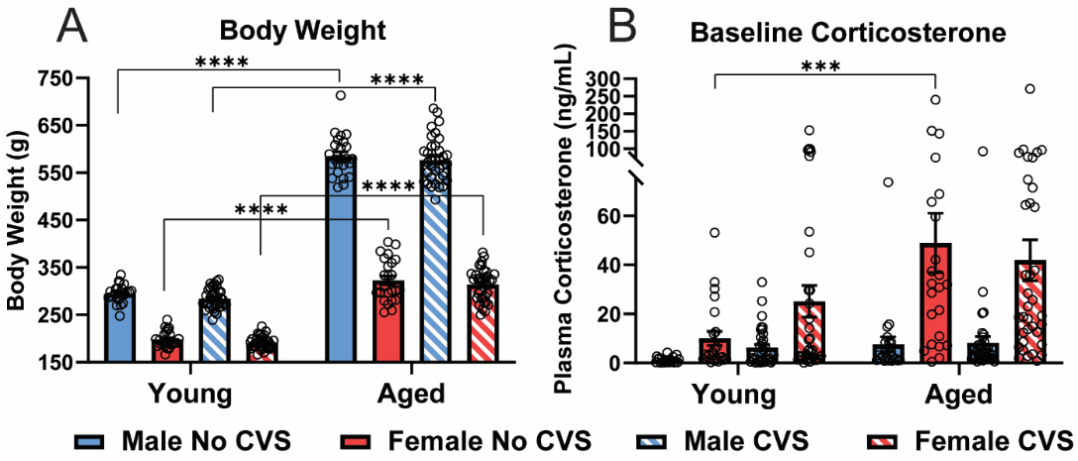

Figure S.1.1: Baseline measures. The effects of age on body weight (**A**) and baseline corticosterone (**B**) for both CVS (n = 36/sex) and No CVS (n = 24/sex) controls. Data are expressed as mean ± SEM. *** $p < 0.001$, **** $p < 0.0001$ within group.

1.2 Age effects: FST

Aging affected both behavioral and hormonal responses to acute psychologic stress (**Fig. S.1.2**). Specifically, passive coping [$F(7, 231) = 20.54$, $p < 0.0001$, $\eta_p^2 = 0.383$] and active coping [$F(7, 231) = 12.04$, $p < 0.0001$, $\eta_p^2 = 0.267$] had age effects. Post-hoc analysis indicated aged males had increased passive coping ($p < 0.0001$) and decreased active coping ($p <$

0.0001) regardless of stress status. Additionally, effects of aging were present in total corticosterone [$F(7, 120) = 6.629$, $p < 0.0001$, $\eta_p^2 = 0.278$] and total glucose [$F(7, 228) = 22.13$, $p < 0.0001$, $\eta_p^2 = 0.404$], where sensitized responses in young chronically stressed females were reduced ($p < 0.0001$). Thus, age impacted FST responses in a sex- and stress-specific manner.

1.3 Age effects: GTT

Aging increased total corticosterone responses [$F(7, 81) = 3.031$, $p = 0.007$, $\eta_p^2 = 0.207$] to GTT (**Fig. S.1.3**) without group-specific effects. Additionally, aging affected glucose tolerance [$F(7, 232) = 5.239$, $p < 0.0001$, $\eta_p^2 = 0.136$] with post-hoc analysis indicating both unstressed ($p < 0.05$) and chronically-stressed males ($p < 0.0001$) had impaired glucose clearance after aging.

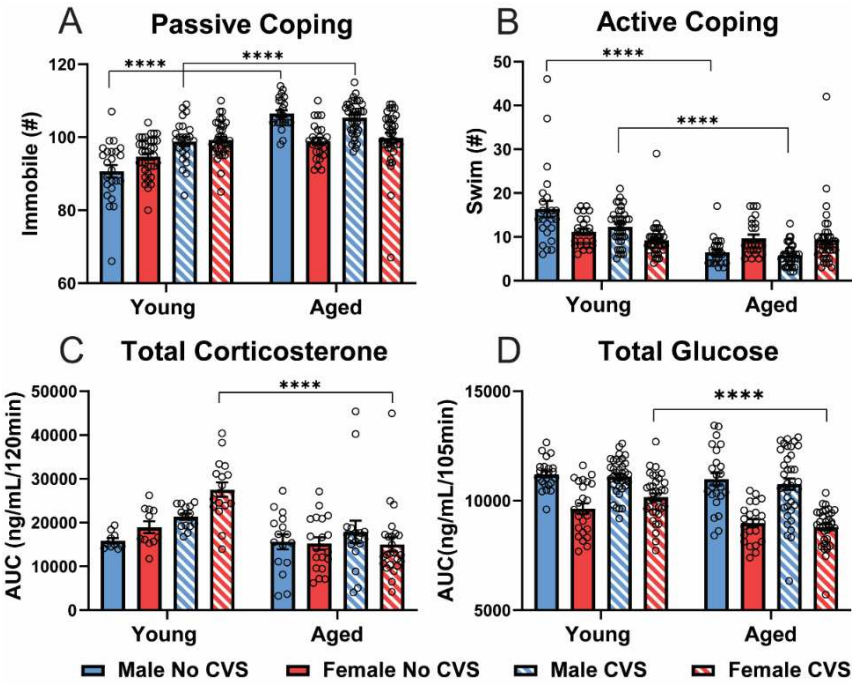

Figure S.1.2: FST. CVS (n = 36/sex) and No CVS (n = 24/sex) controls were assessed for both active (**A**) and passive (**B**) coping. Total corticosterone (**C**) and blood glucose responses (**D**) were calculated from the AUC. **** $p < 0.0001$ within group.

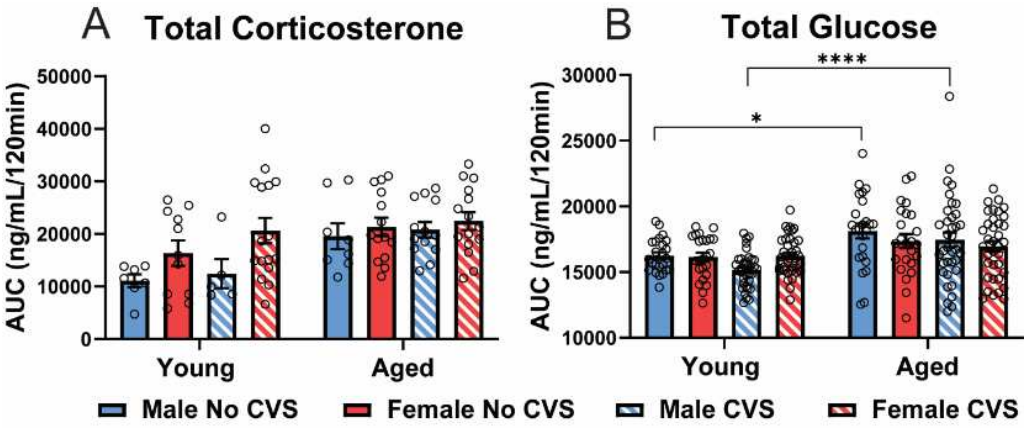

Figure S.1.3: GTT. Total corticosterone (**A**) and blood glucose responses (**B**) were calculated in No CVS (n = 24/sex) and CVS (n = 36/sex) rats from the AUC. Data are expressed as mean ± SEM. * $p < 0.05$, **** $p < 0.0001$ within group.

1.4 Regression analysis: group comparisons

Pearson correlations across measures were analyzed for significant differences between groups (**Fig. S.1.4**). These analyses compared stress condition within sex (**A, B**) and sex within stress condition (**C, D**).

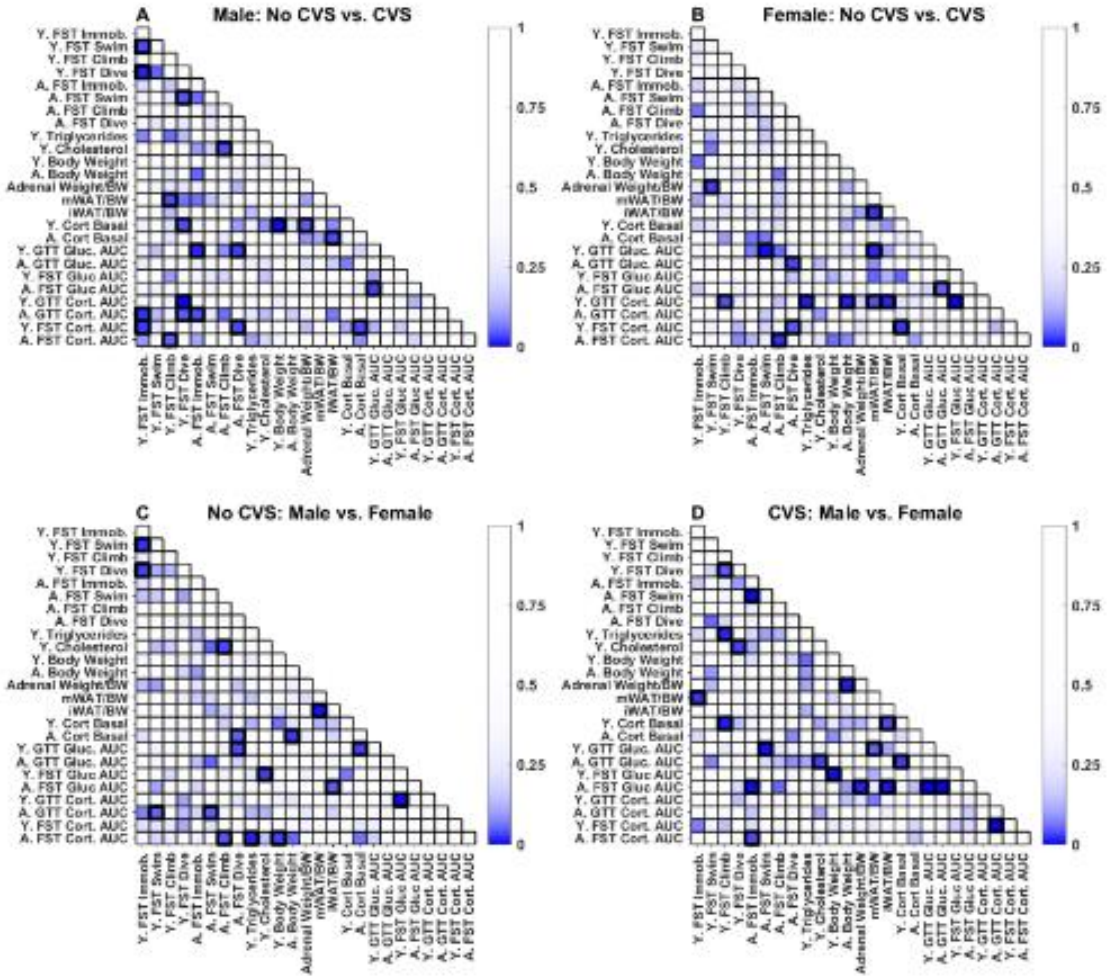

Figure S.1.4: Group comparison of correlation significance. To compare correlations across groups, group correlations were Fisher transformed followed by a two-tailed test. The resultant p values are plotted on the colored scale with significant differences between groups ($p < 0.05$) bolded.

2. Chapter 3 supplemental material

2.1 Glucocorticoid responses: psychogenic stress and metabolic stress

Analysis of FST responses showed numerous sex and stress effects (**Fig. S.2.1**). Baseline corticosterone measures indicated main effects of sex [$(1, 103) = 8.650$, $p = 0.004$, $\eta^2 = 7.006$] and stress [$F(1, 103) = 4.706$, $p = 0.0324$, $\eta^2 = 3.812$] in young animals and a main effect of sex [$F(1, 102) = 24.03$, $p < 0.0001$, $\eta^2 = 17.7$] in aged animals. This is perpetuated in the young total

corticosterone response with both main effects of sex [$F(1, 38) = 13.66$, $p = 0.0007$, $\eta^2 = 14.78$] and stress [$F(1, 38) = 27.81$, $p < 0.0001$, $\eta^2 = 30.09$]. However, aged total corticosterone response to FST shows no significant effect. Significant sex differences were noted in both the young and aged total blood glucose response to FST with a main effect of sex [$F(1, 101) = 48.31$, $p < 0.0001$, $\eta^2 = 29.31$] and [$F(1, 102) = 67.10$, $p < 0.0001$, $\eta^2 = 37.81$] respectively. Interestingly, within the young mid LVH group, young no CVS females mounted a smaller glucose response than both CVS females ($p = 0.0253$) and no CVS males ($p = 0.0007$). Within the high LVH young animals, CVS males had a greater glucose response than CVS females ($p = 0.0047$). Aged animals also showed sex-specific differences with the low LVH no CVS males have a greater glucose response than no CVS females ($p = 0.0076$) and CVS males showing a greater glucose response than their female counterparts in both the mid LVH ($p = 0.0019$) and High LVH ($p = 0.0212$) groups.

While GTT glucocorticoid responses in aged animals impacted LVH, GTT responses in young animals showed only sex effects (**Fig. S.2.2**). Young baseline corticosterone measures showed a main sex effect [$F(1, 90) = 32.51$, $p < 0.0001$, $\eta^2 = 24.63$]. When looking at peak corticosterone levels 30 minutes following intraperitoneal injection of glucose, young animals show no significant differences. Similarly, young animals show no significant effects in total corticosterone response to metabolic challenge.

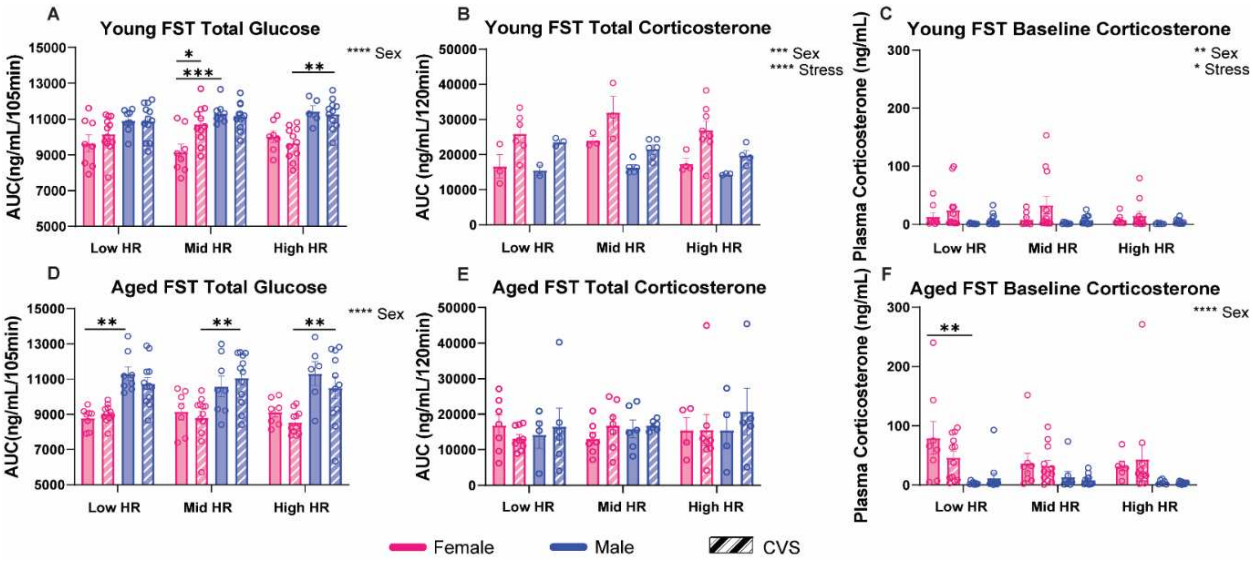

Figure S.2.1. FST glucocorticoid analyses. Total blood glucose and total plasma corticosterone were calculated from the AUC for both the young (A, B) and aged (D, E) animals. Baseline plasma corticosterone was measured (C, F) two days prior to FST. Groups were analyzed according to hypertrophy subpopulations. Data are expressed as mean ± SEM. * p<0.05, ** p<0.01, *** p<0.001, **** p<0.0001.

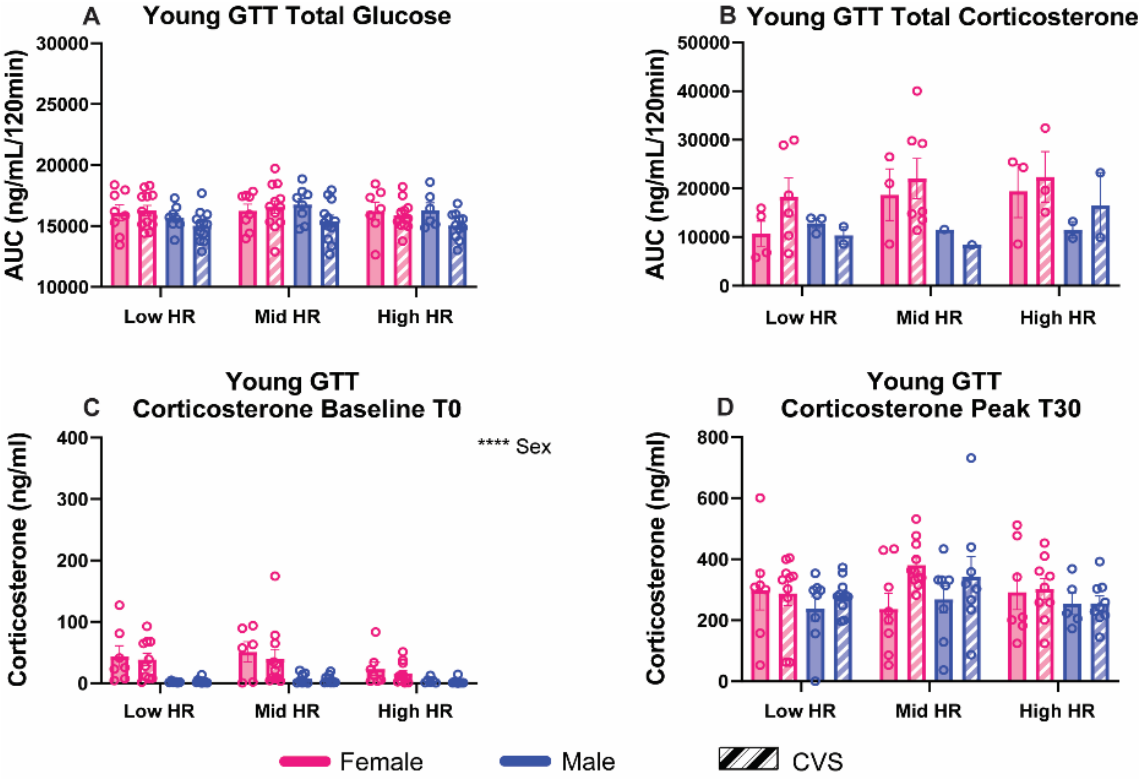

Figure S.2.2. Young GTT glucocorticoid analyses. Young animals were metabolically challenged following chronic stress. Total blood glucose (A) and plasma corticosterone (B) were calculated from an AUC analysis. Baseline corticosterone was measured at T0 taken prior to glucose injection (C). Peak corticosterone response was measured 30 minutes following glucose injection (D). Groups were analyzed according to hypertrophy subpopulations. Data are expressed as mean ± SEM. **** p<0.0001.

2.2 Somatic Measures

Somatic measures of body and organ weights showed sex and stress specific effects (**Fig. S.2.3**). Measures of bodyweight corrected spleen [$F(1, 100) = 13.05$, $p = 0.0005$, $\eta^2 = 10.06$] and adrenal weight [$F(1, 101) = 230.4$, $p < 0.0001$, $\eta^2 = 66.19$] showed main effects of sex. Main effects of sex were also reflected in young cholesterol [$F(1, 101) = 16.01$, $p = 0.0001$, $\eta^2 = 12.36$] and triglyceride levels [$F(1, 101) = 84.15$, $p < 0.0001$, $\eta^2 = 38.71$]. Additionally, young triglycerides showed a main interaction of sex and stress [$F(1, 101) = 5.10$, $p = 0.0261$, $\eta^2 = 2.346$]. Body weight analysis showed main effects of sex both at tissue collection [$F(1, 103) = 1032$, $p < 0.0001$, $\eta^2 = 86.23$] and immediately following chronic stress [$F(1, 103) = 819.0$, $p < 0.0001$, $\eta^2 = 84.04$].

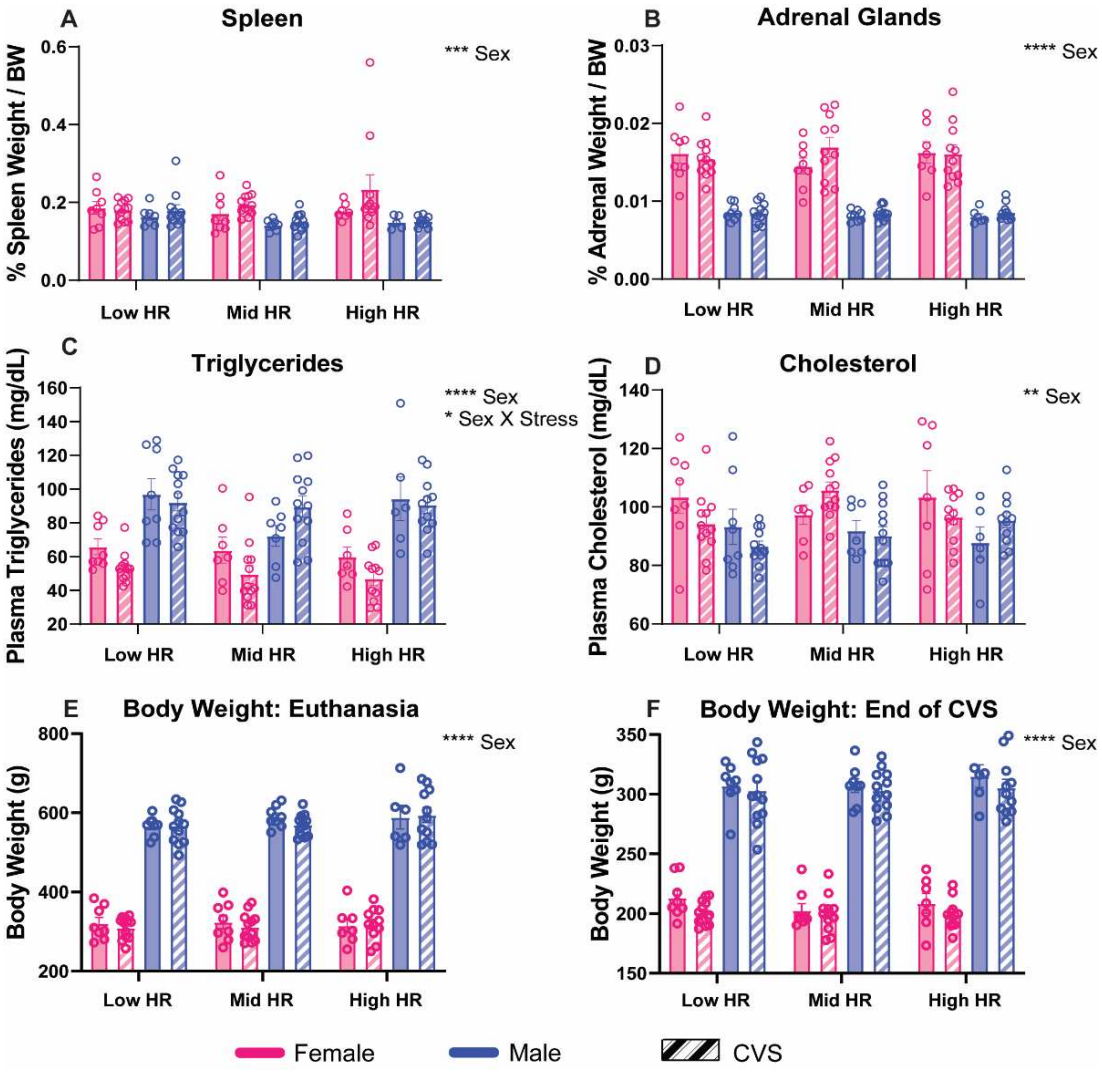

Figure S.2.3 Somatic measures following chronic stress. spleen weight (A), and adrenal weight (B) were measured. Triglycerides (C) and cholesterol (D) were measured following chronic stress from baseline blood samples. Body weight was measured and analyzed at both euthanasia (E) and immediately following CVS (F). Groups were analyzed according to hypertrophy subpopulations. Data are expressed as mean ± SEM. * p<0.05, ** p<0.01, *** p<0.001, **** p<0.0001.

Table S.1: ANOVA table of group comparisons

	ANOVA Table	F(DFn,DFd)	P Value
Figure 11			
Ventricular diameter	Interaction	F (1, 111) = 0.5525	P=0.4589
	Sex	F (1, 111) = 1.902	P=0.1706
	Stress	F (1, 111) = 11.62	P=0.0009

Interior wall thickness	Interaction	F (1, 110) = 0.02195	P=0.8825
	Sex	F (1, 110) = 0.0009537	P=0.9754
	Stress	F (1, 110) = 13.71	P=0.0003
Free wall thickness	Interaction	F (1, 111) = 0.09016	P=0.7645
	Sex	F (1, 111) = 0.2343	P=0.6293
	Stress	F (1, 111) = 19.08	P<0.0001
Hypertrophy ratio	Interaction	F (1, 111) = 1.238	P=0.2682
	Sex	F (1, 111) = 1.641	P=0.2028
	Stress	F (1, 111) = 14.39	P=0.0002
HR tertile comparison	HR	F (2, 103) = 118.1	P<0.0001
	Sex	F (1, 103) = 49.89	P<0.0001
	Stress	F (1, 103) = 4.717	P=0.0322
	HR x Sex	F (2, 103) = 5.932	P=0.0036
	HR x Stress	F (2, 103) = 2.308	P=0.1046
	Sex x Stress	F (1, 103) = 5.520	P=0.0207
	HR x Sex x Stress	F (2, 103) = 1.905	P=0.1540
Figure 12			
Young passive coping	HR	F(2, 103) = 4.786	P=0.0103
	Sex	F(1, 103) = 31.18	P<0.0001
	Stress	F(1, 103) = 4.461	P=0.0335
	HR x Sex	F (2, 103) = 0.8113	P=0.4471
	HR x Stress	F(2, 103) = 3.148	P=0.0471
	Sex x Stress	F (1, 103) = 4.224	P=0.1414
	HR x Sex x Stress	F (2, 103) = 0.5283	P=0.5912
Young active coping	HR	F (2, 103) = 2.557	P=0.0825
	Sex	F (1, 103) = 17.82	P<0.0001
	Stress	F (1, 103) = 10.04	P=0.0020
	HR x Sex	F (2, 103) = 0.4918	P=0.6130
	HR x Stress	F (2, 103) = 1.509	P=0.2260
	Sex x Stress	F (1, 103) = 2.257	P=0.1361
	HR x Sex x Stress	F (2, 103) = 1.506	P=0.2266
Aged passive coping	HR	F (2, 102) = 0.4353	P=0.6483
	Sex	F (1, 102) = 30.75	P<0.0001
	Stress	F (1, 102) = 0.01359	P=0.9074
	HR x Sex	F (2, 102) = 0.9002	P=0.4097
	HR x Stress	F (2, 102) = 0.8090	P=0.4482
	Sex x Stress	F (1, 102) = 0.7146	P=0.3999
	HR x Sex x Stress	F (2, 102) = 0.07626	P=0.9266
Aged active coping	HR	F (2, 102) = 0.8430	P=0.4334
	Sex	F (1, 102) = 14.52	P=0.0002
	Stress	F (1, 102) = 0.07055	P=0.7911
	HR x Sex	F (2, 102) = 0.4101	P=0.6647
	HR x Stress	F (2, 102) = 3.565	P=0.0319
	Sex x Stress	F (1, 102) = 0.09457	P=0.7591
	HR x Sex x Stress	F (2, 102) = 0.5070	P=0.6038
Figure 13			

Aged GTT glucose AUC	HR	F (2, 102) = 2.511	P=0.0862
	Sex	F (1, 102) = 1.299	P=0.2571
	Stress	F (1, 102) = 0.6832	P=0.4104
	HR x Sex	F (2, 102) = 2.238	P=0.1119
	HR x Stress	F (2, 102) = 0.7060	P=0.4960
	Sex x Stress	F (1, 102) = 0.01734	P=0.8955
	HR x Sex x Stress	F (2, 102) = 0.4892	P=0.6145
Aged GTT cort AUC	HR	F (2, 35) = 1.132	P=0.3339
	Sex	F (1, 35) = 0.03862	P=0.8453
	Stress	F (1, 35) = 0.03655	P=0.8495
	HR x Sex	F (2, 35) = 5.042	P=0.0119
	HR x Stress	F (2, 35) = 2.065	P=0.1420
	Sex x Stress	F (1, 35) = 2.002	P=0.1659
	HR x Sex x Stress	F (2, 35) = 0.002035	P=0.9980
Aged GTT cort baseline	HR	F (2, 85) = 0.5794	P=0.5624
	Sex	F (1, 85) = 4.912	P=0.0293
	Stress	F (1, 85) = 0.04995	P=0.8237
	HR x Sex	F (2, 85) = 1.967	P=0.1462
	HR x Stress	F (2, 85) = 2.200	P=0.1171
	Sex x Stress	F (1, 85) = 0.5371	P=0.4657
	HR x Sex x Stress	F (2, 85) = 3.283	P=0.0423
Aged GTT cort peak	HR	F (2, 86) = 0.5056	P=0.6050
	Sex	F (1, 86) = 6.772	P=0.0109
	Stress	F (1, 86) = 1.758	P=0.1884
	HR x Sex	F (2, 86) = 0.3869	P=0.6803
	HR x Stress	F (2, 86) = 0.8288	P=0.4400
	Sex x Stress	F (1, 86) = 0.1867	P=0.6668
	HR x Sex x Stress	F (2, 86) = 0.03880	P=0.9620
Figure 14			
Mesenteric white adipose	HR	F (2, 101) = 3.916	P=0.0230
	Sex	F (1, 101) = 0.3737	P=0.5424
	Stress	F (1, 101) = 2.124	P=0.1481
	HR x Sex	F (2, 101) = 2.131	P=0.1240
	HR x Stress	F (2, 101) = 0.1082	P=0.8975
	Sex x Stress	F (1, 101) = 0.1740	P=0.6774
	HR x Sex x Stress	F (2, 101) = 0.1049	P=0.9006
Inguinal white adipose	HR	F (2, 100) = 2.136	P=0.1235
	Sex	F (1, 100) = 94.98	P<0.0001
	Stress	F (1, 100) = 0.5734	P=0.4507
	HR x Sex	F (2, 100) = 1.945	P=0.1484
	HR x Stress	F (2, 100) = 1.990	P=0.1421
	Sex x Stress	F (1, 100) = 1.554	P=0.2155
	HR x Sex x Stress	F (2, 100) = 3.090	P=0.0499

3. Chapter 4 supplemental material

Table S.2: ANOVA table of group comparisons

	ANOVA Table	F(DFn,DFd)	P Value
Figure 17			
Female body weight	Day	F (4, 132) = 6.825	P<0.0001
	Virus	F (1, 33) = 0.05442	P=0.8170
	Stress	F (1, 33) = 6.641	P=0.0146
	Day x Virus	F (4, 132) = 0.1295	P=0.9714
	Day x Stress	F (4, 132) = 23.80	P<0.0001
	Virus x Stress	F (1, 33) = 0.2910	P=0.5932
	Day x Virus x Stress	F (4, 132) = 0.8380	P=0.5034
Female food intake	Interaction	F (1, 33) = 0.1905	P=0.6653
	Virus	F (1, 33) = 0.5219	P=0.4751
	Stress	F (1, 33) = 13.58	P=0.0008
Female adrenal glands	Interaction	F (1, 33) = 1.712	P=0.1998
	Virus	F (1, 33) = 1.829	P=0.1854
	Stress	F (1, 33) = 0.002132	P=0.9634
Male body weight	Day	F (4, 124) = 44.01	P<0.0001
	Virus	F (1, 31) = 0.2922	P=0.5927
	Stress	F (1, 31) = 2.043	P=0.1630
	Day x Virus	F (4, 124) = 0.4410	P=0.7787
	Day x Stress	F (4, 124) = 49.58	P<0.0001
	Virus x Stress	F (1, 31) = 0.5418	P=0.4672
	Day x Virus x Stress	F (4, 124) = 1.680	P=0.1588
Male food intake	Interaction	F (1, 31) = 0.1795	P=0.6748
	Virus	F (1, 31) = 5.539	P=0.251
	Stress	F (1, 31) = 0.9533	P=0.3364
Male adrenal glands	Interaction	F (1, 28) = 1.273	P=0.2688
	Virus	F (1, 28) = 1.112	P=0.3007
	Stress	F (1, 28) = 20.32	P=0.0001
Figure 18			
Female No CVS glucose	Interaction	F (4, 79) = 1.816	P=0.1340
	Time	F (4, 79) = 16.47	P<0.0001
	Virus	F (1, 79) = 10.36	P=0.0019
Female No CVS insulin	Interaction	F (4, 77) = 0.6094	P=0.6571
	Time	F (4, 77) = 4.104	P=0.0046
	Virus	F (1, 77) = 0.6074	P=0.4381
Female No CVS glucagon	Interaction	F (4, 75) = 0.7674	P=0.5498
	Time	F (4, 75) = 1.103	P=0.3616
	Virus	F (1, 75) = 3.015	P=0.0866
Female No CVS cort	Interaction	F (4, 79) = 2.042	P=0.0965
	Time	F (4, 79) = 19.18	P<0.0001
	Virus	F (1, 79) = 14.41	P=0.0003
Female CVS glucose	Interaction	F (4, 85) = 0.3202	P=0.8637
	Time	F (4, 85) = 20.13	P<0.0001
	Virus	F (1, 85) = 0.008482	P=0.9268

Female CVS insulin	Interaction	F (4, 82) = 1.005	P=0.4098
	Time	F (4, 82) = 1.546	P=0.1965
	Virus	F (1, 82) = 0.06800	P=0.7949
Female CVS glucagon	Interaction	F (4, 80) = 1.183	P=0.3246
	Time	F (4, 80) = 0.8370	P=0.5057
	Virus	F (1, 80) = 0.8857	P=0.3495
Female CVS cort	Interaction	F (4, 83) = 0.5061	P=0.7313
	Time	F (4, 83) = 17.21	P<0.0001
	Virus	F (1, 83) = 0.3916	P=0.5332
Figure 19			
Male No CVS glucose	Interaction	F (4, 70) = 0.5888	P=0.6718
	Time	F (4, 70) = 19.82	P<0.0001
	Virus	F (1, 70) = 2.461	P=0.1212
Male No CVS insulin	Interaction	F (4, 67) = 0.4124	P=0.7991
	Time	F (4, 67) = 1.569	P=0.1928
	Virus	F (1, 67) = 2.308	P=0.1334
Male No CVS glucagon	Interaction	F (4, 63) = 0.6312	P=0.6420
	Time	F (4, 63) = 1.385	P=0.2492
	Virus	F (1, 63) = 4.015	P=0.0494
Male No CVS cort	Interaction	F (4, 68) = 0.4077	P=0.8025
	Time	F (4, 68) = 23.67	P<0.0001
	Virus	F (1, 68) = 1.901	P=0.1725
Male CVS glucose	Interaction	F (4, 81) = 1.623	P=0.1763
	Time	F (4, 81) = 31.22	P<0.0001
	Virus	F (1, 81) = 7.018	P=0.0097
Male CVS insulin	Interaction	F (4, 78) = 1.356	P=0.2570
	Time	F (4, 78) = 1.431	P=0.2315
	Virus	F (1, 78) = 1.270	P=0.2632
Male CVS glucagon	Interaction	F (4, 78) = 0.3960	P=0.8109
	Time	F (4, 78) = 0.8988	P=0.4689
	Virus	F (1, 78) = 2.237	P=0.1388
Male CVS cort	Interaction	F (4, 80) = 0.4972	P=0.7378
	Time	F (4, 80) = 37.56	P<0.0001
	Virus	F (1, 80) = 4.078	P=0.0468
Figure 20			
Female No CVS I:G	Interaction	F (4, 74) = 1.197	P=0.3192
	Time	F (4, 74) = 1.351	P=0.2594
	Virus	F (1, 74) = 0.7814	P=0.3796
Female CVS I:G	Interaction	F (4, 77) = 2.570	P=0.0444
	Time	F (4, 77) = 1.415	P=0.2370
	Virus	F (1, 77) = 1.862	P=0.1764
Male No CVS I:G	Interaction	F (4, 63) = 0.8112	P=0.5227
	Time	F (4, 63) = 0.9507	P=0.4409
	Virus	F (1, 63) = 0.01388	P=0.9066
Male CVS I:G	Interaction	F (4, 76) = 0.5922	P=0.6693
	Time	F (4, 76) = 1.414	P=0.2373
	Virus	F (1, 76) = 5.048	P=0.0276

4. Chapter 5 supplemental material

Table S.3: ANOVA table of group comparisons

	ANOVA Table	F(DFn,DFd)	P Value
Figure 25			
Female body weight	Day	F (4, 132) = 6.825	P<0.0001
	Virus	F (1, 33) = 0.05442	P=0.8170
	Stress	F (1, 33) = 6.641	P=0.0146
	Day x Virus	F (4, 132) = 0.1295	P=0.9714
	Day x Stress	F (4, 132) = 23.80	P<0.0001
	Virus x Stress	F (1, 33) = 0.2910	P=0.5932
	Day x Virus x Stress	F (4, 132) = 0.8380	P=0.5034
Female food intake	Interaction	F (1, 33) = 0.1905	P=0.6653
	Virus	F (1, 33) = 0.5219	P=0.4751
	Stress	F (1, 33) = 13.58	P=0.0008
Female adrenal glands	Interaction	F (1, 33) = 1.712	P=0.1998
	Virus	F (1, 33) = 1.829	P=0.1854
	Stress	F (1, 33) = 0.002132	P=0.9634
Male body weight	Day	F (4, 124) = 44.01	P<0.0001
	Virus	F (1, 31) = 0.2922	P=0.5927
	Stress	F (1, 31) = 2.043	P=0.1630
	Day x Virus	F (4, 124) = 0.4410	P=0.7787
	Day x Stress	F (4, 124) = 49.58	P<0.0001
	Virus x Stress	F (1, 31) = 0.5418	P=0.4672
	Day x Virus x Stress	F (4, 124) = 1.680	P=0.1588
Male food intake	Interaction	F (1, 31) = 0.1795	P=0.6748
	Virus	F (1, 31) = 5.539	P=0.251
	Stress	F (1, 31) = 0.9533	P=0.3364
Male adrenal glands	Interaction	F (1, 28) = 1.273	P=0.2688
	Virus	F (1, 28) = 1.112	P=0.3007
	Stress	F (1, 28) = 20.32	P=0.0001
Figure 26			
Female heart index	Interaction	F (1, 31) = 1.117	P=0.2988
	Virus	F (1, 31) = 7.554	P=0.0099
	Stress	F (1, 31) = 1.152	P=0.2915
Female angiotensin II	Interaction	F (1, 45) = 0.6188	P=0.4356
	Virus	F (1, 45) = 1.981	P=0.1662
	Stress	F (1, 45) = 1.749	P=0.1927
Female pulse wave velocity	Interaction	F (1, 33) = 0.01263	P=0.9112
	Virus	F (1, 33) = 0.003221	P=0.9551
	Stress	F (1, 33) = 0.004723	P=0.9456
Male heart index	Interaction	F (1, 29) = 0.1529	P=0.6987
	Virus	F (1, 29) = 0.1498	P=0.7016
	Stress	F (1, 29) = 2.317	P=0.1388
Male angiotensin II	Interaction	F (1, 48) = 0.4317	P=0.5143
	Virus	F (1, 48) = 1.400	P=0.2425
	Stress	F (1, 48) = 5.321	P=0.0254

Male pulse wave velocity	Interaction	F (1, 29) = 0.9390	P=0.3405
	Virus	F (1, 29) = 0.05101	P=0.8229
	Stress	F (1, 29) = 0.1216	P=0.7298
Figure 27			
Female LV diameter systole	Interaction	F (1, 33) = 2.024	P=0.1642
	Virus	F (1, 33) = 1.434	P=0.2397
	Stress	F (1, 33) = 0.01217	P=0.9128
Female LV diameter diastole	Interaction	F (1, 33) = 0.1055	P=0.7474
	Virus	F (1, 33) = 0.009727	P=0.9220
	Stress	F (1, 33) = 1.001	P=0.3242
Female LV posterior wall systole	Interaction	F (1, 33) = 4.422	P=0.0432
	Virus	F (1, 33) = 0.01762	P=0.8952
	Stress	F (1, 33) = 0.01203	P=0.9133
Female LV posterior wall diastole	Interaction	F (1, 33) = 0.002436	P=0.9609
	Virus	F (1, 33) = 0.5288	P=0.4723
	Stress	F (1, 33) = 4.365e-005	P=0.9948
Female LV diastolic wall strain	Interaction	F (1, 33) = 4.710	P=0.0373
	Virus	F (1, 33) = 0.3813	P=0.5412
	Stress	F (1, 33) = 0.1053	P=0.7476
Male LV diameter systole	Interaction	F (1, 29) = 0.2323	P=0.6334
	Virus	F (1, 29) = 0.01714	P=0.8967
	Stress	F (1, 29) = 0.2416	P=0.6268
Male LV diameter diastole	Interaction	F (1, 29) = 0.2589	P=0.6148
	Virus	F (1, 29) = 0.1014	P=0.7524
	Stress	F (1, 29) = 0.1112	P=0.7412
Male LV posterior wall systole	Interaction	F (1, 29) = 1.279	P=0.2673
	Virus	F (1, 29) = 4.460	P=0.0434
	Stress	F (1, 29) = 2.849	P=0.1022
Male LV posterior wall diastole	Interaction	F (1, 29) = 0.03108	P=0.8613
	Virus	F (1, 29) = 4.943	P=0.0341
	Stress	F (1, 29) = 0.1142	P=0.7379
Male LV diastolic wall strain	Interaction	F (1, 29) = 1.261	P=0.2706
	Virus	F (1, 29) = 0.001706	P=0.9673
	Stress	F (1, 29) = 3.064	P=0.0906
Female fractional shortening	Interaction	F (1, 33) = 2.639	P=0.1138
	Virus	F (1, 33) = 1.970	P=0.1698
	Stress	F (1, 33) = 0.1695	P=0.6832
Female ventricular filling	Interaction	F (1, 24) = 0.01451	P=0.9051
	Virus	F (1, 24) = 0.2578	P=0.6163
	Stress	F (1, 24) = 0.9523	P=0.3389
Male fractional shortening	Interaction	F (1, 29) = 1.404	P=0.2456
	Virus	F (1, 29) = 0.3463	P=0.5607
	Stress	F (1, 29) = 1.285	P=0.2663
Male ventricular filling	Interaction	F (1, 24) = 1.875	P=0.1835

	Virus	F (1, 24) = 2.317	P=0.1411
	Stress	F (1, 24) = 0.3708	P=0.5483
Figure 28			
Female body weight	Day	F (5, 80) = 5.470	P=0.0002
	Virus	F (1, 16) = 5.958	P=0.0267
	Stress	F (1, 16) = 0.4969	P=0.4910
	Day x Virus	F (5, 80) = 0.5658	P=0.7259
	Day x Stress	F (5, 80) = 3.126	P=0.0125
	Virus x Stress	F (1, 16) = 0.5121	P=0.4845
	Day x Virus x Stress	F (5, 80) = 0.4776	P=0.7920
Female heart index	Interaction	F (1, 18) = 3.477	P=0.0786
	Virus	F (1, 18) = 2.376	P=0.1406
	Stress	F (1, 18) = 0.9817	P=0.3349
Female adrenal glands	Interaction	F (1, 18) = 0.8939	P=0.3569
	Virus	F (1, 18) = 1.229	P=0.2822
	Stress	F (1, 18) = 0.02801	P=0.8690
Male body weight	Day	F (5, 94) = 6.889	<0.0001
	Virus	F (1, 19) = 0.5276	0.4765
	Stress	F (1, 19) = 0.6657	0.4247
	Day x Virus	F (5, 94) = 0.8107	0.5449
	Day x Stress	F (5, 94) = 2.040	0.0801
	Virus x Stress	F (1, 19) = 0.1292	0.7232
	Day x Virus x Stress	F (5, 94) = 0.6988	0.6257
Male heart index	Interaction	F (1, 21) = 0.7928	P=0.3833
	Virus	F (1, 21) = 1.412	P=0.2480
	Stress	F (1, 21) = 0.1554	P=0.6974
Male adrenal glands	Interaction	F (1, 19) = 0.5485	P=0.4680
	Virus	F (1, 19) = 1.640	P=0.2157
	Stress	F (1, 19) = 0.3929	P=0.5383
Figure 29			
Female No CVS myogenic tone	Interaction	F (5, 52) = 2.025	P=0.0903
	Virus	F (5, 52) = 1.137	P=0.3527
	Stress	F (1, 52) = 7.717	P=0.0076
Female CVS myogenic tone	Interaction	F (5, 36) = 0.1537	P=0.9776
	Virus	F (5, 36) = 0.9265	P=0.4752
	Stress	F (1, 36) = 13.02	P=0.0009
Male No CVS myogenic tone	Interaction	F (5, 53) = 0.1150	P=0.9885
	Virus	F (5, 53) = 0.9890	P=0.4333
	Stress	F (1, 53) = 1.441	P=0.2352
Male CVS myogenic tone	Interaction	F (5, 42) = 0.09002	P=0.9934
	Virus	F (5, 42) = 0.2496	P=0.9377
	Stress	F (1, 42) = 5.147	P=0.0285
Figure 30			
Female No CVS PE 70	Interaction	F (4, 45) = 0.3596	P=0.8360
	Virus	F (4, 45) = 33.09	P<0.0001
	Stress	F (1, 45) = 3.983	P=0.0520
Female No CVS SNP 70	Interaction	F (6, 63) = 0.2421	P=0.9607
	Virus	F (6, 63) = 3.838	P=0.0025

	Stress	F (1, 63) = 1.931	P=0.1695
Female No CVS ACh 70	Interaction	F (4, 40) = 0.3727	P=0.8267
	Virus	F (4, 40) = 3.101	P=0.0259
	Stress	F (1, 40) = 3.496	P=0.0689
Female CVS PE 70	Interaction	F (4, 35) = 0.3387	P=0.8500
	Virus	F (4, 35) = 17.64	P<0.0001
	Stress	F (1, 35) = 0.04889	P=0.8263
Female CVS SNP 70	Interaction	F (6, 47) = 0.3442	P=0.9098
	Virus	F (6, 47) = 1.560	P=0.1798
	Stress	F (1, 47) = 2.239	P=0.1412
Female CVS ACh 70	Interaction	F (4, 32) = 2.230	P=0.0878
	Virus	F (4, 32) = 3.198	P=0.0257
	Stress	F (1, 32) = 13.06	P=0.0010
Figure 31			
Female No CVS PE 120	Interaction	F (4, 40) = 0.1198	P=0.9746
	Virus	F (4, 40) = 15.19	P<0.0001
	Stress	F (1, 40) = 0.1808	P=0.6729
Female No CVS SNP 120	Interaction	F (6, 56) = 0.07851	P=0.9980
	Virus	F (6, 56) = 3.369	P=0.0066
	Stress	F (1, 56) = 1.712	P=0.1961
Female No CVS ACh 120	Interaction	F (4, 40) = 0.2262	P=0.9221
	Virus	F (4, 40) = 0.4847	P=0.7468
	Stress	F (1, 40) = 1.931	P=0.1724
Female CVS PE 120	Interaction	F (4, 35) = 1.472	P=0.2317
	Virus	F (4, 35) = 18.38	P<0.0001
	Stress	F (1, 35) = 2.923	P=0.0962
Female CVS SNP 120	Interaction	F (6, 42) = 0.5425	P=0.7728
	Virus	F (6, 42) = 0.9339	P=0.4810
	Stress	F (1, 42) = 5.352	P=0.0257
Female CVS ACh 120	Interaction	F (4, 30) = 0.2776	P=0.8901
	Virus	F (4, 30) = 0.4834	P=0.7477
	Stress	F (1, 30) = 12.32	P=0.0014
Figure 32			
Male No CVS PE 70	Interaction	F (4, 45) = 0.8632	P=0.4934
	Virus	F (4, 45) = 36.19	P<0.0001
	Stress	F (1, 45) = 2.230	P=0.1423
Male No CVS SNP 70	Interaction	F (6, 55) = 0.5124	P=0.7964
	Virus	F (6, 55) = 2.835	P=0.0178
	Stress	F (1, 55) = 3.076	P=0.0850
Male No CVS ACh 70	Interaction	F (4, 45) = 0.1974	P=0.9385
	Virus	F (4, 45) = 1.103	P=0.3668
	Stress	F (1, 45) = 0.006874	P=0.9343
Male CVS PE 70	Interaction	F (4, 25) = 0.9660	P=0.4435
	Virus	F (4, 25) = 18.42	P<0.0001
	Stress	F (1, 25) = 0.4439	P=0.5114
Male CVS SNP 70	Interaction	F (6, 35) = 0.04507	P=0.9996
	Virus	F (6, 35) = 5.115	P=0.0007
	Stress	F (1, 35) = 0.7330	P=0.3977
Male CVS ACh 70	Interaction	F (4, 25) = 0.2418	P=0.9119

	Virus	F (4, 25) = 2.132	P=0.1065
	Stress	F (1, 25) = 2.982	P=0.0965
Figure 33			
Male No CVS PE 120	Interaction	F (4, 45) = 0.8531	P=0.4993
	Virus	F (4, 45) = 11.14	P<0.0001
	Stress	F (1, 45) = 0.2821	P=0.5979
Male No CVS SNP 120	Interaction	F (6, 63) = 0.3807	P=0.8887
	Virus	F (6, 63) = 0.6691	P=0.6749
	Stress	F (1, 63) = 6.051	P=0.0167
Male No CVS ACh 120	Interaction	F (4, 45) = 0.6820	P=0.6081
	Virus	F (4, 45) = 0.1974	P=0.9385
	Stress	F (1, 45) = 10.09	P=0.0027
Male CVS PE 120	Interaction	F (4, 25) = 0.7566	P=0.5632
	Virus	F (4, 25) = 14.98	P<0.0001
	Stress	F (1, 25) = 1.087	P=0.3071
Male CVS SNP 120	Interaction	F (6, 35) = 0.2139	P=0.9699
	Virus	F (6, 35) = 2.232	P=0.0629
	Stress	F (1, 35) = 1.966	P=0.1696
Male CVS ACh 120	Interaction	F (4, 25) = 0.3386	P=0.8493
	Virus	F (4, 25) = 0.2632	P=0.8987
	Stress	F (1, 25) = 3.637	P=0.0681